Transcription regulation through chromatin structure and nuclear compartmentalization

Thesis

UNRESTRICTED

CARMELO FERRAI

Transcription regulation through chromatin structure and nuclear compartmentalization

Degree of Doctor of Philosophy (PhD)
in
Molecular and Cellular Biology

September 2007

Sponsoring establishment:
DIBIT-Department of Biological and Technological Research, San Raffaele Scientific Institute
Milan, ITALY

Director of studies:
Dr. Massimo P. Crippa

External supervisor:
Bryan M. Turner

DATE OF SUBMISSION 18 JUNE 2007
DATE OF AWARD 21 DECEMBER 2007

ProQuest LLC.
789 East Eisenhower Parkway
P.O. Box 1346
Ann Arbor, MI 48106 – 1346

CONTENTS

"Il caso aiuta le menti preparate"

"La chance ne sourit qu'aux exprits bien prepares"

"Fortune favours the prepared mind"

Louis Pasteur

DECLARATION

This PhD Thesis has been written by myself and has not been used in any previous application for a degree. All the results presented are original data and were obtained at the laboratory of Molecular Genetics Department, DIBIT San Raffaele Scientific Institute, Milan, under the guidance of Massimo P. Crippa. For the sake of scientific completeness some data obtained in collaboration with other laboratories are presented. However, they are clearly identified at the end of the pertaining result chapter. Some of the work contained in this Thesis has been published and the relative references are reported at the end of the result chapters.

ABSTRACT

Transcription is a very complex multi-step process presenting different levels of regulation. A large amount of general transcription factors and cofactors recruited on the promoters participate, together with the polymerases, in driving RNA production. The formation of chromatin loops allows their interaction with specific transcription factors bound to distant regulatory sequences and the fine tuning of the gene activity. A further level of complexity is provided by the structural and functional compartmentalization of the nucleus. In fact gene transcription takes place in a strongly localized fashion and nuclear architecture can influence genome regulation. One of the most intriguing findings is that an acto-myosin network plays a role in gene transcription. However, the *in vivo* role of such proteins in gene expression is still largely unclear. During my PhD I developed a technical approach coupling MNase digestion to ChIP by which I showed that the enhancer and minimal promoter of the human uPA gene function as a single transcription control unit forming a stable structure, that is required to sustain the early elongation step of RNAP-II. I next studied the uPA gene in an inducible cell system showing that it is associated with an inactive RNAP-II transcription factory before the onset of its expression while transcriptional induction promotes its association with an active transcription factory. This finding indicates inactive factories as distinct entities from the active ones supporting the notion of specialized transcription factories. I also studied the involvement of MyosinVI in transcription, characterizing its role in regulating RNAP-II activity. MyosinVI is required for phosphorylation of RNAP-II CTD at level of Serin-2 that, in turn, is required for the

enzyme to proceed in the elongating phase. Finally, I showed that the transcription factor Prep1 and MyosinVI are associated in a complex and that the recruitment of MyosinVI on the Prep1-target genes is mediated by the transcription factor itself.

INTRODUCTION

1.1. Transcription is regulated at multiple levels.

The regulation of gene expression is a fundamental problem in modern biology because all biological events depend on the correct transcriptional onset of subsets of genes. Eukaryotic gene transcription is a remarkably complex biochemical multi-step process, each one which is tightly regulated. During the life of every organism the activation of specific gene expression programs in development and cellular differentiation, is the result of an intricate regulatory network. Local chromatin remodeling, as well as the correct recruitment of the transcriptional machinery, is known to be crucial steps and their synergistic action eventually determines the correct gene regulation (Lemon and Tjian, 2000). However, recent lines of evidence show that also nuclear architecture can influence genome regulation (Misteli, 2007) making clear that the modulation of gene expression programs involve different levels of structural organization in the cell nucleus (Misteli, 2007).

1.2. Long range interaction of cis control elements.

At the most basic level gene expression is controlled through the action of DNA regulatory elements. Eukaryotic genes contain complex arrays of specific sequences that combine

more commonly shared core promoter elements with largely different gene-specific cis-elements called enhancers. Both these sequences are required and cooperate to define different expression patterns (Dynan, 1989) through the recruitment of the general transcriptional machinery, including RNAP-II and a large number of transcription factors and cofactors with chromatin-modifying activities (Lemon and Tjian, 2000). The enhancers have been defined as elements that can increase transcription irrespective of their orientation and position relative to the transcription start site (Dillon and Sabbattini, 2000). It is well known that these regulatory elements can be located at considerable distances (up to one megabase or more) from the genes they regulate (Chakalova et al., 2005). Other control elements such as insulators, silencers and LCRs, which play a fundamental role in the control of many complex genetic loci, also regulate gene expression over long distances (Grosveld, 1987; Sun and Elgin, 1999; West et al., 2002).

1.2.1. Models for long-range interaction.

Since the initial discovery of distal regulatory sequences, a debate has focused on how such elements communicate their regulatory effects to the linked genes over large spans of intervening DNA. Two main models were proposed: the "looping" and the "linking" model (Hatzis and Talianidis, 2002). In the former, transcriptional activators bound to the enhancer directly contacted other factors bound to the promoter, causing the looping of the IVS (see Figure 1.1). In the latter, the establishment of modified chromatin domains between the enhancer and the promoter was achieved through the action of facilitator proteins that generated a progressive chain of higher order complexes over the chromatin fiber of the IVS (see Figure 1.1). Other models extended those reported above, differing

only in the manner in which the contact between enhancer and promoter is established. In the "tracking" model (Hatzis and Talianidis, 2002), for instance, a complex recruited on the enhancer slides along the IVS and eventually contacts the promoter (see Figure 1.1). In another model the progressive chain of higher order complexes over the chromatin fiber of the IVS causes its bending and allows the contact between the regulatory regions (see Figure 1.1) (Hatzis and Talianidis, 2002).

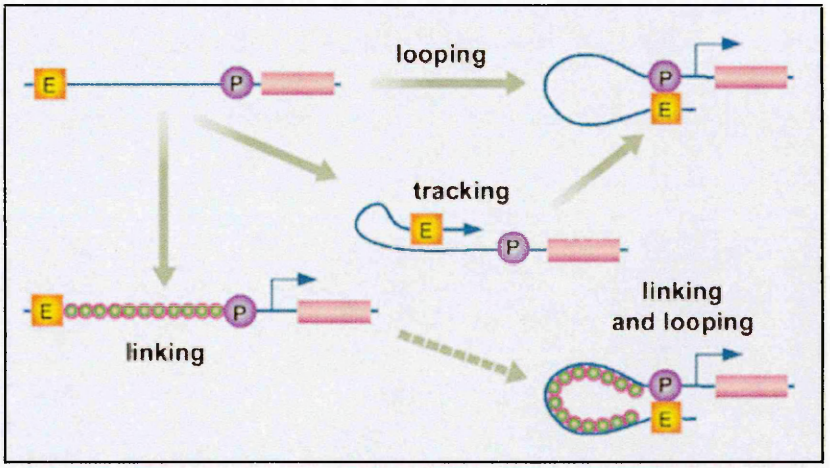

Burger et al. 2002 Nat. Genet.

Figure 1.1. Scheme of long range interaction mechanism between distal regulatory sequences.
The figure shows the main interaction models of distal regulatory elements like an enhancer (yellow box with E) and the promoter (violet ball with P) of a gene (pink box).

1.3. Transcriptional regulation by organization of the chromatin three-dimensional looped structure.

Despite these models have been speculated about for years, only recently the mechanism of long-range interaction has been partially solved. In fact thanks to two novel techniques, the RNA TRAP (Figure 1.2) and the 3C (Figure 1.3), the spatial proximity of distal genomic elements was shown for the first time for the β-globin locus in erythroid cells, implying the looping out of the 50 Kb long IVS (Carter et al., 2002; Tolhuis et al., 2002). Since then, other loci have been found to be folded into looped structures, in which distal enhancers are in close proximity to the promoters of the relevant genes (Eivazova and Aune, 2004; Liu and Garrard, 2005; Spilianakis and Flavell, 2004). However, the looping between distal regulatory regions is not a peculiarity of actively transcribed gene. In fact, other regulatory elements, such as silencers, insulators and boundary elements are also involved in the formation of loops that, in turn, might exert their function limiting (or favoring) the interaction of enhancers to their target gene promoters. For example, differentially methylated regions, known to be involved in the control of imprinted gene expression, seem to be important in setting up specific loop structures that might partition nearby, differentially expressed genes into distinct loops of active versus silent domains (see Figure 1.4A) (Murrell et al., 2004). So rather than a prerequisite of actively transcribed gene, looped higher order structures have to be thought of as general features of the genome organization (Marenduzzo et al., 2007), generated by the contribution of different regulatory sequences. This complex three-dimensional structure would reflect the transcriptional program of the cell, in which genes may result in an "on" or "off" state

according to their local retention within specific neighborhoods with active versus silent features (Dillon, 2006; Misteli, 2007), as schematized in the model shown in Figure 1.4B.

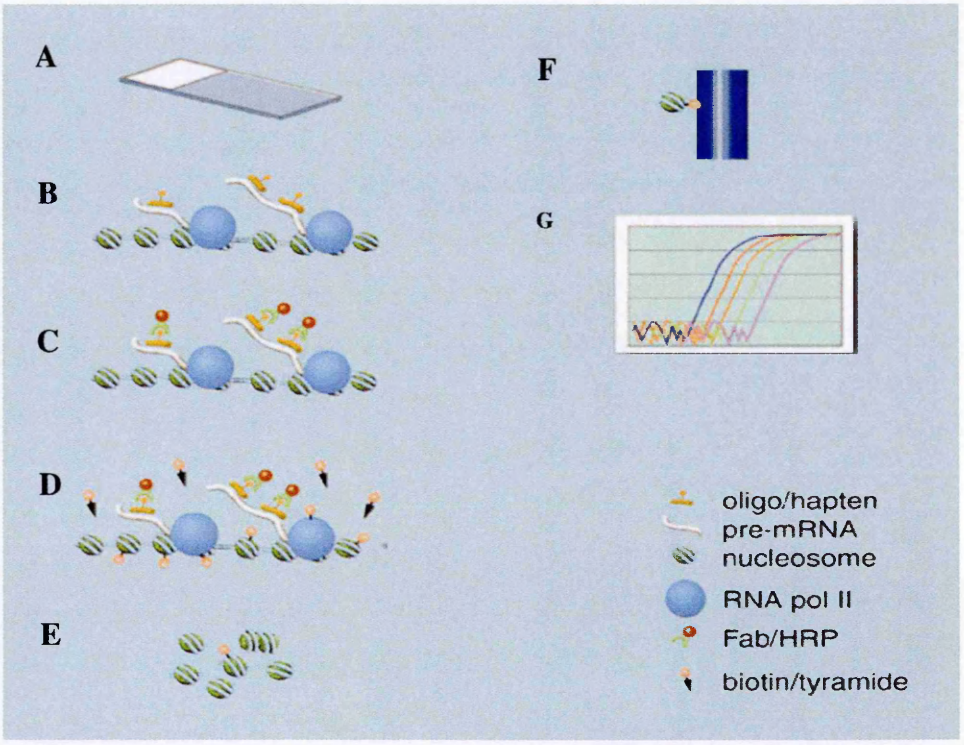

Carter, D. et al. 2002 Nat. Genet.

Figure 1.2. RNA TRAP.
In this technique (Carter et al., 2002) **(A)** nuclei are isolated and after formaldehyde fixation **(B)** hybridized with a digoxigenin-labeled oligonucleotide probe specific for a nascent, unprocessed mRNA. **(C)** Horseradish peroxidase–conjugated antibodies against digoxigenin are then used to localize horseradish peroxidase enzymatic activity to the site of transcription. **(D)** Biotin-tyramide is added to the sample and is activated by horseradish peroxidase, resulting in the covalent linkage of biotin to electron-rich moieties on proteins in the same region. **(E)** At this point, the cells are disrupted by sonication to fragment the chromatin and **(F)** biotin-conjugated chromatin fragments are isolated by affinity chromatography on a streptavidin column. **(G)** The enrichment of specific genomic sequences bound to the column can then be determined by quantitative PCR.

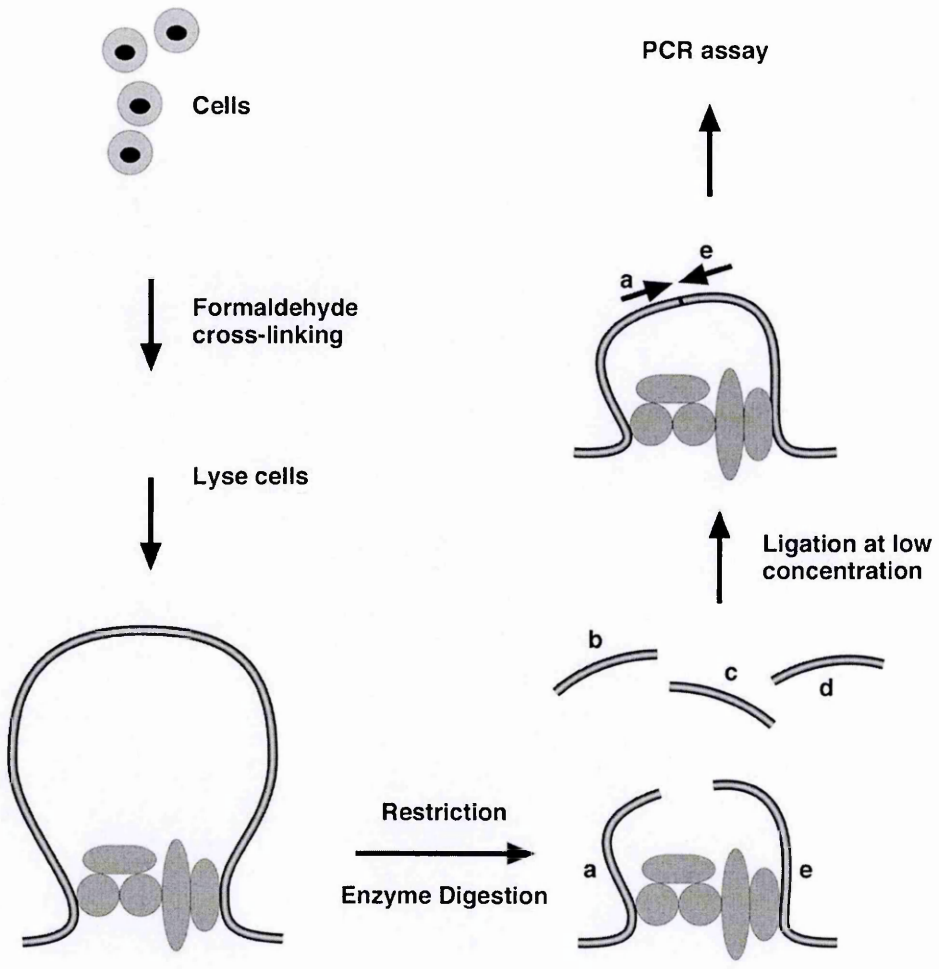

Liu, Z. et al. 2005 Mol. Cell Biol.

Figure 1.3. Chromosomal Conformation Capture (3C).
In this technique (Dekker et al., 2002) the cells are treated with formaldehyde to crosslink proteins to DNA or other nearby proteins and than lysated. The genomic DNA in cross-linked DNA-protein complex is then subjected to restriction enzyme cleavage. Digestion is followed by ligation at low DNA concentrations. Under these conditions, ligations between crosslinked DNA fragments is favored with respect to the ligation of random fragments because of their close spatial proximity. After ligation, the crosslinks are reversed and ligation products are detected and quantified by PCR.

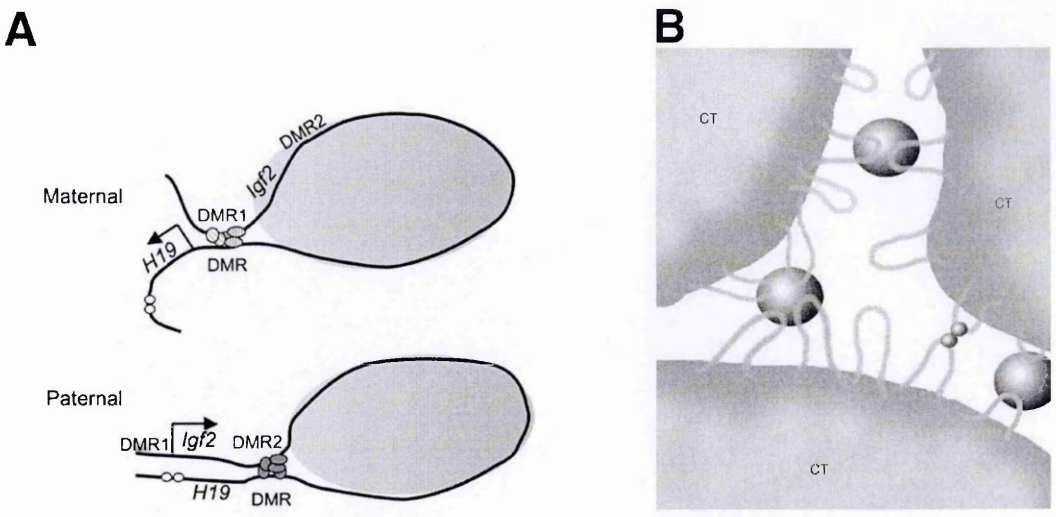

Murrel, A. et al. 2004 Nat. Genet.

Fraser, P. 2006 Curr. Opin. Genet. Dev.

Figure 1.4. Organization of the chromatin fiber in looped structures tether genes into distinct loops of active versus silent domains.
(**A**) Parent-specific interactions between distinct Differentialy Methylated Region (DMR) provide the transcriptional switch for Igf2. In the maternal allele the unmethylated H19 DMR interacts (through CTCF) with the Igf2 DMR1, segregating Igf2 in an inactive domain (shaded area). Conversely, in the paternal allele the interaction between DMR2 and DMR relocate Igf2 in an active chromatin domain as shown. (**B**) The complex three-dimensional structure organization reflects the transcriptional program of the cell. Chromatin fibers that contain genes are organized in different loops and are retained within specific neighborhoods with active (big spheres) or silent (small spheres) domains through the interaction with specific protein resulting in their "on" or "off" transcriptional state.

1.4. Nuclear compartmentalization.

The fact that in the nucleus there are no "membrane-enclosed" sub-compartments, such as the endoplasmic reticulum or the Golgi apparatus in the cytoplasm, led to the notion that functions and molecules were randomly distributed in this organelle. Instead, several lines of evidence showed the structurally and functionally complex organization of the eukaryotic cell nucleus interior. Most nuclear events do not occur ubiquitously throughout

the nucleoplasm, but are limited to specific and spatially defined sites (Lamond and Spector, 2003; Misteli, 2005). The nuclear volume contains morphological distinct higher-order chromatin domains, such as condensed heterochromatin, and a number of membraneless proteinaceous subcompartments, including the nucleolus, speckles, PML bodies, Cajal bodies, etc., that contain several nuclear components (Dellaire and Bazett-Jones, 2004; Handwerger and Gall, 2006). The physically distinct nature of each compartment not only contributes to the spatial partition of the nuclear volume, but also creates distinct functional subdomains within the nucleus. An additional layer of complexity is generated by the non-random spatial organization of the genome itself (Misteli, 2007). However, the functional significance of spatial positioning is not yet known and it represents one of the big challenges in modern molecular biology.

1.5. Chromosome territories and nuclear position.

The chromosomes contain the whole genome. In early microscopy studies it was readily observed that during mitosis all chromatin fibers of the chromosomes were tightly packaged yelding the typical "X" shape. However, once the cell enters interphase the chromosomes unfold and become entangled. A more organized view of the spatial organization of mammalian chromosomes in interphase came later from a study in Chinese Hamster cells. Small portions of the nucleus were irradiated with UV laser light and the damaged sites were visualized at the following metaphase. Instead of obtaining a signal scattered across several chromosomes, the authors observed the discrete labeling of only a few chromosomes (Figure 1.5) (Cremer et al., 1982), which suggested that chromatin was highly compartmentalized within the nucleus. However, direct visualization of

chromosomes in interphase nuclei was achieved only after the development of whole chromosome paint probes, in combination with FISH. This approach definitively showed that each chromosome occupied a spatially defined nuclear sub-volume, named CT (Figure 1.6). Further studies reported that these territories are non-randomly arranged within the nuclear space, but occupy preferential positions relative to the center of the nucleus (Parada and Misteli, 2002). Small chromosomes tend to occupy more central nuclear positions and bigger ones are positioned toward the nuclear periphery (Bolzer et al., 2005). Similar correlations have also been made for the nuclear radial positioning of chromosomes depending on their gene density. Experiments performed in lymphocytes showed that gene-poor chromosomes are more peripheral than gene-rich chromosomes, located in the nuclear interior (Boyle et al., 2001).

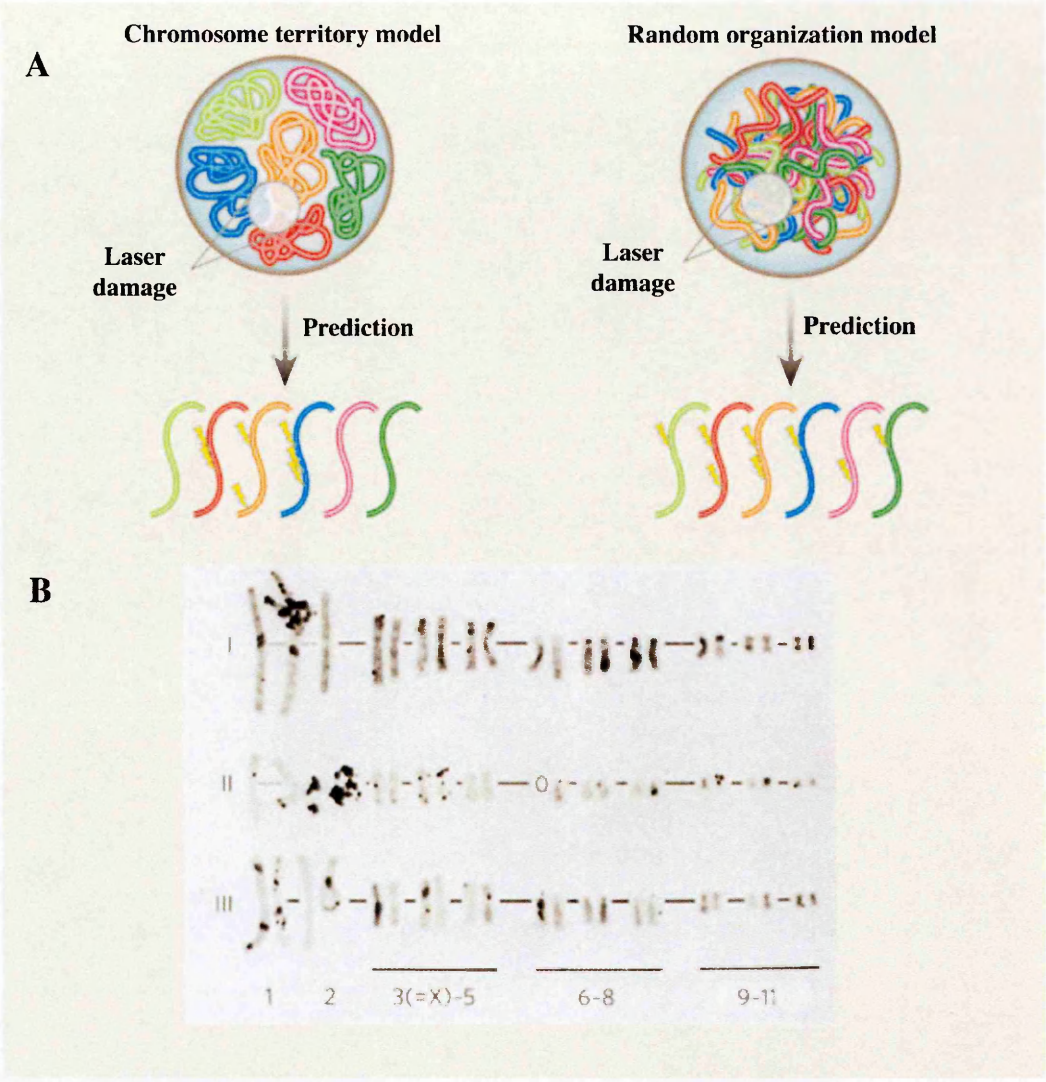

Meaburn, K.J. et al. 2007 Nature

Figure 1.5. Scheme of the experiment used to show the existence of chromosome territories.

(A) Thomas and Christoph Cremer used a microlaser approach to induce local genome damage. The prediction was that inflicting DNA damage within a small volume of the nucleus would yield different results, depending on how chromosomes were arranged. Occupation of distinct territories (A, left panel) will result in the fact that only a small subset of chromosomes will be affected by the localized damage, whereas if the chromatin fibers of each chromosome were randomly distributed throughout the nucleus (A, right panel), many chromosomes would be damaged. In panel **(B)** are shown metaphase chromosomes recovered after laser damage. Only a subset of the chromosomes was damaged, as indicated by the black grains of radioactivity, most prominently indicating that chromosomes are not randomly distributed, but occupy a defined position.

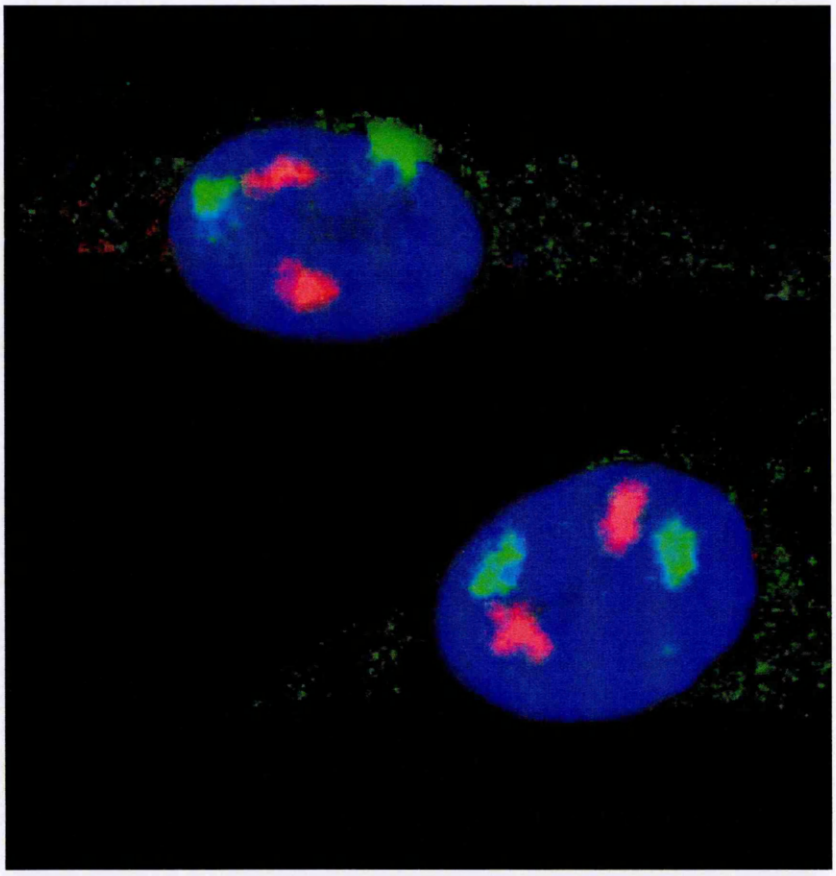

Oliver, B. and Misteli, T. 2005 Genome Byology

Figure 1.6. Chromosome detection using paint probes.
The figure shows liver cells stained with probes specific for Chromosome 12 (green) and chromosome 15 (red). DNA is stained in blue. Chromosomes are clearly organized in chromosome territories, occupying a discrete sub-volume in the nucleus.

1.5.1. Structural organization of the CT.

The discovery of the discrete territorial organization of chromosomes in the nucleus during interphase prompted to appreciate the importance of the genome nuclear compartmentalization for gene transcription. How are genes and regulatory regions organized within the CTs and how does this partition affect transcription? Because of their functional relevance, the structural organization of CTs has been carefully investigated using different approaches leading to different models.

1.5.2. CTs are inter-connected by a network of channels: the inter-chromatin domains.

Initial studies, aimed at mapping sites of transcription relative to the CT, showed that transcriptionally active genes are preferentially positioned outside to the CT area (Zirbel et al., 1993). Conversely, inactive genes were located inside the CTs (Zirbel et al., 1993). This finding was supported by other studies showing that specific chromatin segments, corresponding to coding sequences, were often located near the periphery of the CTs and non-coding sequences were found inside the CTs (Kurz et al., 1996). These lines of evidence led to a model in which the genome is organized in CT-IC shown in Figure 1.7. In this model active genes are located at the periphery of CTs, in a space called inter-chromosome domain, where they would be accessible to transcription and splicing factors (Cremer et al., 1993). Since inactive chromatin remains inside CTs the model hypothesized

that such positioning would reduce the accessibility of the genomic regulatory sequences to transcriptional machinery.

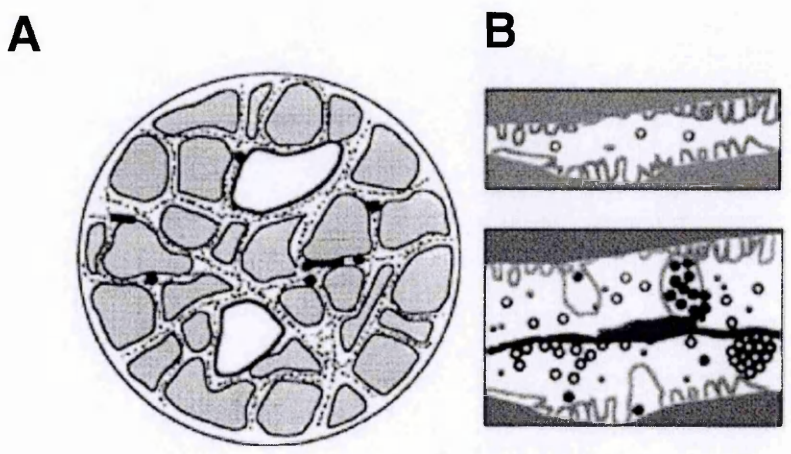

Figure 1.7. Scheme describing the CT- Inter-Chromosome (IC) model.
In (**A**) CTs are shown separated from each other by an inter-chromosomal space. (**B**) The enlargements shows that this space is rich in the transcriptional machinery and RNA processing factors (white and black circles respectively). The genes that are located in this space interact with the molecular components of the transcriptional machinery determining its active state wile the positioning of gene inside the CTs would prevent such interaction and is associated with their inactive state.

Other observations showed that some genes looped out of their CTs upon activation (Chambeyron et al., 2005; Volpi et al., 2000), whereas silenced genes occupied an internal position to the CT as in the case of "X" chromosome inactivation during ES cell differentiation (Chaumeil et al., 2006). However, it is now known that transcription is scattered all over the nucleus, including inside the CTs (Abranches et al., 1998; Branco and Pombo, 2006; Verschure et al., 1999). In light of these lines of evidence a model in which CTs are subdivided into "~ 1 megabase pairs (Mbp) chromatin domains", that constitute a

level of chromatin fiber organization above 30 nm was proposed (Figure 1.8) (Cremer and Cremer, 2001).

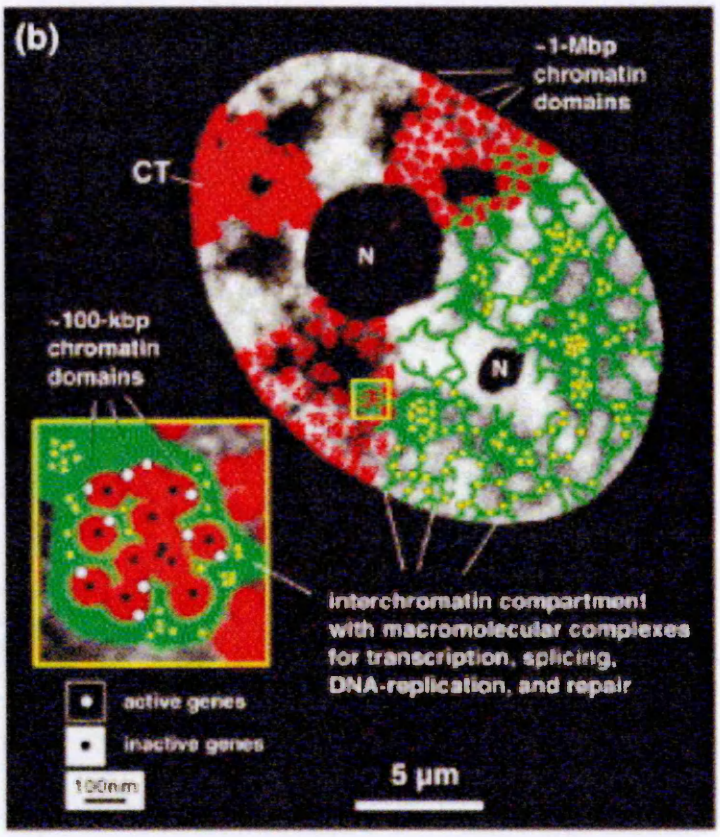

Figure 1.8. Scheme describing the "1 Mbp chromatin domains" composition of CT-IC model.
CTs are composed of "~1Mbp chromatin domains" which, in turn, are made by "~100 Kbp chromatin domains". The IC compartment (containing molecular complexes necessary for transcription) extends into CT contacting the surface of the "~100 Kbp chromatin domains" where active genes are located. Inactive genes are located inside the "~100 Kbp chromatin domains"

In this model the IC are represented as a network of gaps between chromatin domains, allowing proteins to reach the inner portion of CTs. So the IC part of the acronym CT-IC

indicated the inter-chromatin domain compartment (rather than inter-chromosome domain compartement). There are no experimental evidences showing how chromatin is organized in these 1Mbp domains. The model suggests that each 1Mbp domain is built as a rosette of small loops, termed "~100 kilobase pair (Kbp) chromatin domains", which are in contact with the inter-chromatin compartment (Cremer et al., 2006). An important aspect of the CT-IC model is that both CTs and also ICs exhibit little or no intermingling between them (Cremer et al., 2000).

1.5.3. CTs as a net of chromatin fibers: the lattice model.

Early electron microscopy studies on the structure of isolated chromatin fibers revealed structures with a 10 nm diameter, which were shown to further fold into 30 nm fibers (Dehghani et al., 2005). However, visualization of such structures in the interphase mammalian nucleus was hampered by the lack of contrast between chromatin and all of the proteins and RNA present in the nucleus. Different staining methods were developed to provide such contrast, but yet they did not provide a global high-resolution picture of chromosome organization (Dehghani et al., 2005). An improvement was obtained by using ESI, although the results obtained by ESI did not show the 1Mbp looped domains and, thus, did not support the CT-IC model (Dehghani et al., 2005). However, the ESI technique confirmed earlier electron microscopy studies showing that chromatin was mainly organized in 10 and 30 nm fibers without a particular structure organization (Dehghani et al., 2005). These evidences led to the proposal of yet another model to explain the CTs structure called "Lattice"(see Figure 1.9).

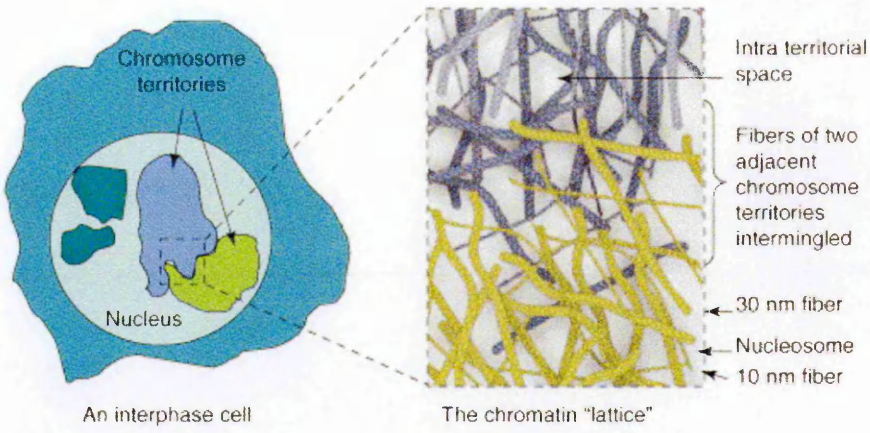

Figure 1.9. Scheme showing the Lattice model.
This model proposes that interphase chromosomes are organized as a network of 10nm and 30nm fibers. There are no large channels or gaps devoid of chromatin, but only the small spaces within the Lattice structure. This kind of organization would provide enough accessibility for macromolecules to interact with the genes. Moreover chromatin fibers from different CTs would intermingle at CT boundaries.

In this model each chromosome maintains its own (limited) space in the nuclear volume, but is organized in a relatively uniform net of chromatin fibers. This is in agreement with experiments showing that the nuclear volume is fully accessible to macromolecules moving by diffusion (Verschure et al., 2003). Importantly, the lattice model does not support the existence of channels, as postulated by CT-IC model, and suggests that folding of chromatin into a 30 nm fiber would be sufficient to regulate gene activity inside the of CTs. Recently, long-range interactions between regulatory elements on the same chromosome (or on different chromosomes) have been described, revealing extensive interactions across the genome (Fraser, 2006). The degree of genome flexibility and dynamics, suggested by the detection of inter-chromosomal associations, points to a higher degree of intermingling between CTs than initially thought. New insights on this issue

come form a recent publication (Branco and Pombo, 2006) in which the authors show a significant degree of intermingling between CTs corresponding to approximately 20% of the nuclear volume (Branco and Pombo, 2006).

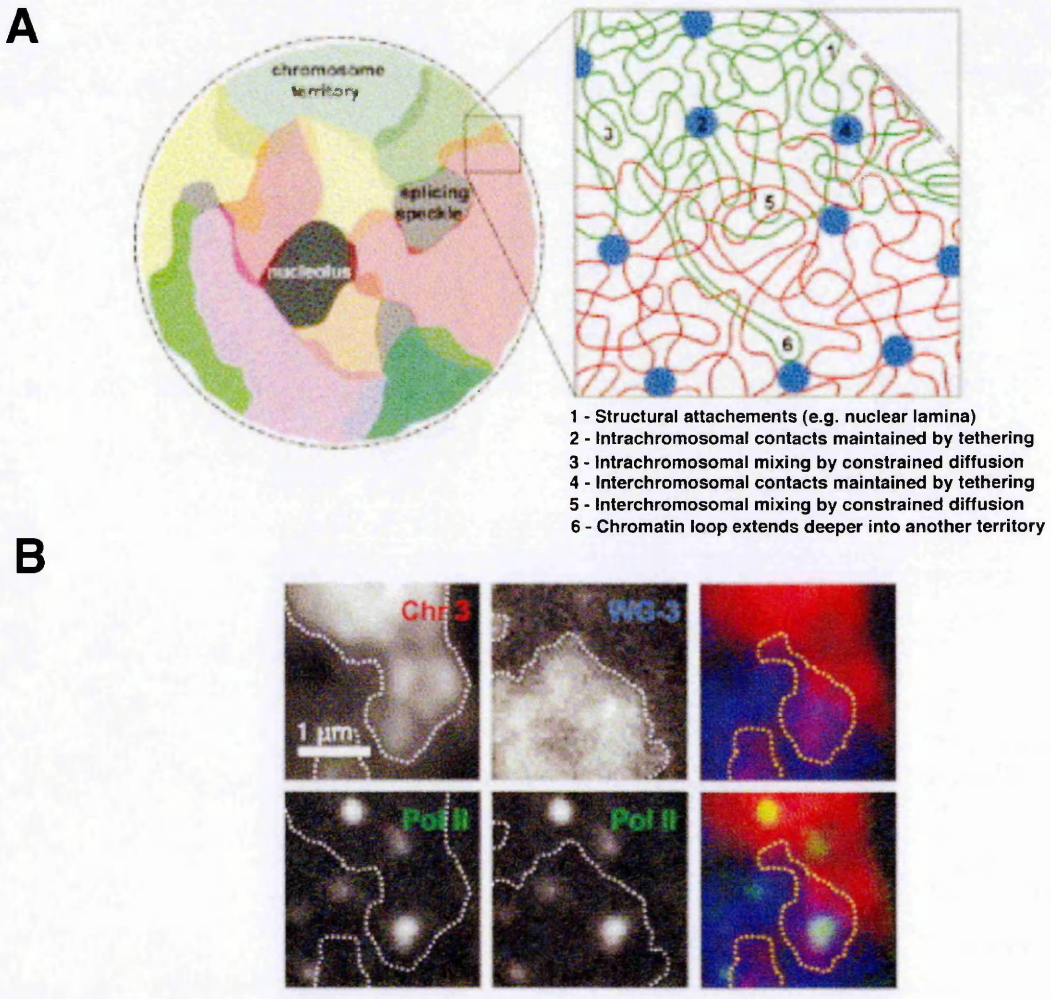

Figure 1.10. Scheme showing an updated version of the Lattice model.
This model incorporates recent findings about intra- and inter-chomosomal associations with respect to chromosome organization. **(A)** Functional interactions within the same CT and between different CTs might be mediated by RNAP-II or other nuclear components (e.g. nuclear lamins) which together with the physical properties of the chromatin fiber would influence nuclear distribution of CTs. **(B)** Functional interactions between CTs would be mediated by RNAP-II transcription factories. In fact simultaneous labeling of chromosome 3 (Chr3, red), of the whole genome except of chromosome 3 (WG-3, blue) and RNAP-II (Pol II green) reveals that intermingling areas contain RNAP-II foci.

This evidence suggested a new arrangement in interphase nuclei in which chromatin fibers branch out from CTs that maintain their spatial position and intermingle with fibers from other CTs that occupy a different nuclear space (see Figure 1.10). This view is consistent with different reports in which large chromatin loops were located far from their respective CT, as shown in Figure 1.11 (Chambeyron et al., 2005; Mahy et al., 2002; Volpi et al., 2000).

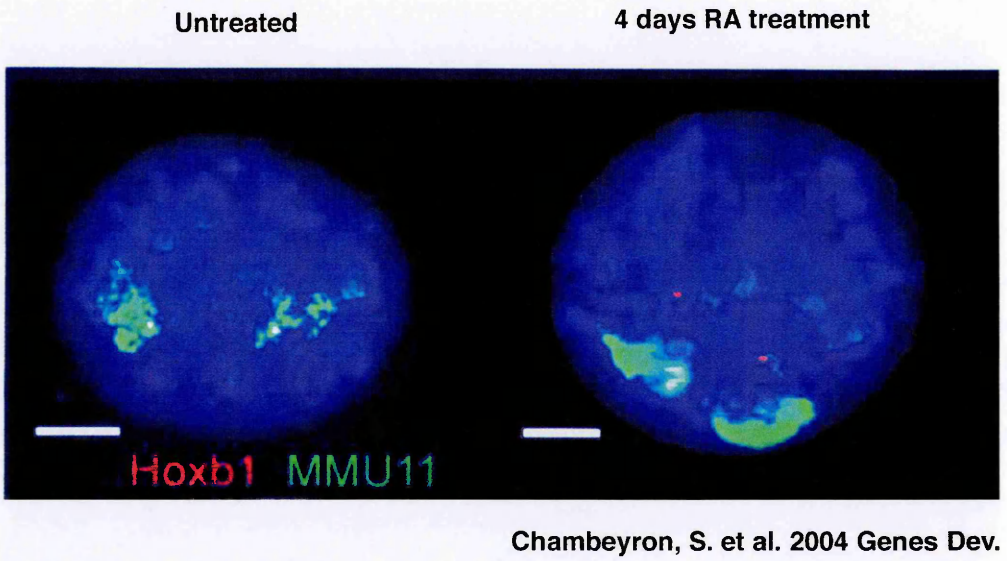

Figure 1.11. Changes in chromatin structure at HoxB locus after RA induced differentiation in ES cells.
In undifferentiated ES cells, the Hoxb1 gene (red staining) is condensed with the MMU11 CT (green staining). However, the HoxB1 gene is at the edge of the territory, poised to respond to transcriptional induction by RA. After 4 days of induction with RA, the chromatin fiber containing HoxB1 decondenses, and the gene is extruded from the CT. Nuclei are stained with DAPI (blue staining).

Moreover, inter-chromosome proximity may favor translocation events and, thus, the development of aberrant karyotypes observed in many cancers (Branco and Pombo, 2006).

1.6. Nuclear spatial organization of transcription: transcription factories.

Transcription, as well as other nuclear processes, is a compartmentalized event. Pulse labeling experiments of nascent RNA showed that transcription does not occur homogeneously throughout the nucleoplasm, but appears to be concentrated in distinct sub-nuclear foci (Figure 1.12) (Jackson et al., 1993; Wansink et al., 1993).

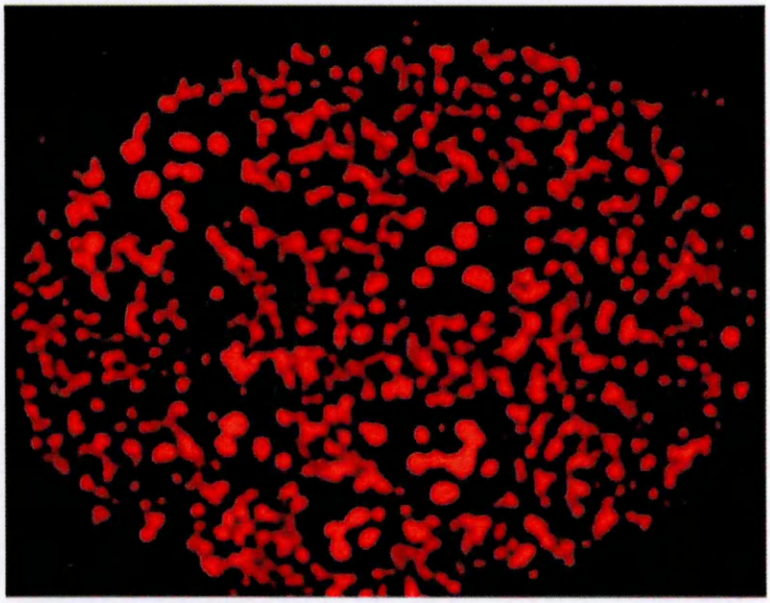

Figure 1.12. Transcription is concentrated in sub nuclear foci.
Experiment showing BrUTP incorporation in the nucleus. Cells are permeabilized and incubated with a physiological buffer containing BrUTP. BrUTP incorporation in to nascent RNAs can be detected with specific anti-BrUTP antibodies. The confocal image shows that nascent transcripts are clustered in defined spots (in red) indicating that transcription is restricted to distinct nuclear foci.

It was long assumed that this distribution represents elongating RNAP distributed along genes. It is now clear that these sites correspond to subnuclear transcription centers (Cook, 1999; Osborne et al., 2004). In normal cell lines active RNAP molecules are estimated to be approximately 65,000, whereas transcription sites are less that 10,000 (Cook, 1999). The limited number of transcription sites per nucleus as compared to the larger number of active RNAPs led to the prediction that more than one RNAP is present in each focus (Jackson et al., 1998) and, thus they were called "transcription factories". The consideration that most active genes are associated with only one active RNAP at any given time, allowed to predict that each transcription factory would simultaneously transcribe more than one gene (Cook, 1999). Recently this model was supported by experiments showing that genes as far as 40 Mb apart often co-localize in a shared factory when transcribed (Osborne et al., 2004).

1.6.1. Transcription factories: Importance of clustering transcription in a spatially defined fashion.

The ordered assembly of the transcription pre-initiation complex was originally proposed on the basis of the formation of active transcription complexes *in vitro* (Buratowski, 1994). It was observed that a stepwise addition of purified basal factors was required for promoter binding and transcriptional initiation from naked DNA templates. Moreover, the direct or indirect interaction of activators with constituents of the general transcriptional machinery, have long been observed to affect the rates of complex formation and, in turn, of transcription (Chi et al., 1995; Horikoshi et al., 1988; Lin and Green, 1991). The large number of additional co-factors observed to interact with the core machinery and required

to regulate activated transcription would render an initiation complex extremely large (Inostroza et al., 1992; Kim et al., 1994; Nakajima et al., 1997). Therefore considering the limited concentration of effectors in the nucleus and the structural problem exerted by the multiple levels of genome organization, it would appear that such an assembly is unlikely or, at least, inefficient. Thus the assembly of such complex on the large number of active promoters at any given time in the cell would not occur in a feasible time scale. Clustering of the transcription process in transcription factories, on the other hand, ensures that the local concentration of RNAPs and promoters is high, enabling them to interact efficiently (Cook, 1999). For example in HeLa cells the RNAP-II is present in a dispersed pool at a concentration of ~ 1 μM. However, the concentration of the sub-fraction locally associated with transcription factories is ~ 1000-fold higher (Cook, 2002). This would appear particularly useful in the case of functionally linked genes or of inducible arrayed genes, where the compartmentalization of transcription might facilitate the responsiveness to signaling cascades, leading to transcriptional activation, by obviating to the limited nuclear concentration of individual transcriptional components (Cook, 1999; Misteli, 2007).

1.6.2. Specialized transcription factories.

Many lines of evidence suggest that different transcription factories may specialize in the transcription of different groups of genes. Nucleoli represent a distinct nuclear compartment where the 45S rRNA genes and all the machinery essential for its transcription are localized and provide an important evidence in support of this issue (Martin and Pombo, 2003). Human loci encoding rRNA (contained in several tandem repeats) are located on chromosomes 13, 14, 15, 21 and 22, with each locus carrying a

NOR that promotes their association with nucleoli even when they are inactive (Sullivan et al., 2001). A typical nucleolar factory in HeLa cells contains ~ 500 RNAP-I molecules engaged around four templates and was shown to have a peculiar sub-compartmentalization with areas dedicated to storage, RNA synthesis and processing (Hozak et al., 1994; Jackson et al., 1998). Also RNAP-II and RNAP-III gather in transcription factories, although they are smaller than those found in nucleoli and are devoid of a particular substructural organization. Different approaches suggested that factories containing RNAP-II do not contain RNAP-III and, thus, localize to spatially distinct foci (Martin and Pombo, 2003; Pombo et al., 1999). Whether RNAP-II nucleoplasmic factories further specialize in the transcription of particular gene sets is yet not known. However, that different transcription factories contain distinct set of transcription factors and cofactors components, and thus create a specific transcriptional environment (Bartlett et al., 2006; Misteli, 2007) is a very attractive hypothesis. Recent results showing that some of the genes expressed in the erythroid lineage (Hbb-b1and Eraf) (distant 25 Mbp from each other) share the same RNAP-II factory corroborate such an idea (Osborne et al., 2004). Nevertheless, to date there are no evidences showing functional or structural specificity among RNAP-II transcription factories. Thus the question on the "specialization" between RNAP-II transcription factories is still open.

1.6.3. Active genes undergo on and off cycles of transcription depending of its association with a transcription factory.

From a functional standpoint, genes are assumed to be either active or inactive depending on the detection of a specific mRNA. In this simplistic view, an active gene is continuously transcribed when associated with the transcriptional machinery until a negative signal stops this process and determines its inactivation. However, a detailed RNA FISH analysis of several genes showed that many active genes are not continuously transcribed (Levsky et al., 2002; Ross et al., 1994). They seem to go through on/off transcription cycles, spending more time in the off state than in the on state (Osborne et al., 2004). The transcription of a given gene occurs in pulses of a certain frequency in each cell. This implies that, at any given time, different cells of the same population will have similar, but not identical, subsets of actively transcribed genes. Importantly, the actively transcribed genes localize to transcription factories, whereas temporarily non-transcribed gene do not (Osborne et al., 2004). These evidences suggest a model in which the "on" state correlate with factory occupancy and the "off" state with the relocation away from the factory, as shown in the Figure 1.13 (Osborne et al., 2004).

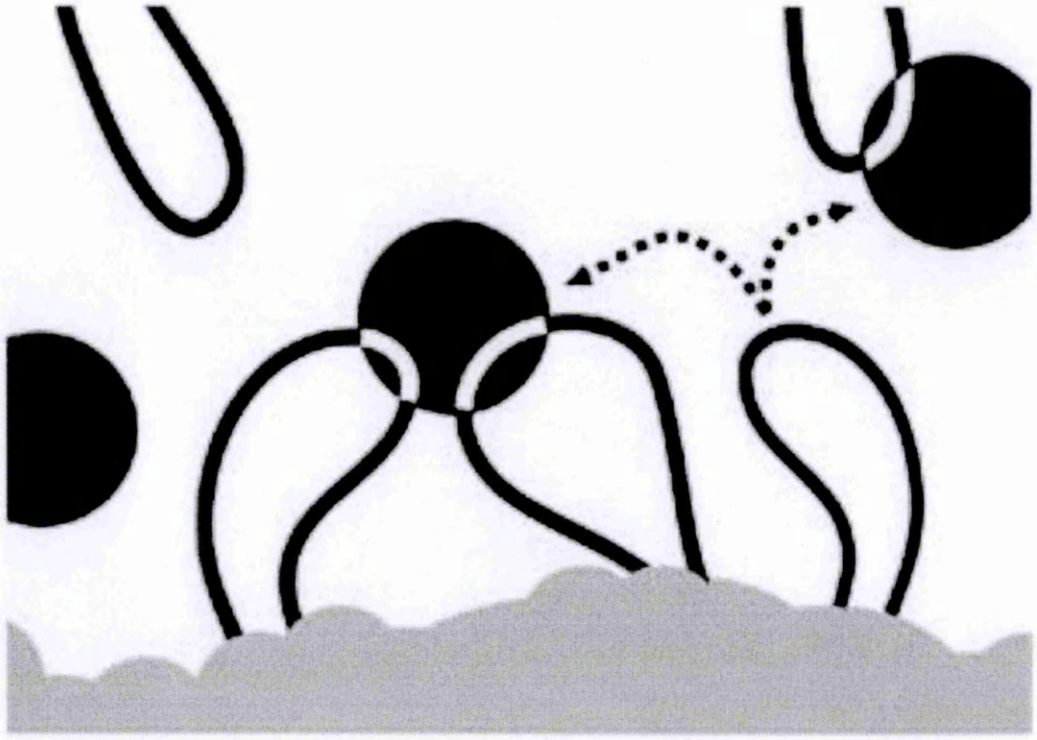

Figure 1.13. Model of dynamic associations of genes with transcription factories. In the scheme chromatin loops (black) are distinct from the rest of CT (gray). Transcribed genes (white portion of the loop) are recruited to transcription factories (black circles) whereas untranscribed genes are located away from the factory. The model suggests that gene transcription correlates with its recruitment in the transcription factory. The association with factories is dynamic and genes goes through waves of "on"/"off" phases. This implies that a given gene will be "more transcribed" than another when it will be associated with a transcription factory more frequently or for more time spans (Fraser, 2006).

1.7. RNAP-II activity and carboxy-terminal domain phosphorylation.

In eukaryotes RNAP-II enzyme transcribes protein-coding genes. The vast majority of studies aimed at elucidating the molecular mechanism of transcriptional regulation by RNAP-II focused on the early stages of the process, such as the formation of the PIC and initiation. However, the finding that many steps of RNA processing and maturation are

modulated through interactions with the RNAP-II transcriptional elongation complex generated a more focused attention on the relevance of this enzyme (Sims et al., 2004). RNAP-II exists in a hypo- or hyper-phosphorylated state (IIA and IIO respectively) (Dahmus, 1981). Phosphorylation targets the CTD of Rpb1, the largest subunit of RNAP-II. The CTD is made up of multiple tandem repeats (from 26 in yeast to 52 in Human) of the evolutionarily conserved heptapeptide sequence $Y_1S_2P_3T_4S_5P_6S_7$ (Corden, 1990) and is essential for life (Corden, 1990). The structural conservation of CTD in tandem repeats is also crucial as the insertion of an alanine residue between heptapeptide sequences is lethal in yeast, whereas the insertion of the same aminoacid between heptapeptide pairs can be tolerated (Stiller and Cook, 2004). Early experiments clarified that the hyperphosphorylated state of RNAP-II was associated with the enzyme activity (Christmann and Dahmus, 1981) and that it was distributed in discrete foci throughout the nucleus, where it colocalized with nascent transcripts (Cook, 1999; Iborra et al., 1996; Wansink et al., 1993). Biochemical experiments showed that the IIO form, differently from the IIA form, is highly insoluble as it is resistant to various extraction procedures (Kimura et al., 1999). Importantly, RNA run-on experiments performed with soluble extracts, containing the IIA form of the protein, and with the resulting pellets containing the IIO form showed that all the activity was essentially retained in the pellets, suggesting that the hyperphosphorylated form corresponds to the active RNAP-II (Kimura et al., 1999). "In vivo" FRAP experiments performed with a GFP tagged RNAP-II protein, confirmed with FLIP experiments, unexpectedly showed that the enzyme had a rapid diffusion kinetic (Kimura et al., 2002). On the other hand two kinetically distinct fractions were detected: one faster and the other slower corresponding to the free (IIA) and engaged (IIO) form of

RNAP-II respectively (Kimura et al., 2002). This implies that the enzyme engaged in the transcription factories (Cook, 1999) exchanges with the soluble fraction (Misteli, 2001a). Phosphorylation of the RNAP-II CTD occurs on serine 2 and serine 5 of the repeats, although the two different modifications are not equivalent (Sims et al., 2004). In particular, the form phosphorylated at serine 5 (CTD-S5p) corresponds to a poised form of RNAP II and is commonly found enriched on the promoter of active genes, while the form phosphorylated at serine 2 (CTD-S2p) corresponds to the elongating form of the enzyme and is typically associated with the internal portions of transcribed genes (Gomes et al., 2006; Komarnitsky et al., 2000; Sims et al., 2004). Transcription enters the initiation phase when RNAP-II is phosphorylated at CTD-S5p becoming poised, and a further phosphorylation event at CTD-S2p determines the transition to the elongation phase (Gomes et al., 2006; Komarnitsky et al., 2000; Sims et al., 2004).

1.8. Nuclear positioning of genes during transcriptional activation.

The association of genes with the nuclear periphery is generally considered a hallmark of silencing, as transcriptionally silent heterochromatin is preferentially located at the edges of the nucleus in many organisms (Misteli, 2004). Moreover, many evidences show the existence of a link between the nuclear radial position of a gene and the regulation of its expression. An example is the gene for the CFTR that is associated with peripheral heterochromatin in cells where the locus is silent (Zink et al., 2004). On the other hand, the locus dissociates from the periphery and moves towards the inner part of the nucleus in cell types where CFTR is expressed (Zink et al., 2004). Additional evidence for a role of peripheral localization of gene silencing comes from studies in which several

differentiation-specific genes were found near the nuclear periphery in their inactive state (Brown et al., 1999; Kim et al., 2004; Kosak et al., 2002; Skok et al., 2001). However, although many genes show preferential positioning relative to the nuclear center, this position may not be critical for function. In fact, in a cell population some genes can be found at virtually any position in the nucleus regardless its active or inactive state (Bartova et al., 2000; Kim et al., 2004; Kozubek et al., 2002; Roix et al., 2003). It seems more likely that the positioning observed for some loci is largely the consequence of the positioning of chromosomes to which the gene belongs. A complex relationship seems to exist between transcription and the position of genes within the CT and both the dissociation from territories, as well as the preferential positioning of genomic regions at the surface of CTs, has been suggested to contribute to proper gene function (Chambeyron and Bickmore, 2004b; Ragoczy et al., 2003). In human and mouse cells several loci in the genome have been characterized by FISH experiments, showing that they are extruded from their CTs and loop several micrometers away from the main body of chromosomes (Mahy et al., 2002; Volpi et al., 2000; Williams et al., 2002). Multiple lines of evidence suggest that there is a correlation between transcriptional activity and the location outside of CTs of some genes (Chambeyron and Bickmore, 2004b; Mahy et al., 2002). This is the case for the HoxB cluster in mouse ES cells, where the sequential activation of the genes of the cluster following RA treatment is associated with the gradual protrusion of the chromatin fiber that contains the locus from the CT as shown in Figure 1.11 (Chambeyron and Bickmore, 2004a). Although the role of positioning in gene function is still unclear, it is tempting to speculate that the relocation of genes away from CT may be required to move it toward a factory, as proposed by (Osborne et al., 2004) (Figure 1.13).

1.9. What are the molecular ties that determine nuclear genome organization?

The complex spatial organization of the nucleus has given rise to the provocative concept that a defined structure, in the form of a karyoskeleton or matrix, may contribute to spatially organize the multitude of nuclear compartments (Nickerson, 2001; Pederson, 2000). Many protein molecules have been found implicated in affecting nuclear architecture, but the definition of such a nuclear scaffold remains elusive. It has been reported that the over-expression of the non-chromosomal protein EAST in Drosophila it causes alterations in the nuclear architecture, determining the expansion of the extrachromosomal space and of the whole nucleus (Wasser and Chia, 2000). This suggested that the protein might be part of a putative nuclear skeleton, or at least to be involved in the control of its expansion. In human thymocytes the protein SATB1 appears to form a cage-like network of proteinaceous filaments to which genes can be attached (Cai et al., 2003). Obvious candidates as scaffold components are the well-characterized lamin proteins. This protein family is known to form a structural meshwork underlying the nuclear envelope, referred to as the nuclear lamina (Goldman et al., 2002). Recent observations strongly suggest that lamin A, B and C are not selectively restricted to the nuclear periphery, but protrude also toward the nuclear interior and are functionally important for transcription and replication processes (Goldman et al., 2002; Kumaran et al., 2002). However, lamin A and C do not seem essential for the formation of the splicing factor compartment and other nuclear bodies (Vecerova et al., 2004) and to date it is unclear what it should be their contribution to the inner nuclear structures. A further

prominent candidate as a structural component of the karyoskeleton is actin. Filamentous actin has been shown to be present in the nucleus (McDonald et al., 2006) and, moreover, many evidences support its fundamental role in transcription (de Lanerolle et al., 2005). Transcription levels are affected by the use of reagents that block actin filament formation, albeit no global reorganization of transcription sites has been observed (McDonald et al., 2006). The difficulties in defining a static nuclear skeleton and the highly dynamic nature of the nuclear architecture has lead to suggest that the molecular constituents of the nucleus possess "self organizing" capabilities (Cook, 2002; Misteli, 2001b). The model predicts that the morphological appearance and spatial organization of a self-organizing system is a reflection of the sum of all ongoing functions (Cook, 2002; Misteli, 2001b). At the same time the resulting structural features support and enhance ongoing activities in a self-reinforcing manner. In favor of this model are evidences showing that inhibition of a specific nuclear process (e.g. transcription) abolishes looping and determines a general de-condensation of the genome (Marenduzzo et al., 2007). In this context the clustering of active RNAPs molecules in transcription factories would directly contribute to genome organization, suggesting that RNAPs and transcription factors may act as molecular ties (Cook, 2002).

1.10. The acto-myosin system: new players in transcriptional regulation.

One of the most intriguing developments in the field of gene regulation is that structural proteins, mainly cytoplasmic, such as actin and myosins, play an important role in

transcription (de Lanerolle et al., 2005). Early studies showed evidences that actin was implicated in transcription (Egly et al., 1984; Scheer et al., 1984). However, biochemical observations supporting this idea encountered strong criticism, mainly because nuclear preparations were thought to be contaminaited by cytoplasmic actin. Moreover the use of a classic tool, like phalloidin staining, to detect actin filaments in the nuclear compartment failed to reveal such a structure, although it was clearly visible in the cytoplasm. Several recent publications show that actin is found associated with all three RNAPs and that it modulates their activity (Hu et al., 2004; Philimonenko et al., 2004). Moreover, other proteins, like NMI, Myosin VI and N-WASP, have been reported to be present in the nucleus and to modulate transcriptional activity (Philimonenko et al., 2004; Vreugde et al., 2006; Wu et al., 2006). These findings prompted the speculation that an acto-myosin mechanism is implied in transcriptional regulation. However, the *in vivo* role of actin and myosins in gene expression is still largely unclear.

1.10.1. Nuclear actin.

Important clues concerning the role of nuclear actin came from the identification of its interactors. Many Swi/Snf-like complexes and histone-modifying factors have been found associated with actin in different organisms (Bettinger et al., 2004; Olave et al., 2002). These results argue in favor of a functional link between actin and the regulation of chromatin structure (Bettinger et al., 2004; Olave et al., 2002). As mentioned above, actin is associated with all three RNAPs and anti actin antibodies reduce the activity of RNAPs *in vivo* as well as *in vitro* (Philimonenko et al., 2004), suggesting that the role of actin in the three different systems would be similar. RNAP-I abortive transcription-initiation

assays have shown that antibodies against actin do not affect the incorporation of the first nucleotide by the enzyme. However, they do inhibit the subsequent elongation step, since further incorporation of nucleotides is abolished (Philimonenko et al., 2004). Actin also associates with hnRNPs (Kukalev et al., 2005), a family of proteins involved in pre-mRNA processing and in the transport, localization and stability of mRNA (Dreyfuss et al., 2002). This suggests that actin is involved in a process that occurs shortly after transcription initiation. However, an alternative interpretation of the results would suggest that the steric hindrance of the actin-bound antibodies could affect only the recruitment of a subset of specific cofactors, required in defined steps of transcription. This would imply that actin might have a different role in multiple steps of the transcription process. In fact actin is associated with both active and inactive RNAP-I, unlike NMI that is associated only with the complex containing the active enzyme (see next paragraph). A feasible hypothesis might be that the fundamental function of actin in transcription is to mediate dynamic protein-protein interactions and to act as an allosteric factor in the remodeling of large multimolecular complexes, such as the transcriptional apparatus.

1.10.2. Nuclear Myosin I.

NMI was the first myosin found in the nucleus (Pestic-Dragovich et al., 2000). This, together with the finding of nuclear actin, suggested that the two proteins may functions in a concerted manner, an idea strengthened by the fact that both proteins have been found in mammalian nucleoli (Andersen et al., 2005; Andersen et al., 2002; Fomproix and Percipalle, 2004). ChIP experiments showed that NMI and actin are associated to actively transcribing ribosomal genes (Philimonenko et al., 2004). Importantly, while actin is

associated with both active and inactive RNAP-I, NMI binds to the enzyme containing transcriptional machinery through the TIF-IA (Philimonenko et al., 2004). This implies that actin and NMI are not recruited to the transcriptional machinery at the same time, suggesting that they may have specific roles in different steps of the RNAP-I dependent of transcription. However, *in vivo* inhibition of RNAP-I transcription by siRNA NMI protein depletion, as well as *in vitro* by NMI antibodies, clearly supports a role for NMI in RNAP-I transcription (Philimonenko et al., 2004). An intriguing question is whether NMI also plays a role in regulating other RNAPs, since the activity of all RNAPs seems to be inhibited by NMI blocking antibodies (Philimonenko et al., 2004). A recent publication showed that NMI is implicated in the formation of the initial phosphodiester bond by RNAP-II (Hofmann et al., 2006), supporting the idea of its possible involvement also in the regulation of RNAP-II activity.

1.10.3. Nuclear Myosin VI.

Myosin VI is a ubiquitously expressed non-conventional myosin (Buss et al., 2004) found in the Golgi complex, in membrane ruffles at the cell's leading edge, in clathrin-coated vesicles and in a cytosolic pool (Buss et al., 2001; Buss et al., 1998). Within the myosin superfamily, Myosin VI motor properties are unique, since the direction of its movement is towards the pointed (minus) end of actin filaments, opposite to all other characterized myosins (Wells et al., 1999). Moreover at high load and low ATP concentrations Myosin VI stops moving along the actin filament and acts as an anchor, tethering tail-associated proteins to actin (Altman et al., 2004). In mouse and Human Myosin VI plays a role in different biological processes such as embryonic development and spermatogenesis

(Friedman et al., 1999), while several mutations are associated with hereditary hearing loss and hypertrophic cardiomyopathy (Buss et al., 2004). In addition, Myosin VI regulates cell migration and its high expression levels correlate with the disseminating potential of tumor cells (Yoshida et al., 2004). Recently, new evidences show that Myosin VI is also present inside the nucleus of a number of cell lines, where it displays a speckled distribution and colocalizes with nascent transcripts and with RNAP-II (Vreugde et al., 2006). Moreover, ChIP experiments show that the molecule is recruited to promoters and intragenic regions of actively transcribed genes. Finally, the *in vivo* depletion of Myosin VI protein and the inhibition of transcription with antibodies against Myosin VI in *in vitro* assays show that it plays a role in RNAP-II gene transcription (Vreugde et al., 2006). Nevertheless there are no data on its mechanism of action. A reasonable idea would be that Myosin VI takes part in the process of elongation, since it is associated with intragenic regions of different analyzed genes (Vreugde et al., 2006).

1.11. Transcription factors confer target specificity to gene expression and define transcription programs.

The evolution of complex cellular and developmental processes depends on the maintenance and regulation of large amounts of genetic information. Animal cells normally transcribe thousand of genes and they evolved tightly regulated transcription programs in order to direct spatial and temporal patterns of gene expression in response to metabolic requirements. The need to discriminate between different genes requires specialized adapters that selectively target genes with the transcriptional apparatus. Transcription factors are the molecules dedicated to control and maintain this essential

biological process. They are DNA-binding proteins that recognize specific sequences in the regulatory regions of the genes, such as promoters and/or the enhancers. Transcription factors have an activation domain (through which interact with RNA polymerase and other transcription factors) and a DNA-binding domain. The presence of different DNA binding motifs has led to a classification of transcription factor according to the structure of such motifs, the most common of which are:

a) Zinc-Finger motif, composed of amino-acids that bind a zinc ion (Zn2+) forming a protruding loop, like a finger. Several loops, repeated in tandem, denote α-helical structures that bind the major groove of DNA. Sp1 and the steroid nuclear receptors belong to this class of transcription factors.

b) Leucine-Zipper motif, in which leucine residues are repeated every seven amino acids to form an amphipathic α-helix, allowing the interaction with other leucine-zipper-containing factors to form homo and/or heterodimers. The Jun and Fos families of transcription factors belong to this class.

c) HLH motif is a 40-50 amino acid long sequence forming two amphipathic α-helices separated by a linker region (loop) of variable length. α-helices can bind to DNA and also dimerize with other factors. MyoD and Myc belong to this class.

d) Homeodomain motif, which shows a correlation with the HTH motif of prokaryotic repressors, and forms three α-helices. Several homeodomain (or homeobox)-containing transcription factors are involved in the development of most eukaryotes. Prep1, Pbx and Hox proteins belong to this class.

Regulation of gene expression is the result of the mixing and matching of different types of transcriptional activators and repressors in a coordinated fashion. Moreover, it is now

evident that some transcription factors may also have time-, developmental- and tissue-restricted expression (Lemon and Tjian, 2000). This increases the finesse of tuning transcriptional regulation, considering the broad diversity of molecular signals that must be integrated by the transcriptional apparatus.

1.12. The transcription factor Prep1.

Prep1 belongs to the MEINOX family of a homeodomain-containing transcription factors. Experimental data show that it heterodimerizes with Pbx family proteins in a DNA-independent manner, that such complexs are translocated to the nucleus where they bind DNA (through the homeodomains of Prep1 and its Pbx partner) and act as transcriptional regulators (Berthelsen et al., 1999). Prep1 is ubiquitously expressed in adult mouse tissues (although with great variability) and in embryos where it plays and important role during development (Berthelsen et al., 1998; Ferretti et al., 2006). Pbx is known to interact with Hox family proteins. Prep1 forms trimeric complexes with Pbx Hox proteins and enhances their transcriptional activity. EMSA show that the trimeric complex Prep1-Pbx-Hox binds on the ARE of the HoxB1 (b1-ARE) gene (Berthelsen et al., 1998), while transient transfections, using a b1-ARE-driven reporter plasmid, have shown a Prep1 mediated up regulation of transcription (Berthelsen et al., 1998) in line with other *in vivo* findings (Ferretti et al., 2005; Ferretti et al., 2000; Jacobs et al., 1999; Ryoo et al., 1999). Besides its role in development and differentiation, the role of Prep1 in apoptosis was also recently investigated. Prep1 knock-down in zebrafish (by using a morpholino antisense oligonucleotides strategy) showed an associated massive apoptosis in the central nervous system during early development (Deflorian et al., 2004). Analogous experiments were

performed in our laboratory where, a Prep1 hypomorphic (Prep1$^{i/i}$) mouse model was developed (Ferretti et al., 2006). Embryos from Prep1$^{i/i}$ mice express low (up to 10%) residual levels of Prep1 mRNA and protein. Moreover Prep1$^{i/i}$ embryos show several defects in angiogenesis, hematopoiesis and eyes development. The role of Prep1 in apoptosis has been investigated using MEF obtained from WT and Prep1$^{i/i}$ embryos at E14.5. The results show that Prep1$^{i/i}$ MEF were spontaneously more prone to apoptosis and more sensitive to genotoxic stimuli. Very interestingly, the study found that Bcl-X and p53 genes were direct transcriptional targets of Prep1, indicating that Prep1 controls the apoptotic response by directly regulating the expression of these genes (Micali et al., In preparation).

1.13. uPA and the plasminogen activation system.

Extra-cellular targeted proteolysis is essential for cell migration and tissue remodeling. One major system involved in these processes is the activation of plasminogen. The conversion of plasminogen to the active proteolitic form (plasmin) leads to the degradation of extracellular matrix molecules, like fibronectin and laminin, and this event is a crucial step in a number of biological processes, both in physiological (e.g. fibrinolysis, embryogenesis etc.) as well as in pathological conditions (e.g. tumor metastasis formation, angiogenesis etc.) (Crippa, 2007). Mammalian cells contain two types of Plasminogen Activators, the urokinase type (uPA) and the tissue type (tPA), of which uPA is primary involved in extracellular matrix degradation (Andreasen et al., 1997; Danø et al., 1999).

1.13.1. uPA expression and cancer.

Increased expression of uPA has been reported in various malignancies, including prostate (Gaylis et al., 1989; Van Veldhuizen et al., 1996), breast (Look and Foekens, 1999), colon (Pyke et al., 1991) and lung (Skriver et al., 1984) cancers. These represent the most common type of malignancies in many Western industrialized countries and have a high level of incidence. In many cases, its increased expression seems to be associated with an increased metastatic potential and poor survival (Hsu et al., 1995; Miyake et al., 1999a; Miyake et al., 1999b; Yang et al., 2000). To be able to invade surrounding tissues and to metastasize, cancer cells must degrade the extra cellular matrix components, a process in which uPA plays a major role.

1.13.2. Transcriptional regulation of the uPA gene.

Transcription of the uPA gene is modulated by a number of chemical and physical stimuli (Besser et al., 1996; Cirillo et al., 1999). Such stimuli have been shown to act (at least in part) through the enhancer element, located approximately 2 kb from the start of transcription (Verde et al., 1988) (Figure 1.14). However, recent findings in our laboratory showed that a GC-/GA-rich region, associated with the proximal promoter (Figure 1.14), plays an important role in the transcriptional regulation of uPA through the binding of Sp1 and that such binding may occurs when the transcription factor is phosphorylated through the JNK pathway (Benasciutti et al., 2004; Ibanez-Tallon et al., 2002; Milanini et al., 1998; Milanini-Mongiat et al., 2002).

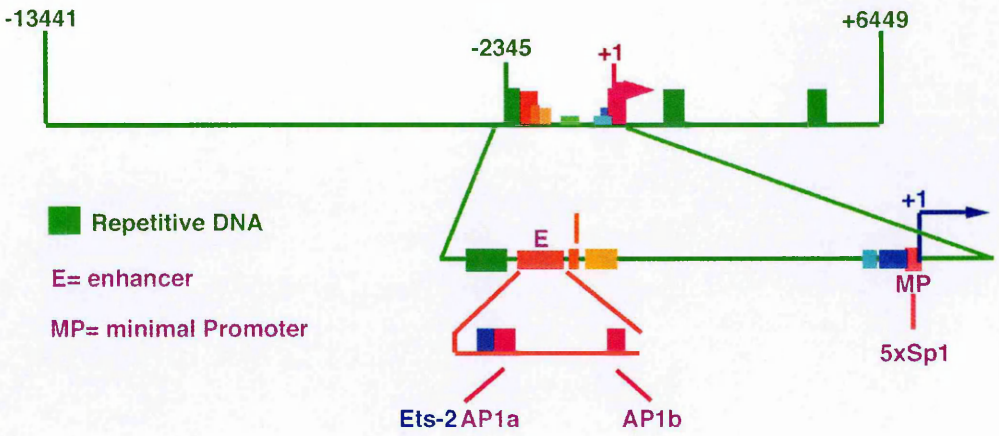

Figure 1.14. Scheme of uPA gene.
The scheme reports the locations of the enhancer and minimal promoter of uPA gene. The enhancer contains two AP-1 binding sites and the minimal promoter five Sp1 binding sites, referred to in the text, as GC-/CA-rich region.

1.13.3. Phorbol esters induce uPA in HepG2 cells.

TPA is a potent stimulator of cell migration, cell scattering and a general enhancement of the metabolic activity levels in many cultured cell lines. TPA activates the phospholipid dependent PKC pathway (Cirillo et al., 1999), determining the upregulation of Jun and Fos protein family members which, in turn, lead to the targeted activation of AP-1 regulatory elements. The induction of uPA transcription by TPA has been well established by a number of studies (Cirillo et al., 1999; Ibanez-Tallon et al., 1999) and this regulation

targets the enhancer of uPA, containing two AP1 binding sites (Rorth et al., 1990). Previous results in HepG2 cells, where the uPA gene is not expressed in basal conditions, showed that TPA treatment for 1-3 hours induces uPA transcription (Ibanez-Tallon et al., 1999). Transcriptional activation is accompanied by an increase of the DNaseI hypersensitivity and accessibility of the regulatory region to restriction nucleases (Ibanez-Tallon et al., 1999). However, the presence of a modest DNaseI hypersensitivity and restriction enzyme accessibility also before induction suggests a limited, if any, chromatin remodeling event following TPA treatment (Ibanez-Tallon et al., 1999). This led to speculate that the gene might be in a poised state and that other changes in terms of regulation of the uPA gene contribute to its transcriptional induction.

AIM OF THE WORK

The aim of my thesis was to study the interaction between the enhancer and the minimal promoter of the uPA gene through the looping of the IVS in PC3 cells where the gene is constitutively expressed. In order to address this issue I set up a technical approach in which MNase digestion of the cross-linked chromatin was coupled to ChIP. This allowed me to precisely map the interacting DNA sequences and characterize their proteins content. In order to gain insights on the dynamics of such interaction I applied this approach to another cell system (HepG2 cells), where uPA gene transcription can be induced by the treatment with phorbol esters. The finding that in uninduced HepG2 cells the uPA gene is associated with a poised RNAP-II form, prompted me to ask if the transcriptionally inactive gene was hosted by distinct nuclear sub-structures similar to, but distinct from, transcription factories, known to be active sites of transcription. Sites of nascent RNA synthesis are associated with non-conventional Myosin VI. This observation led to experiments aimed at clarifying its implication in transcription and to elucidate its effects on the activity of RNAP-II. Finally I studied the mechanism of Myosin VI recruitment on specific target genes through the interaction with the transcription factor Prep1. In summary this thesis provides some new clues on the three-dimensional organization of cis-regulatory regions and how it affects transcriptional regulation. Moreover, it gives a new outlook on the link between transcription and nuclear compartmentalization, supporting the importance of nuclear architecture and structural proteins in regulating gene expression.

MATERIAL AND METHODS

2.1. Cells culture and treatments.

PC3, HepG2, NT2-D1 and MEF cells were grown at 37 °C under a 5% CO_2 atmosphere in DMEM (Gibco), containing 10% (v/v) FBS (Gibco), 0.2 mg/ml streptomycin (Gibco), 20 U/ml penicillin (Gibco,), 2mM glutamine (Gibco) and 1mM sodium pyruvate (Gibco).

2.1.1. Treatment of PC3 cells with α-amanitin.

α-amanitin (Sigma) was dissolved in water and were added to the culture medium to the final concentration of 10mg/ml for 24 hours, as prevously described (Casse et al., 1999). In ChIP experiments on PC3 cells (Figures 3.10 B,C and 3.13 C) the concentration of α-amanitin was 10 μg/ml for 24 hours.

2.1.2. Treatment of the HepG2 cells with TPA.

Treatment of HepG2 cells with TPA (Sigma) was performed on starved cells (0.5% (v/v) FBS for two hours) by adding new medium containing 100ng/ml TPA and 10% (v/v) of FBS for 15 minutes to three hours.

2.1.3. Treatment of the NT2-D1 cells with RA and TSA.

Treatment of NT2-D1 cells with RA (Gibco) was performed by adding RA directly to the medium at a final concentration of 3μg/ml and incubating cells for 48 hours.

Treatment of NT2-D1 cells with RA + TSA was performed by adding RA directly to the medium to a final concentration of 3μg/ml and after incubating cells for 42 hours adding TSA directly to the medium to a final concentration of 10 ng/ml and incubating for 6 hours more.

2.2. RNA detection.

2.2.1. RNA extraction and reverse transcription.

Total RNA was extracted with an RNeasy mini kit (Qiagen), quantitated by spectrophotometry (Nanodrop). 5 µg of total RNA were reverse-transcribed using a SuperScript™ First-Strand kit using random primers (Invitrogen) according to the manufacturer's instructions.

2.2.2. RNA quantization by real-time PCR.

For qRT-PCR, 5 ng of reverse-transcribed RNA were amplified and the amplification products detected using the TaqMan gene expression assay (Hs00170182_m1, Hs00181192_m1, Hs00158272_m1, and Hs00355782_m1, Applied Biosystems, Foster City,CA94404 USA) primers and probes specific for uPA, LDLR, ITGB4BP, and CDKN1A, in an ABI PRISM 7900HT Sequence Detection System. 18S rRNA levels were used to normalize the results (TaqMan gene expression assay 4319413E). Target gene expression was normalized to the values obtained with the pIRES-EGFP vector

2.2.3. RNA detection by non-quantitative PCR.

To check for the presence of RNA in the enhancer and coding region of the uPA gene (Figure 3.12) total RNA was extracted from untreated cells, reverse transcribed as above and 5, 10 and 20 ng of reverse transcribed products were amplified with primers corresponding to different fragments of the enhancer and coding region of uPA. PCR reactions were performed as follows: First denaturation 1: 95° C for 3 minutes; second denaturation: 95° C, 1 minute; annealing step (see Table 1 for temperatures of the primer sets), 1 minute; extension: 72° C, 1 minute; final extension: 72° C, 3 minutes. The second denaturation, annealing and extension steps were repeated for 40 cycles. Primer sequences, location with respect to the uPA sequence (Verde et al., 1988) and annealing temperatures used for each primer set are reported in Table 1. PCR products were analyzed on 2% agarose gels in 1X TAE buffer.

2.3. Cells cross-linking and chromatin preparation.

Cells were cross-linked with 1% formaldehyde (Sigma) for 10 minutes and chromatin prepared essentially as described in (Orlando et al., 1997) by using 10 sonication cycles (35 seconds at 60-70 Watt, in an Ultrasonic Processor XL Sonicator (Miosonix), followed by a 2 minutes rest on ice). Cross-linked chromatin-containing fractions were pooled and stored at –80° C.

2.4. Restriction enzyme digestion of cross-linked chromatin.

Cross-linked chromatin fractions were first dialyzed against TE buffer (10 mM EDTA, 50 mM Tris-HCl, pH 8) and then diluted 1:10 in water. 10 μg of dyalized chromatin samples were digested with 100 U of the restriction enzymes MseI and DraI (Roche) overnight at 37°C. Following digestion, the material was treated with RNase A (50 μg/ml) for 30 minutes at 37° C and by proteinase K (500 μg/ml) in 0.5% (w/v) SDS at the same temperature overnight. Formaldehyde cross-links were reverted by heating the samples at 65° C for 5 hours and the DNA was purified by phenol extraction. For the experiments shown in Figure 3.2 the DNA was resuspended in distilled water, quantitated at the spectrophotometer (Nanodrop) (OD_{A260}) and equal amounts (100 ng or 10 ng) of material for each time point were used as template in PCR reactions.

2.5. Micrococcal nuclease digestion of cross-linked chromatin.

Cross-linked chromatin fractions were first dialyzed against 25mM KCl, 50 mM Tris-HCl, pH 8 and then diluted with dialysis buffer to a concentration of 200 μg/ml. MNase digestions were performed in bulk by adding $CaCl_2$ to a final concentration of 2mM and 2U/ml MNase (Sigma) and incubating at 37°C. Aliquots (1 ml) were withdrawn from the digestion mixture at each time point and directely added to the digestion stop solution (1% SDS; 0.1 M NaCl; 10 mM EDTA; 10 mM EGTA; 50 mM Tris-HCl pH 8). Digested chromatin was treated with proteinase K (Roche) (500 μg/ml) for 5 hours at 37°C, cross-links were reverted by heating overnight at 65°C and the DNA was purified using phenol extraction and resuspended in distilled water. The DNA was then treated with RNAse A

(Roche; 50 μg/ml) for 30 minutes at 37°C, again with proteinase K (500 μg/ml) for 5 hours at 55°C, phenol extracted, precipitated and resuspended in distilled water. For the experiments shown in Figures 3.3, 3.4, 3.6, 3.7, 3.8, 3.10 DNA quantitated at the spectrophotometer (Nanodrop) (OD_{A260}) and equal amounts (100 ng) of material for each time point were used as template in PCR reactions.

For ChIP assays, cross-linked material was digested for 50 minutes at 37°C and MNase digestion stopped by adding RIPA buffer (1 mM EDTA; 0.5 mM EGTA; 10 mM Tris; pH 8; 1% Triton; 0.1% (w/v) Na Deoxycholate; 0.1% (w/v) SDS; 140 mM NaCl ; 1 mM PMSF). The resulting material was used directly in ChIP assays.

2.6. ChIP.

This protocol was used both for MNase-digested and undigested cross-linked chromatin. Each aliquot of cross-linked chromatin (200 µg) was precleared with 25 μl of rProtein A-Sepharose beads (Amersham Pharmacia Biotech), previously coated with 10 μg/ml each of poly-(dI-dC), poly-(dG-dC) and poly-(dA-dT) (Sigma) and with 100 μg/ml of bovine serum albumin (BSA; Roche) in RIPA buffer. The aliquots were then incubated overnight with 1 μg of the appropriate antibodies (or without antibodies for the mock controls) in a total volume of 1 ml of RIPA buffer and immunoprecipitated as described (Orlando et al., 1997). Following immunoprecipitation, the material was treated with RNase A (50 μg/ml) for 30 minutes at 37° C and by proteinase K (500 μg/ml) in 0.5% (w/v) SDS at the same temperature overnight. Formaldehyde cross-links were reverted by heating the samples at

65° C for 5 hours, the DNA was purified with phenol extraction and resuspended in 250 μl of distilled water. Resuspended material (4 μl) was used as a template in PCR reactions.

2.6.1. non-quantitative PCRs of immuno precipitated DNA.

Semi-quantitative PCRs were performed as follows: First denaturation step: 95° C for 3 minutes; second denaturation step: 95° C, 1 minute; annealing step (see Table 1 for temperatures of the primer sets), 1 minute; extension step: 72° C, 1 minute; final extension step: 72° C, 3 minutes. The second denaturation, annealing and extension steps were normally repeated for 33 cycles. To exclude the presence of a signal from other immunoprecipitated material, the number of cycles in the PCR reactions was raised to 40. Primer sequences, location with respect to the uPA sequence (Verde et al., 1988) and annealing temperatures for each primer set are reported in Table 1. For the amplification of the 1,574 bp genomic fragment shown in Figures 3.1 and 3.2 (primers F14/R26) an elongation step of 2 minutes was used.

PCR products were analysed on 2% (w/v) agarose gels in 1X TAE buffer.

2.6.2. Quantitative PCRs of immunoprecipitated DNA.

ChIP-enriched DNA of indicated amplicons (see Table II) was quantified by QT-PCR in a light cycler instrument (Roche) using FastStart DNA mix SYBR Green I kit (Roche). PCR conditions were as follows: First denaturation and DNA polymerase activation step: 95° C for 10 minutes; second denaturation step: 95° C, 15 seconds; annealing step (see Table II for temperatures of the primer sets), 6 seconds; extension step: 72° C, 20 seconds. Three independent ChIP experiments were performed and ChIP-samples were analysed in

triplicate PCRs. The relative enrichment of genomic DNA was determined by calculating the ratio of DNA in the immunoprecipitates compared with DNA in the input chromatin.

TABLE I – List of the primer sets used.

Primer sets	Primers Sequences (5' to 3' orientation)	Primers position in uPA sequence	PCR annealing temperature for primer sets
F8	TGTCCAGGAGGAAATGAAGTCATC	-1981/-1958	57°C
R11	GAAACTCCCAGGTTAGTTATCAGG	-1836/-1859	
F8	TGTCCAGGAGGAAATGAAGTCATC	-1981/-1958	57°C
R12	GACCAGAACATAAACAGAGATGCTG	-1792/-1816	
F8	TGTCCAGGAGGAAATGAAGTCATC	-1981/-1958	57°C
R14	CTCTAGAAGACTGTGGTCAGTTTTG	-1731/-1755	
F5	GATTAGCGCATGGATAAGGAAGTTC	-2105/-2081	54°C
R14	CTCTAGAAGACTGTGGTCAGTTTTG	-1731/-1755	
F22	CAGTAATCTGGCCTTGCCTTTCC	-645/-623	60°C
R26	GAGGAATCGAGAGGCTTGTAAATTC	-181/-205	
F26	GAATTTACAAGCCTCTCGATTCCTC	-205/-181	60°C
R31	GGGATCTCAGGACCGCGG	+114/+97	
F22	CAGTAATCTGGCCTTGCCTTTCC	-645/-623	60°C
R31	GGGATCTCAGGACCGCGG	+114/+97	
F21	CCCAATCCTTATCAAGCCCTGTC	-700/-678	60°C
R26	GAGGAATCGAGAGGCTTGTAAATTC	-181/-205	
F22	CAGTAATCTGGCCTTGCCTTTCC	-645/-623	60°C
R27	CGCAACGCTCACAAAGATTTG	-114/-134	
F26	GAATTTACAAGCCTCTCGATTCCTC	-205/-181	60°C
R34	ACCAGGCTCCCCAGCTGTC	+304/+286	
F26	GAATTTACAAGCCTCTCGATTCCTC	-205/-181	60°C
R36	GAGGTCGGGGCGCTAGACG	+420/+402	
F26	GAATTTACAAGCCTCTCGATTCCTC	-205/-181	60°C
R37	CAGGACGCAGAGAAGCAGG	+465/+447	
F25	GAGCTGGGCGAGGTAGAGAGTC	-313/-292	60°C
R31	GGGATCTCAGGACCGCGG	+114/+97	

F7	GGGAGAAAGGGTGTCACGC	-2024/-2006	57°C
R10	GCCGTCATGATTCATGTTGCTCC	-1872/-1894	
F3	GAGGACCCCTTGAACCCAGAAG	-2192/-2171	57°C
R6	CCGTGCCACCTCTTCACCTAGC	-2043/-2064	
F11	CCTGATAACTAACCTGGGAGTTTC	-1859/-1836	57°C
R15	CTTCAGAGCCAACCTTGCTACTTC	-1707/-1730	
F18	GAGTCCTACTGGGTTCAAAATGAC	-1354/-1331	57°C
R21	GACAGGGCTTGATAAGGATTGGG	-726/-748	
F6	GCTAGGTGAAGAGGTGGCACGG	-2064/-2043	54°C
R10	GCCGTCATGATTCATGTTGCTCC	-1872/-1894	
F9	GCATGACAGCCTCCAGCCAAG	-1942/-1922	57°C
R12	GACCAGAACATAAACAGAGATGCTG	-1816/-1792	
F19	CTCCAGTCTCCCAATTCCTCTAC	-948/-926	54°C
R22	GGAAAGGCAAGGCCAGATTACTG	-623/-645	
F7	GGGAGAAAGGGTGTCACGC	-2024/-2006	54°C
R11	GAAACTCCCAGGTTAGTTATCAGG	-1836/-1859	
F14	CAAAACTGACCACAGTCTTCTAGAG	-1755/-1731	60°C
R26	GAGGAATCGAGAGGCTTGTAAATTC	-181/-205	
F27	CAAATCTTTGTGAGCGTTGCG	-134/-114	57°C
R31	GGGATCTCAGGACCGCGG	+114/+97	
F32	GGGATCTCAGGACCGCGG	+194/+213	57°C
R36	GAGGTCGGGGCGCTAGACG	+420/+402	
F18	GAGTCCTACTGGGTTCAAAATGAC	-1354/-1331	57°C
R22	GGAAAGGCAAGGCCAGATTACTG	-623/-645	
F29	GCTGCAAGACAGGGGAGGGAG	-85/-65	60°C
R31	GGGATCTCAGGACCGCGG	+114/+97	

TABLE II – List of the primer sets used in ChIP quantitative PCR's.

Primer sets	Primers Sequences of promoter regions Used in HepG2 cells (5' to 3' orientation)	PCR annealing temperature for primer sets

Fw- p21WAF1 **Rev-p21WAF1**	**CTGGAACTCGGCCAGGCTCAGC** **GCGAATCCGCGCCCAGCTCCG**	**60°C ***
Fw-uPA **Rev-uPA**	**CAAATCTTTGTGAGCGTTGCG** **GGGATCTCAGGACCGCGG**	**60°C ***
Fw-p27/eIF6 **Rev-p27/eIF6**	**CCTAAAAAGCTCCTGAATG** **GCACACTTGGACAGGATG**	**57°C**
Fw-LDLR **Rev-LDLR**	**TGTTAACAGTTAAACATCGAGAA** **CCCGCGATTGCACTCGGGGC**	**60°C**
Primer sets	**Primers Sequences of exonic regions (5' to 3' orientation)**	**PCR annealing temperature for primer sets**
Fw- p21WAF1Int. **Rev-p21WAF1Int**	**CTGTCACTGTCTTGTACCCTTGTGCC** **GTTAGCTAGTGGTCTTTGCTGCCTAC**	**60°C ***
Fw-uPAInt. **Rev-uPAInt**	**CGACTATCTCTATCCGGAGC** **ACACTCACCTGGCAGGAATC**	**58°C ***
Fw-p27/eIF6Int. **Rev-p27/eIF6Int**	**ATCCCGCATGCTGGTGGCAATGGT** **TGGGTCATTACCTGCCACAGTTTGG**	**60°C**
Fw-LDLRInt. **Rev-LDLRInt.**	**ATCTCCTCAGTGGCCGCCTCTACTG** **CAGTTTTCTGCGTTCATCTTGGCTTGA**	**60°C**
Primer sets	**Primers Sequences used in MEF cells (5' to 3' orientation)**	**PCR annealing temperature for primer sets**
Fw- p53 **Rev- p53**	**GGTGGTGCGATACCAAGTATCTCG** **GTAAGTGGACCGCCACTGTTCTG**	**60°C**
Fw- Bcl-XL **Rev- Bcl-XL**	**CGGACTCAGACCTTCATAAGAGCC** **CCAAAACACCTGCTCACTTACTGG**	**60°C**

* PCR mix contained 1.2M (final concentration) of betaine PCR reagent (Sigma, Cat. No. B0300).

2.7. BrUTP incorporation assay.

Cells grown on glass coverslips for 24-36 hours (less than 60% confluent) were washed once with ice-cold PBS, equilibrated in transcription buffer (TB; 100 mM KCl, 5 mM $MgCl_2$, 0.5 mM EGTA, 1 mM PMSF, 5 U/ml RNAsin (Promega Co., Madison, WI), 25% glycerol and 50 mM Tris–Cl, pH 7.4) for 10 minutes on ice and permeabilised with 0.05% Triton X-100 in TB for 3 minutes on ice. Samples were then incubated for 20 minutes at room temperature in TBN (TBN: TB containing 0.5 mM ATP, 0.5 mM GTP, 0.5 mM CTP (Promega) and 0.25 mM BrUTP) (Sigma), washed in PBS, fixed in 3% paraformaldehyde in PBS for 10 minutes at room temperature. Incorporated BrUTP was detected by immunofluorescence with anti-BrdU monoclonal antibodies from Roche using confocal microscopy analysis (See below).

2.8. Immunofluorescence and confocal microscopy analysis.

Cells were grown at least for 24-36 hours on 13 mm glass coverslips (VWR international). Cells where washed three times with cold PBS, fixed with paraformaldehyde solution (3% (w/v) paraformaldehyde; 2% (w/v) sucrose; 1X PBS) for 10 minutes. at room temperature (RT) and then washed again three times with cold PBS. Cells where then permeabilized by incubation in Hepes-Triton solution (20mM Hepes pH7.4; 300mM Sucrose; 50nM NaCl; 3mM $MgCl_2$; 0,5% (v/v) Triton X-100) for 5 minutes at RT washed three times with 1X PBS + 0,2% (w/v) BSA and after incubation for 20 minutes at 37°C in 1X PBS + 2% (w/v) BSA were added the primary Ab (1:100 final dilution) and incubated 30 minutes at 37°C. After three washes with 1X PBS + 0,2% (w/v) BSA, 1X PBS + 2% (w/v) BSA were added and cells incubated for 20 minutes at 37°C before adding the secondary antibody (1:100

final dilution) and incubated for 30 minutes at 37°C. Cells were washed again three times with 1X PBS + 0,2% (w/v) BSA and then incubated with 4'6-diamidino-2-phenylindole dihydrochloride (DAPI) nuclear staining (Fluka) previously resuspended in 1X PBS. After an incubation of 3 minutes at RT cells were washed twice with cold PBS and cover slips were mounted with Immu-Mount (Thermo electron corporation). Images were obtained with a Leica DMIRE2 (Confocal System Leica TCS SP2) and a Delta vision (Delta Vision RT deconvolution System) confocal microscopes.

2.9. Protein extraction and western blot analysis.

2.9.1. Total protein extraction.

Cells were detached with cold PBS additioned with 1mM EDTA and washed with cold PBS. $1x10^6$ cells were resuspended in lysis buffer (Tris pH 7.6, 50 mM; NaCl, 0.8 M; EDTA, 1 mM; Triton X-100, 1%; NP-40, 0.5%; PMSF, 1mM; phosphatase inhibitor cocktail 1, 1:100; phosphatase inhibitor cocktail 2, 1:100; Protease inhibitors, 1:1000) (phospatase inhibitor cocktails 1 and 2 were from Sigma; protease inhibitors were from Roche) and lysed by passing them trough a syringe. Lysates were kept in agitation for 15 minutes at 4 °C, additioned with an equal volume of 2X SDS gel-loading buffer and heated for 10 minutes at 95 °C and chilled on ice for 2 minutes. Equal volumes were loaded in a 5-15% gradient SDS-PAGE (Laemmli, 1970).

2.9.2. Cytoplasmic and Nuclear protein extraction.

Cells were detached with cold PBS containing 1mM EDTA and washed with cold PBS. $1x10^6$ cells were added of buffer A (Hepes-KOH pH 7.8 10 mM; $MgCl_2$ 1.5 mM; KCl 10 mM; phosphatase inhibitor cocktail 1, 1:100; phosphatase inhibitor cocktail 2, 1:100; Protease inhibitors, 1:1000) and gently pipetted and then incubated on ice for 10 minutes. 10% Triton X-100 (Sigma) was added to the cells in buffer A as 1/30 of the volume and the suspension vortexed for 30 seconds. An aliquot of treated sample was observed under the microscope (CK2 Olimpus) to control that cytoplasmic membranes were broken and nuclei released. Samples were centrifuged for 1 minute at 11,000 rpm in an Eppendorf microfuge at 4°C to pellet nuclei. The supernatant, representing the cytoplasmic fraction, was additioned with an equal volume of 2X SDS gel-loading buffer and heated for 10 minutes at 95 °C. Equal volumes for each sample were loaded in a 5-15% gradient SDS-PAGE (Laemmli, 1970). The pelleted fraction (representing the whole nuclei) was washed twice with buffer A to eliminate cytoplasmic protein contaminants, additioned with an equal volume of 2X SDS gel-loading buffer, heated for 10 minutes at 95 °C and equal volumes were loaded in a 5-15% gradient SDS-PAGE (Laemmli, 1970).

2.9.3. Detection of proteins.

Following SDS-PAGE proteins were transferred to nitrocellulose as previously described (Towbin et al., 1979). Filters were blocked for 16 hr at 4°C with PBS 1X supplemented with 5% non-fat dry milk (Regilat), washed 5 times for 5 minutes with PBS 1X supplemented with 0.1% Tween 20 (PBS-T) and incubated with primary antibodies (see Table III) at RT. After 1 hour blots were washed twice for 10 minutes with PBS-T,

incubated for 30 minutes at RT with a peroxydase-conjugated secondary anti-mouse (Amersham, Cat. No. NA9310V) or anti-rabbit (Amersham, Cat. No. NA9340V) or anti-goat antibody (depending on the primary antibody used, see Table III) used at final concentration of 1:5000, washed 5 times for 10 minutes with PBS-T and finally developed with Super Signal West pico chemiluminescence substrate system (Pierce, Cat. No. 34080).

2.10. Southern Blotting.

2.10.1. Gel fractionation of genomic DNA and transfer on a nylon membrane.

Cross-linked chromatin has been prepared, digested with MNase and genomic DNA purified and quantitated as described before (see above). 15 μg of genomic DNA for each time point of MNase digestion were fractionated on a 0.8% (w/v) agarose, 1X TAE gel overnight. The gel was incubated for 30 minutes in an acid solution (0.25 M HCl), rinsed with water, incubated twice in a basic solution (0.6 M NaCl, 0.2 N NaOH) for 15 minutes and finally incubated 15 minutes in a neutralizing solution (0.5 M Tris pH 7.5, 1.5 M NaCl). DNA was transfered overnight in 20X SSC by capillarity on Hybond N+ nylon transfer membrane (Amersham pharmacia biotech). The membrane was previously floated in water and than soaked in SSC 20X. The following day after, the membrane was soaked in SSC 2X and gently rubbed with a gloved finger to remove all agarose, incubated 30 seconds in a basic solution (0.4 N NaOH), transferred for 5 minutes in a equilibrating

solution (0.2 M Tris pH 7.5; SSC 2X), air dried and than DNA on the membrane fixed using UV cross-linker (Stratalinker,).

2.10.2. Probes preparation.

Probes specific for the enhancer and MP were obtained by PCR using primer sets F5/R14 and F22/R26 (see Table I) and the following PCR conditions:

First denaturation 1: 95° C for 3 minutes; second denaturation: 95° C, 1 minute; annealing step (see Table 1 for temperatures of the primer sets), 1 minute; extension: 72° C, 1 minute; final extension: 72° C, 3 minutes. The second denaturation, annealing and extension steps were normally with 40 amplification cycles. Specific amplified fragments were isolated by agarose gel extraction using Wizard SV Gel and PCR clean-up system (Promega), quantitated by the spectrophotometer (Nanodrop) (OD_{A260}) and radiolabeled using ^{32}P-α-dCTP (Amersham, Cat. No. AA0005) with Rediprime ^{TM} II random prime labelling system (Amersham, Cat. No. RPN1633) according to the manufacture's instructions.

2.10.3. Hybridization and signal detection.

The membrane was prehybridized at 65°C shaking for 6 hours in hybridization buffer (1% SDS (w/v); 10X Denharts; 0.2% BSA (w/v); 1 M NaCl; 100 μg/ml herring sperm) using a Kapak scotchpak heat sealable pouch (Kapak corporation, Cat. No. 403). The hybridization buffer was then replaced, radiolabeled probes (previously denatured) were added and the membrane incubated at 65°C overnight with shaking. The following day the membrane was washed twice with wash solution A (2XSSC; 0.1% SDS (w/v)) at RT for 10 minutes, once with wash solution B (1XSSC; 0.1% SDS (w/v)) at 65°C for 15 minutes and once

with wash solution C (0.1XSSC; 0.1% SDS (w/v)) at 65°C for 10 minutes. Radioactive membranes were exposed for the appropriate time for autoradiography and revealed using Typhoon 8600 phosphoimager (Molecular Dynamics) and signal intensity was measured using a using the inbuilt software.

TABLE III – List of the Antibodyes used.

Name of the antibody	Company and Cat. No.	Final concentration in ChIP	Final concentration in W.B.
Anti Phospho-Ser-2 of RNAP II CTD (a-CTD-P-S2)	Covance, MMS-129-RA	1µg/ml	1:500
Anti Phospho-Ser-5 of RNAP II CTD (a-CTD-P-S5)	Covance, MMS-134-RA	1µg/ml	1:500
α-Myosin VI (KA-15)	Sigma, M5187-.2 ML	1µg/ml	1:1000
α-Histone H3-K4me2	Upstate, 07-030	1µg/ml	#
α-Histone H3-K9me2	Upstate, 07-212	1µg/ml	#
α-Histone H3-K14ac	Upstate, 07-353	1µg/ml	#
α-Histone H3-K9ac	Upstate, 07-352	1µg/ml	#
α-Histone H2B	Upstate, 07-371	#	1:2000
α-c-Jun	Santa Cruz, sc-1694X	1µg/ml	1:1000
α-p300 (N-15) X	Santa Cruz, sc-584X	1µg/ml	#

α-Sp1 (PEP2) X	Santa Cruz, sc-59X	1μg/ml	#
α-Lamin A/C (N-18)	Santa Cruz, sc-6215	#	1:1000
α-Lamin A/C (636)	Santa Cruz, sc-7292	#	#
α-RNAP II (N20)	Santa Cruz, sc-899	1μg/ml	1:800
α-BrU	Roche, Cat. No. 11170376001	#	
α-HMGN1	Kindly provided by Dr. Michael Bustin, NCI, Bethesda	1μg/ml	
α-HMGN2	Kindly provided by Dr. Michael Bustin, NCI, Bethesda	1μg/ml	
α-uPAR	Produced in our laboratory	1μg/ml	

2.11. Transient transfections.

Transient transfections were performed using lipofectamin 2000 (Invitrogen, Life Technologies) according to manufacturer's instructions. For the experiment shown in Figure 5.4 the transfection of HepG2 cells was performed in 24 well plates using at a total of 0,8 μg of DNA/well (either the control pEGFP-C1 empty vector (Clontech) or the full length pEGFP-MyosinVI (Aschenbrenner et al., 2003), (kindly provided by Dr. T. Hasson) containing 5-7 X 10^4 cells on glass coverslips. For the experiment shown in Figure 6.3 the transfection on NT2-D1 cells was performed in 6 well plates. 6 μg of DNA per well of either control pIRES-EGFP empty vector or pIRES-EGFP-MyosinVI AS (Yoshida et al., 2004) (kindly provided by Dr. H. Naora) with 10^6 cells/well were used.

2.11.1. Selection of stably transfected cells.

To establish stable clones expressing the myosin VI antisense RNA transfections on HepG2 cells were done as described above and cells were routinely passed in complete, selective medium (see above), containing 0.9 mg/ml G418 (neomycin; Gibco).

2.12. Tandem Affinity Purification (TAP) of Prep-1-associated proteins.

Prep1-TAP cDNA and purification are described elsewhere (Diaz *et al.*, in preparation).

2.13. Mouse embryo primary fibroblasts preparation.

Prep1$^{i/i}$ and WT primary mouse embryo fibroblasts (MEFs) were obtained from embryos 14.5 days after fertilization. Mice were sacrificed by carbon monoxide inhalation. Each embryo was dissected and treated with 0.25% trypsin, 0.02% EDTA in PBS for 30 minutes on ice in 24 wells-plates. Trypsinization was blocked by the addition of complete-DMEM. After mechanical dissociation, embryo fragments were cultured in 6 cm dishes containing complete-DMEM, and were maintained at 37° C, in a humidified incubator with 5% CO2. Genotyping was performed as described in (Ferretti et al., 2006).

2.13.1. Amplification and maintenance of cultured MEF.

MEF were incubated until confluent and split every 2-3 days in 15 cm dishes with 20 ml of DMEM and mantained at 37 °C, in a humidified incubator with 5% CO2. MEF were used for experiments between passages 4 and 5.

2.14. Cell fixation for cryo-section (Protocollo Ana).

Cell fixation are described in (Branco and Pombo, 2006).

2.14.1. Cryo-section and Immuno-FISH analysis.

Cryosections and immuno-FISH analysis are described in (Branco and Pombo, 2006).

RESULTS AND DISCUSSION -I-

Interaction between enhancer and MP of the uPA gene by looping of the intervening sequence.

RESULTS -I-

3.1.1. Anti-Sp1 and anti-p300 antibodies immunoprecipitate uPA MP and enhancer sequences.

Formaldehyde cross-links molecules with reactive groups at a maximum distance of 2 Å. This may occur between proteins bound to distant regulatory elements if such groups are close enough, implying their interaction. We tested this hypothesis for the MP and the enhancer of the uPA gene, located 2 kb upstream, by performing conventional ChIP experiments on cross-linked, sonicated chromatin from PC3 cells with antibodies against Sp1, which uniquely binds the MP (Cirillo et al., 1999; Ibanez-Tallon et al., 2002; Nerlov et al., 1992; Nerlov et al., 1991), and the cofactor p300. We asked if the DNA immunoprecipitated with one or the other antibody contained both enhancer and MP

sequences, by amplifying the recovered material with specific primers (F5/R14 and F27/R31 in Figure 3.1A). Indeed both genomic DNA sequences were immunoprecipitated with either antibody, whereas the IVS was not detected (Figure 3.1B) even by increasing the number of PCR cycles. Thus, the results are consistent with a close physical proximity of the regulatory elements and the extrusion of the IVS. However, amplification of the input DNA with the F14/R26 primer set did show the presence of a PCR product (Figure 3.1B), indicating that the IVS was not fully broken by sonication. To make sure that the regulatory elements were located on separate genomic fragments in the immunoprecipitated material we decided to enzymatically cleave ChIP ready chromatin prior to immunoprecipitation.

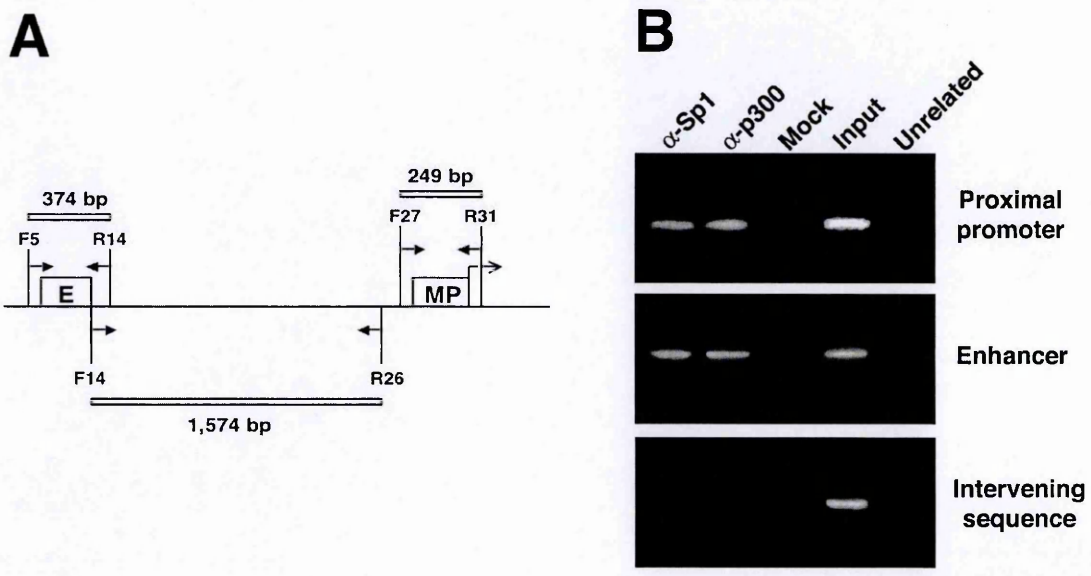

Figure 3.1. Both uPA enhancer and MP sequences are present in genomic DNA immunoprecipitated with either anti-Sp1 or anti-p300 antibodies.
ChIP-ready chromatin was immunoprecipitated with anti-Sp1 and anti-p300 polyclonal antibodies. Purified DNA was amplified by PCR with the F5/R14, F27/R31 and F14/R26 primer sets (Table I). The PCR products were fractionated on a 2% agarose 0.5x TBE gels

and stained with EtBr. (**A**) Scheme of the regulatory region of the uPA gene (E = enhancer; MP = minimal promoter) and location of the primer sets (not drawn to scale). The regulatory elements are located approximately 2 kb apart. Arrows with full heads: primers and their orientation; empty arrowhead: transcription start site. Empty boxes: amplified fragments. (**B**) PCR amplification products of immunoprecipitated genomic DNA. Both enhancer and MP sequences, but not the intervening sequence, are present in the material recovered after immunoprecipitation with anti-Sp1 or anti-p300 antibodies.

3.1.2. Restriction enzyme digestion, following sonication, does not fully cleave the IVS.

We tried to digest ChIP-ready chromatin with restriction enzymes. We chose 4- (Mse I) or 6-cutter (Dra I) enzymes because they have multiple recognition sites (6 for Mse I and 2 for Dra I) in the region between the 3' end of the enhancer (-1,879) and the 5' end of the MP (-86), but not within the regulatory elements themselves (Figure 3.2A). Moreover these enzymes do not have cytosines (or guanines) in their cognate sequence that may interfere with the digestion, since cytosines are involved in the formation of protein-DNA cross-links, together with the amino groups of lysines (Orlando et al., 1997). Cross-linked chromatin was digested overnight, purified DNA was quantitated at the spectrophotometer (OD_{A260}) and used as template in PCR reactions using different set of primers that were designed in order to amplify regions of DNA across the cutting sites of the restriction enzymes (Figure 3.2A). Figure 3.2B shows that the enzymes failed to digest ChIP-ready chromatin as the region between the regulatory elements of uPA can still be amplified.

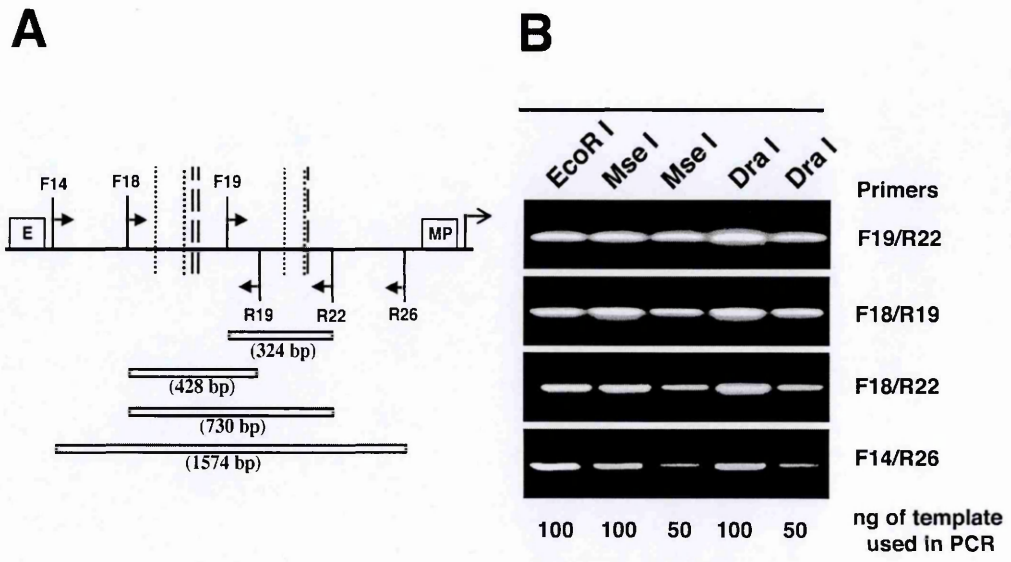

Figure 3.2. The restriction enzyme digestion does not completely cut the IVS between the enhancer and MP of uPA.
Aliquots of ChIP-ready chromatin were digested with restriction enzymes that do not cut (EcoRI) or cut (MseI and DraI) the IVS, as described in material and methods. After purification recovered DNA was measured and used as template in PCRs reactions. (**A**) Scheme (not to scale) of the amplified regions using the indicated primer sets (see Table I). Restriction sites of MseI and DraI are reported as dotted or broken vertical lines, respectively. White boxes: amplified fragments. Arrows with full heads: primers and their orientation; empty arrowhead: transcription start site. Empty box with E: enhancer. Empty box with MP: minimal promoter. 100 or 50 ng of genomic DNA from the different digestions were amplified by PCR, and DNA products were fractionated on a 2% agarose 0.5x TBE gels and stained with EtBr. (**B**) Amplification of specific IVS fragments, across restriction sites, still occur after digestion.

3.1.3. ChIP-ready chromatin is accessible to MNase cleavage.

We then decided to digest ChIP-ready chromatin, with MNase, an enzyme widely employed in chromatin studies (Turner, 2001) (van Holde, 1989). MNase is a processive enzyme that binds and cleaves unprotected chromatin DNA in a processive manner (typically the internucleosomal linker), converting it to free nucleotides. The digestion

ends when the enzyme meets a physical barrier to cleavage. As a result the amount of DNA recovered at each digestion time point, and measured as $O.D._{A260}$, decreases (Figure 3.3A). The pattern of MNase digestion obtained in a time-course experiment shows that ChIP-ready chromatin from PC3 cells was readily and increasingly cleaved by the enzyme to poly-, mono- and sub-nucleosomal particles (Figure 3.3B). Next, equal amounts of genomic DNA from the various digestion time-points of Figure 3.3B was subjected to PCR reactions with sets of primers that amplified increasingly larger (from 145 to 250 bp) fragments in the uPA enhancer region (Figure 3.3C). The results showed that only nucleosome-size genomic fragments could be amplified using material from all the digestion time points (Figure 3.3D), thus confirming the accessibility to and the cleavage by MNase of the uPA enhancer region.

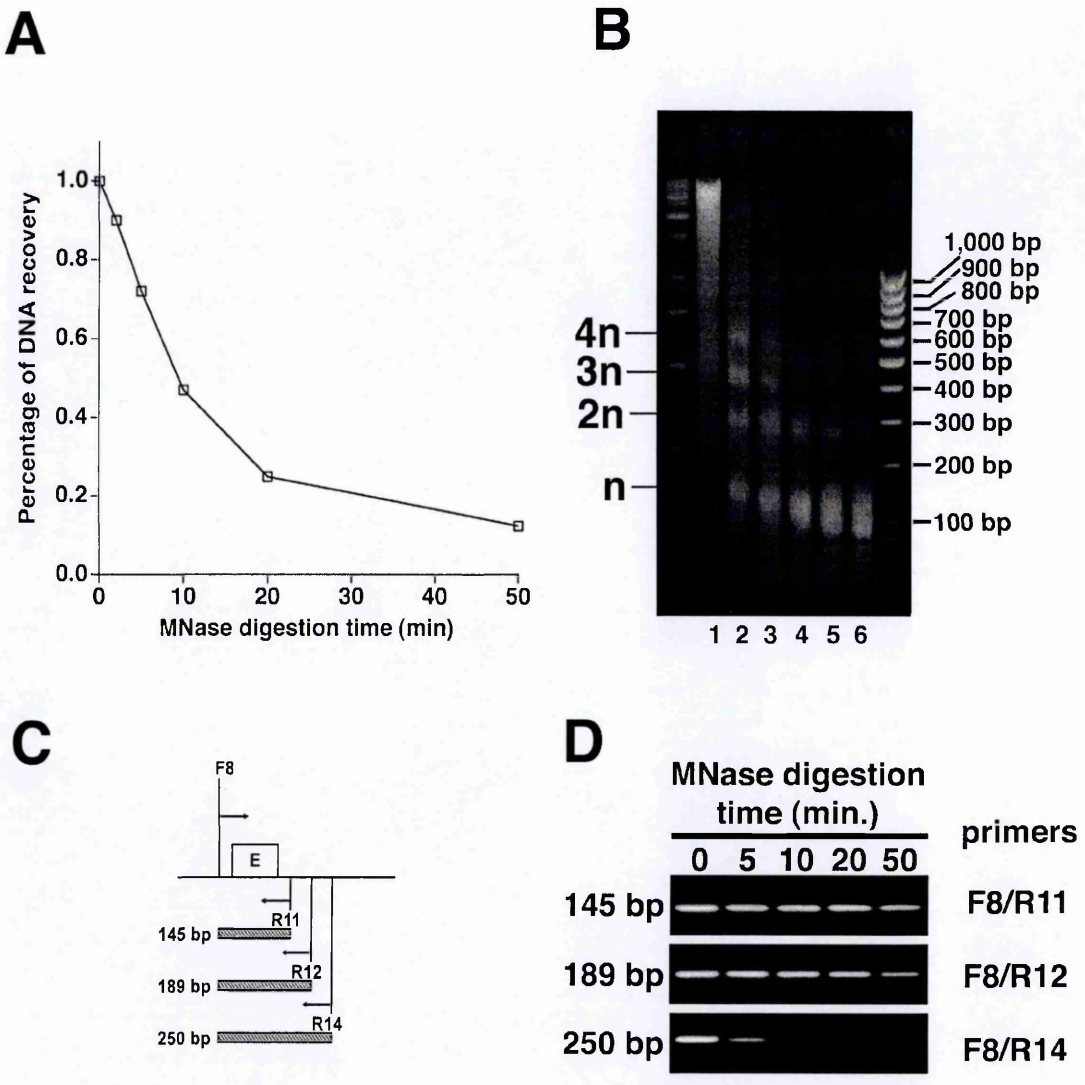

Figure 3.3. MNase digestion time-course of ChIP-ready chromatin and detection of nucleosome-size fragments in the enhancer region. (**A**) 1,200 μg of ChIP-ready chromatin were digested with MNase. At increasing times, aliquots of the reaction were withdrawn, the digestion was stopped and genomic DNA purified. After purification, DNA was measured and the percentage of recovery plotted in graph. (**B**) Equal amounts of genomic DNA from each time point were fractionated on a 2% agarose gel in 0.5x TBE and visualized with EtBr. M: markers; left marker: 1 kb DNA ladder (Fermentas); right marker: Mass Ruler DNA Ladder (100 bp ladder; Fermentas). n, 2n, etc. = mononucleosomes, dinucleosomes, etc. (**C**) Scheme (not to scale) of the amplified region using the indicated primer sets (see Table I). Striped boxes: amplified fragments. Arrows: primers and their orientation. White box with E: enhancer. Equal amounts of genomic DNA from the different digestion time points (panel A-B) were amplified by PCR. (**D**)

Only mononucleosome-size fragments (145 – 189 bp) can be amplified in the enhancer region using genomic DNA from all digestion time points

3.1.4. PCR reactions with genomic DNA from MNase digested ChIP-ready chromatin reveals fragments with a distinctive amplification pattern.

We then repeated the PCR amplification protocol in the uPA MP region. Since we wanted to exclude the presence of genomic fragments larger than 200 bp (mononucleosome size), we deliberately designed two sets of primers spanning 464 bp and 320 bp respectively (Figure 3.4A), and expected to be able to amplify genomic DNA only by using material from the early digestion time points (see Figure 3.3B). As shown in Figure 3.4B, primer sets F22/R26 and F26/R31 showed that the amplification signal decreased by using genomic DNA from early and intermediate MNase digestion time-points, but was rescued with material from later (20 and 50 minutes) time points. However, the amplification of two fragments of similar size upstream of F22 and one in the enhancer region displayed the progressive loss of the PCR signal, as expected. The amplification pattern of fragments F22/R26 and F26/R31 apparently contradicts the MNase digestion kinetics and the results obtained in the enhancer region, shown in Figure 3.3. However, one must recall that MNase is a processive endonuclease, as mentioned before, that causes a generalized loss of genomic DNA with increasing digestion and, consequently, an increase in the relative ratio of MNase-resistant to -sensitive material. If our interpretation were correct, the lowest amplification signals should then be rescued by "spiking" the material from the specific

digestion time-points with genomic DNA from the 50 minutes digestion time-point. We therefore mixed equal amounts of the material yielding the lowest PCR signal for the amplicons amplified by primer sets F22/R26 and F26/R31 (10 and 20 minutes, respectively; Figure 3.4B) with material from the 50 minutes digestion time point and subjected the samples to PCR reactions. As shown in Figure 3.4C the signal for both amplicons was rescued, indicating that the 50 minutes digestion time point contains more amplifiable copies of the specific genomic fragments, originating from the cleavage-resistant chromatin population.

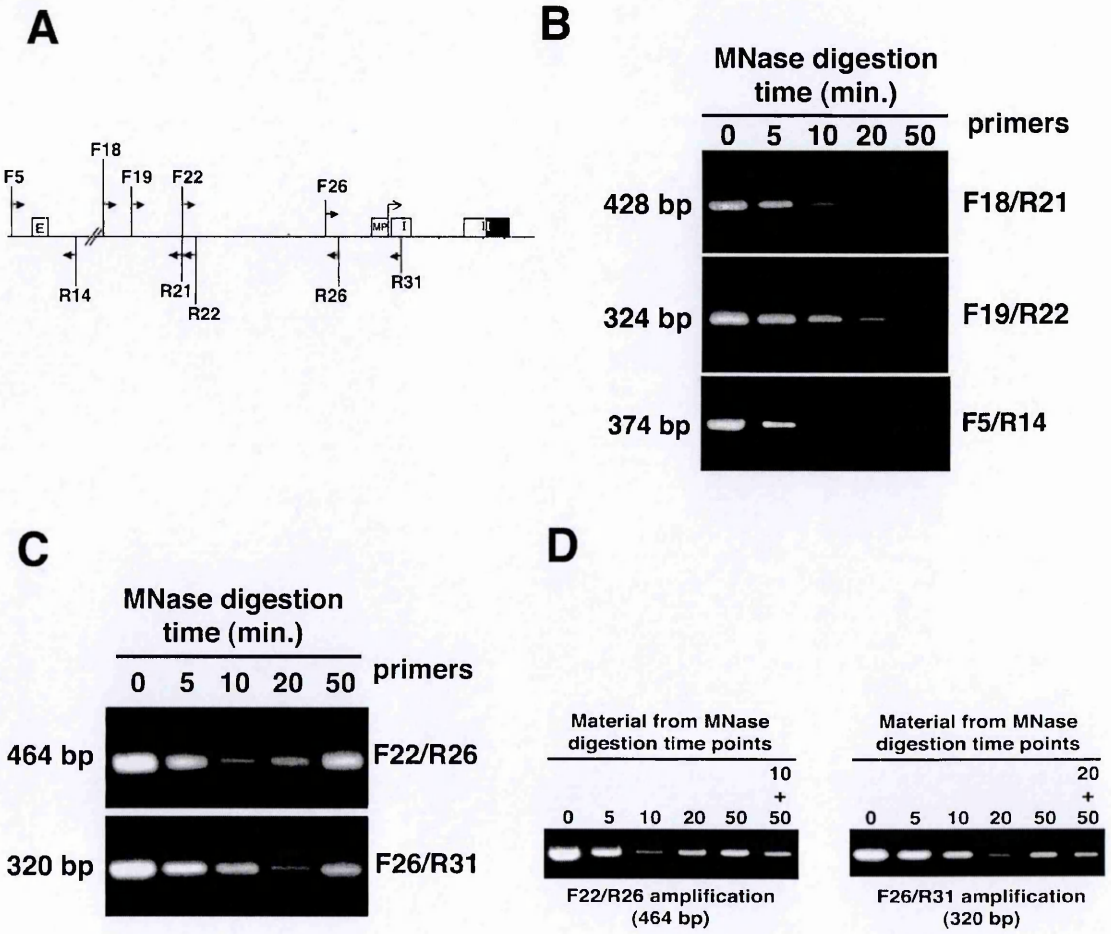

Figure 3.4. Detection and characterization of DAF amplicons in the MP region of the uPA gene.
(**A**) Scheme (not to scale) of the amplified regions and primers used. Full arrowheads: primers (Table I) and their orientation. Empty arrowhead: transcription start site. White and hatched boxes: amplified fragments; MP: minimal promoter; roman number I: first, untranslated exon of the uPA gene; white and black boxes with roman number II: untranslated and translated portions, respectively, of the second exon of the uPA gene. Equal amounts of genomic DNA from each MNase digestion time-point were amplified with the appropriate primers (panel A) and PCR products revealed on a 2% agarose gel in 0.5x TBE stained with EtBr. Amplification products of the enhancer region (primer set F5/R14) or the region upstream of MP (primer sets F18/R21 and F19/R22) are visible at the 0 minutes time points and the signal is lost in the following time points digestion (**B**). In panel (**C**) amplicons F22/R26 and F26/R31 show a loss of PCR signal using material originated from early and intermediate MNase digestion time points. The signal is then recovered at later time points revealing the presence of amplicons resistant to MNase digestion. Equal amounts of the material yielding the lowest PCR signal for the DAF-A and DAF-B amplicons (10 and 20 minutes, respectively; Panel C) were mixed with material from the 50 minutes digestion time point and subjected to PCR reactions with specific primers. As shown in panel (**D**) the signal for both amplicons was rescued, indicating that the 50 minutes digestion time point contains more amplifiable copies of the specific genomic fragments, originating from the cleavage-resistant chromatin population.

A model depicting the interpretation of this result is shown in Figure 3.5. In PC3 cells the uPA gene is present in multiple copies, but not all copies are transcriptionally active (Helenius et al., 2001). We postulate that the regulatory region of the gene is found in two chromatin configurations which differ in their sensitivity to MNase cleavage: one configuration is sensitive to digestion, while the other is resistant. However, these populations represent a minute amount of the total chromatin of PC3 cells, since the vast majority is represented by non-uPA chromatin. These three populations (sensitive and resistant uPA chromatin, plus non-uPA chromatin) also make up total ChIP-ready chromatin from PC3 cells and their differential sensitivity to MNase affects the genomic DNA content of samples at different digestion time points. The rate at which the enzyme

cleaves the non-uPA and the sensitive uPA chromatin populations is the same, but their presence is detected in significantly different ways. Since non-uPA chromatin represents the vast majority of ChIP-ready chromatin from PC3 cells, its amount can be measured as $O.D._{A260}$ at each digestion time point and can be considered a good estimate of the total DNA recovered (represented by the large circles in the Figure 3.5). On the other hand, in our experimental set-up uPA chromatin can only be revealed by PCR amplification of specific sequences, which are, therefore, "amplifiable" (small white circles in the Figure 3.5). A single double-stranded MNase cut in an "amplifiable" sequence renders it "non-amplifiable" (crossed-out circles Figure 3.5) and dramatically reduces their PCR detectable pool, so that, at intermediate digestion, all the sensitive uPA chromatin population is converted to "non-amplifiable" material (compare the number of white vs. crossed-out circles in each large circle in the Figure 3.5). Conversely, the MNase-resistant uPA chromatin population (black circles Figure 3.5) is not affected by cleavage and, thus, is present in the same amount in the recovered DNA at each digestion time point and is amplifiable. Therefore: since the amount of amplifiable material from the resistant uPA chromatin population is constant, while that from the sensitive uPA chromatin population decreases, the relative ratio of resistant/sensitive "amplifiable" material increases at each digestion time point (compare the number of black vs. white circles in each large circles in the Figure 3.5). In other words: at early digestion time points amplifiable DNA from uPA chromatin originates from both the sensitive and the resistant population, whereas at intermediate and late digestion time points amplifiable DNA originates only from the resistant population. By the same token, the amount of total recovered DNA at each digestion time point (as $O.D._{A260}$ or as percentage of the undigested sample; large circles

Figure 3.5) decreases (Figure 3.3A) and, consequently, also its concentration will decrease if each sample is resuspended in the same volume. However, the relative ratio of resistant/total chromatin DNA increases at each digestion time point, since the amount of DNA from resistant uPA chromatin is constant (black circles Figure 3.5), and this will also increase the ratio of "amplifiable/non-amplifiable" sequences. Thus, PCR samples loaded with the same amount of genomic DNA (100 ng) contain more "amplifiable" sequences if the material is taken from the late digestion time point than from the early ones. As a result, samples containing material from the early digestion time points (few "amplifiable" sequences) display a loss of the PCR signal, whereas samples containing material from the late digestion time point show a rescue of the PCR signal (Figure 3.4B). Since F22/R26 and F26/R31 amplicons have a distinctive amplification pattern they were named DAF.

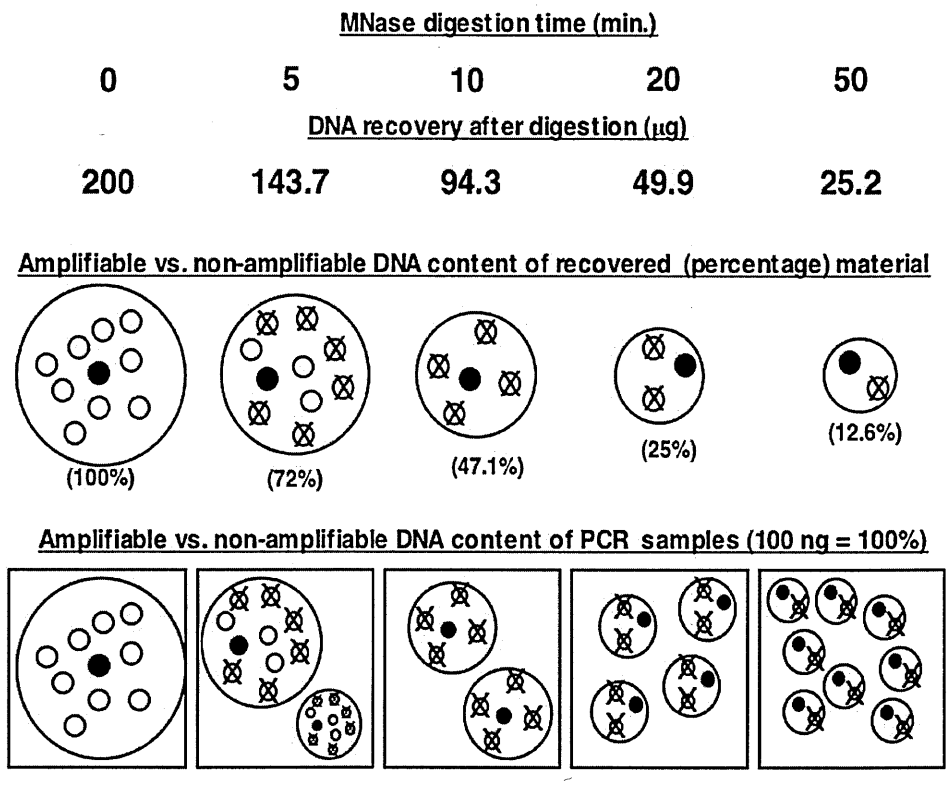

Figure 3.5. Scheme representing the interpretation of the distinctive amplification pattern of fragments amplifyed by PCR.

MNase cleaves unprotected DNA converting it to free nucleotides in a processive manner and, as a result, the amount of DNA recovered at each digestion time point decreases (see also Figure 3.3 A and B). The decrease in genomic DNA recovery is indicated in the figure and depicted by the decrease in size of the large circles. We postulate that the regulatory region of the gene is found in two chromatin configurations: one is more represented and sensitive to digestion (small white circles in the figure), while the other is less represented and is resistant to digestion (black circles). During MNase digestion a single nick in an "amplifiable" sequence renders it "non-amplifiable" (crossed-out circles), but the MNase-resistant uPA chromatin population is not affected. Therefore the relative ratio of resistant/sensitive "amplifiable" material increases at each digestion time point (compare the number of black vs. white circles in each large circles in the figure), implying that at intermediate and late digestion time points amplifiable DNA originates only from the resistant population. As mentioned above also the amount of total recovered DNA at each digestion time point (large circles) decreases and, consequently, the relative ratio of resistant/total chromatin DNA increases at each digestion time point. As a result loading the same amount of total of DNA in a PCR (large squares) for each digestion time point, samples containing material from the early digestion time points will have an high number of "amplifiable" sequences, that will decrease in the middle time points and that will increase again at late time points giving the PCR pattern shown in Figure 3.4C and D.

3.1.5. Different resistant fragments are presents in the MP region of uPA.

Amplicons F22/R26 and F26/R31 share a common primer (F/R26 in Figure 3.4A); however, they displayed the lowest amplification signal at different time points. Thus we asked if they belonged to the same or different genomic populations by amplifying the region spanning both fragments using primers F22 and R31 (Figure 3.6A). In this case the amplification signal decreased with increasing digestion time (Figure 3.6B). Thus amplicons F22/R26 and F26/R31, specifically located at and upstream of the MP region of the uPA gene, belong to different DNA fragments, which become evident after enzymatic cleavage of the overlapping sensitive population to non-amplifiable material. Since that F22/R26 and F26/R31 amplicons were named DAF-A and DAF-B respectively.

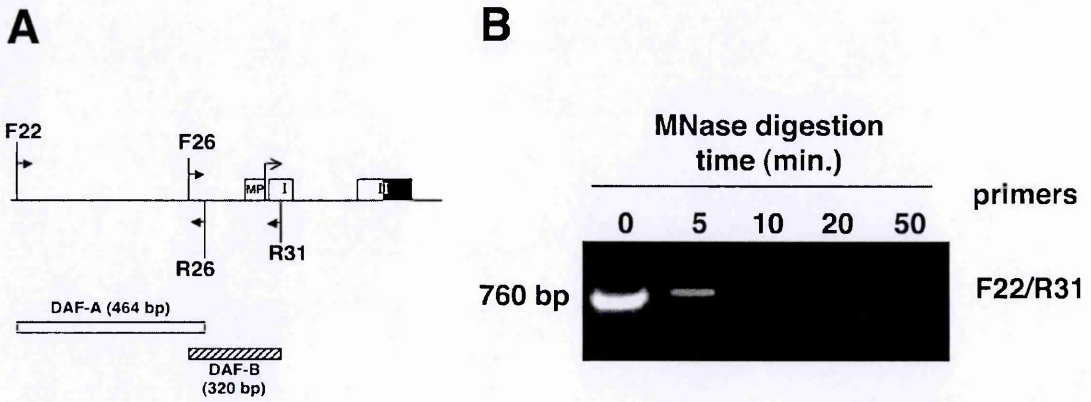

Figure 3.6. Presence of different DAFs amplicons in the MP region of the uPA gene. (**A**) Scheme (not to scale) of the amplified regions and primers used. Full arrowheads: primers (Table I) and their orientation. Empty arrowhead: transcription start site. White and hatched boxes: amplified fragments; MP: minimal promoter; roman number I: first,

untranslated exon of the uPA gene; white and black boxes with roman number II: untranslated and translated portions, respectively, of the second exon of the uPA gene. **(B)** Equal amounts of genomic DNA from each MNase digestion time-point were amplified by using the F22/R31 primer set (panel A) and PCR products revealed on a 2% agarose gel in 0.5x TBE stained with EtBr. Amplification products are visible only at the 0 and 5 minutes digestion time points, indicating that amplicons F22/R26 and F26/R31 do not belong to the same genomic fragment, but represent different chromatin populations.

3.1.6. Southern analysis of MNase digested ChIP-ready chromatin shows that DAF regions are subpopulation of the uPA regulatory region.

The speculation that DAF fragments originate from a MNase-resistant chromatin population implies that: 1) overlaying a Southern blot with the appropriate probe could show the presence of a specific resistant fragment at the late digestion time points; 2) the accumulation of mono-nucleosomes from a sensitive chromatin population would be different (more rapid), at the different digestion times, from that of a mixed (sensitive + resistant) chromatin population (slower). ChIP-ready chromatin was digested with MNase, as described in Materials and Methods. After purification, 15 μg aliquots of genomic DNA from each time point were fractionated on two separate agarose, gels, stained with EtBr and photographed (Figure 3.7 left panels in A and B). Fractionated DNA was transferred to a nylon membranes and the blots were incubated with specific probes for the enhancer (Figure 3.7 right panel in A) and DAF-A (Figure 3.7 right panel in B). We chose to use DAF-A as probe since the rescue of its PCR signal already occurred at 20 minutes, as compared to DAF-B and –Bx, where it occurred only at 50 minutes (see Figure 3.4B and C). Moreover, the enhancer region was chosen as a comparison because it did not show any recovery of the PCR signal (Figure 3.3C) and, therefore, it might represent a chromatin

population homogeneously more sensitive to cleavage than bulk. Genomic DNA in the EtBr stained gels was quantitated normalized to the value obtained for the 0 time point (sonicated material, no MNase digestion, arbitrarily set to 1) and plotted, together with the percentage of DNA recovery after MNase digestion at each digestion time point (see Figure 3.7C). The radioactive membranes were exposed and the radioactivity signals from each lane of both Southern blots (Figure 3.7 right panels in A and B) were acquired and quantitated by phosphoimager, normalized to the respective bulk chromatin values (EtBr stain; Figure 3.7 left panels in A and B) and then plotted as percentage of the value obtained for the 0 time point (sonicated chromatin, no MNase digestion, arbitrarily set to 1). The plot in Figure 3.7C shows that both gels were loaded essentially with the same amount of material at each digestion time point, thus compensating for the loss of genomic DNA due to MNase processivity. An analysis of the Southern blot labeled with the DAF-A probe (Figure 3.7 right panel in B) did not reveal the presence of a 464 bp band, corresponding to DAF-A at any digestion time point. Therefore we asked whether it was possible to show a differential accumulation of mono- and sub-nucleosomes between the enhancer and DAF-A regions, which we postulate to be made up by a homogeneously sensitive vs. mixed (i.e. sensitive and resistant) chromatin population, respectively. To our surprise a comparison of the radiolabeled blots with their respective EtBr stained gels (Figure 3.7 right and left panels, respectively, in A and B) indicated that the enhancer and DAF-A regions yielded a substantial mono- and sub-nucleosomal fraction already after sonication, as compared to bulk chromatin. This suggested that chromatin in the regulatory region of the uPA gene was more sensitive to "mechanical" severing than bulk chromatin and corroborated the result shown in Figure 3.1, where the 1,574 bp fragment was

detectable only in the input sample, but not in the immunoprecipitated material. A technical implication of this result was that sonication did not equally affect all chromatin. It appeared, then, that further MNase digestion of such material had a reduced chance to highlight a difference in the accumulation of mono- and sub-nucleosomes from a sensitive (enhancer) vs. mixed (DAF-A) population. However, when we plotted the quantitation results of the probed Southern blots (Figure 3.7D), we could observe a different behavior of the enhancer and DAF-A regions. The former was rapidly digested and reached a plateau after 5 minutes, indicating that no further conversion to mono- and sub-nucleosomes could occur. The DAF-A region, on the other hand, was converted to mono- and sub-nucleosomes more slowly and reached the plateau after 10 minutes. Interestingly, Figure 3.3B shows that the lowest PCR signal (approximately 50 fold less than the signal at the 0 time point) yielded by the DAF-A fragment occurs at this digestion time point, when further conversion of this region to mono- and sub-nucleosomes could not occur. This observation, together with the lack of a detectable fragment in the Southern blot (Figure 3.7 right panel in B), indicates that such DAFs are present in a very low amount as the Southern blot technique is not sufficiently sensitive to reveal DAF-A. However, they are detectable by the exponential amplification provided by PCR that represents a more sensitive detection system.

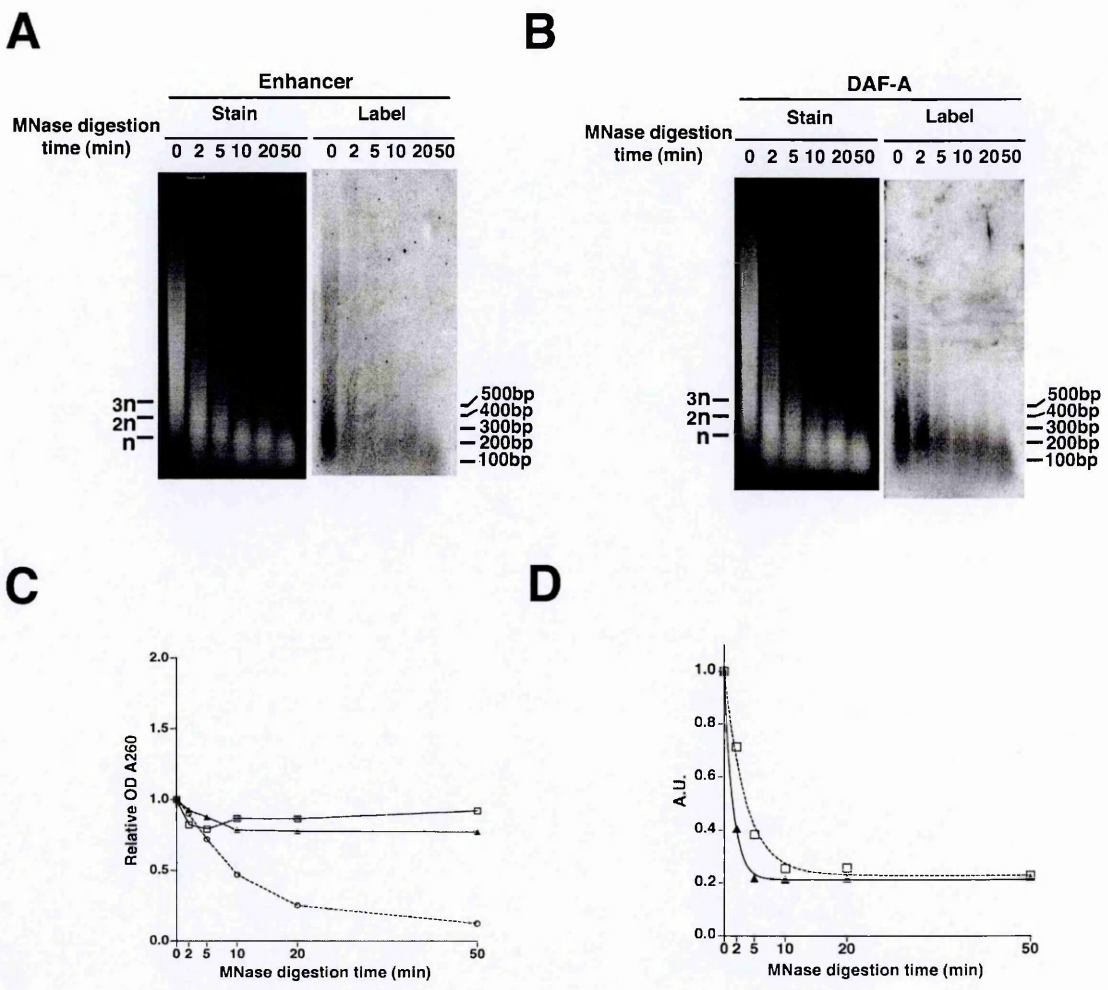

Figure 3.7. DAFs correspond to a low represented subpopulation of uPA gene.
ChIP-ready chromatin was digested with MNase, as described in Materials and Methods. After purification, 15 μg aliquots of genomic DNA from each time point were fractionated on two separate 1% agarose, 0.5x TBE gels, stained with EtBr and photographed (**left panels in A and B**). Fractionated DNA was transferred to nylon membranes as described in material and methods. The blots were incubated with specific radiolabeled probes for the enhancer and DAF-A obtained by PCR using primers F5/R14 and F22/R26, respectively (see Table I). The radioactive membranes were exposed and the acquired images are shown in (**A and B right panels**). Genomic DNA in the EtBr stained gels was quantitated using Image Quant software, normalized to the value obtained for the 0 time point (sonicated material, no MNase digestion, arbitrarily set to 1) and plotted in (**C**) (full triangles: EtBr stain of the left panel in A; empty squares, EtBr stain of the left panel in B), together with the percentage of DNA recovery after MNase digestion at each digestion time point (empty circles). The radioactivity signals from each lane of both Southern blots (right panels in A and B) were quantitated with Image Quant software, normalized to the

respective bulk chromatin values (EtBr stain; left panels in A and B) and then plotted as percentage of the value obtained for the 0 time point (sonicated chromatin, no MNase digestion, arbitrarily set to 1) in **(D)**. Full triangles: enhancer probe signal; empty squares: DAF-A probe signal. A.U.: arbitrary units. The graph in (C) shows that both gels were loaded essentially with the same amount of material at each digestion time point, thus compensating for the loss of genomic DNA due to MNase processivity. The quantitation results plotted in (D), show a different behavior of the enhancer and DAF-A regions. The former was rapidly digested and reached a plateau after 5 minutes, indicating that no further conversion to mono- and subnucleosomes could occur. The DAF-A region, on the other hand, was converted to mono- and sub-nucleosomes more slowly and reached the plateau after 10 minutes. However the analysis of the Southern blot labeled with the DAF-A probe (right panel in B) did not reveal the presence of a 464 bp band, corresponding to DAF-A at any digestion time point, indicating that the Southern blot technique is not sufficiently sensitive to reveal DAF-A and that DAFs correspond to a little represented subpopulation of uPA gene only detectable by PCR.

3.1.7. Defining the borders of DAF-A and DAF-B.

Since DAF-A and DAF–B represent different chromatin populations we next established their size by amplifying increasingly longer fragments, assuming that the amplification pattern of amplicons F22/R26 and F26/R31 would be maintained if longer fragments belonged to the same chromatin populations. Figure 3.8B shows that the amplification pattern of DAF-A was lost using either primer F21 (5' extension) in combination with R26 or primer R27 (3' extension) in combination with F22. This suggests that primers F22 and R26 are located close to or at the borders of DAF-A. On the other hand we could extend the amplification pattern of DAF-B in the 3' direction, using primers R34 and R36, but not R37, in combination with F26 (Figure 3.8C). However, by using primer F25 in combination with R31 the pattern of amplicon DAF-B was lost in the 5' direction. Thus DAF-B could be extended to the untranslated portion of the second exon of the uPA gene

(Figure 3.8A) and (Riccio et al., 1985). Amplicon F26/R36 was named DAF-B "extended" (DAF-Bx).

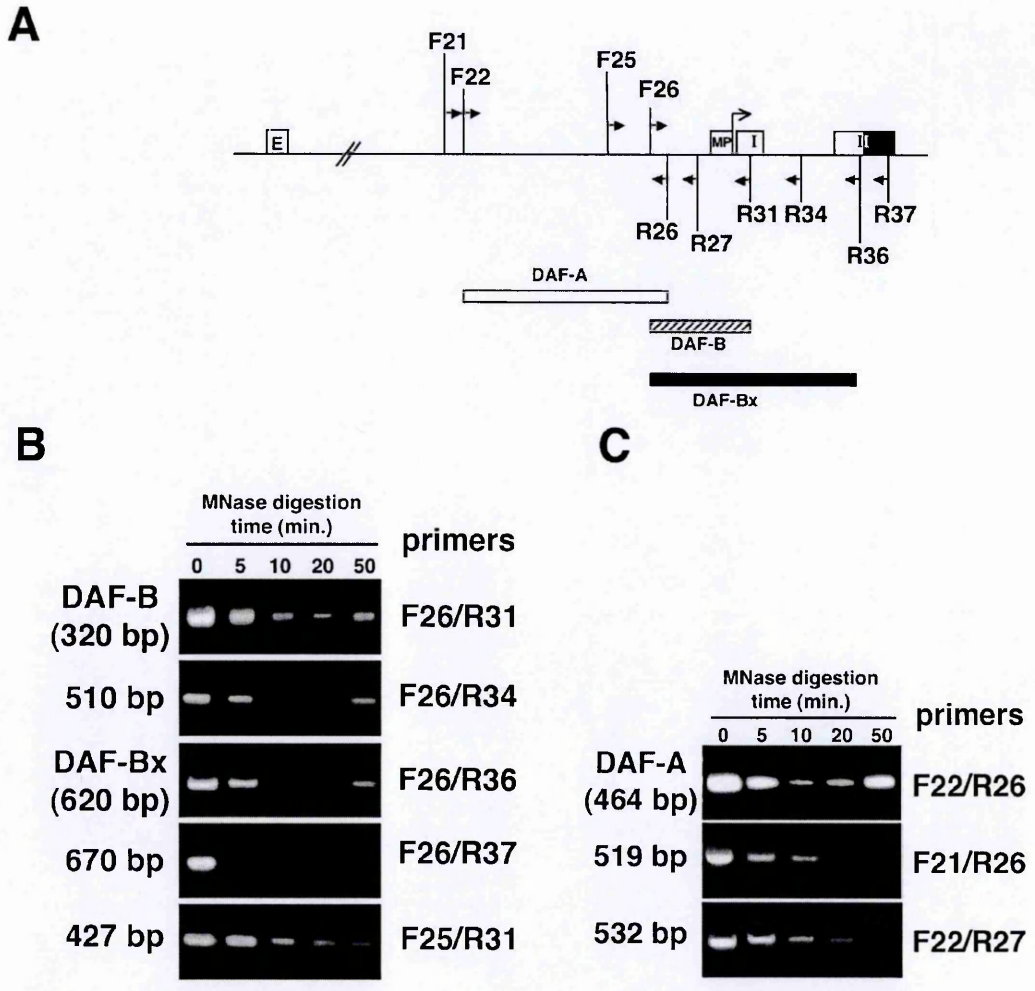

Figure 3.8. Defining the borders of DAF-A and -B.
Genomic DNA prepared as in Figure 3.3 was amplified with primers located upstream and downstream of DAF-B (F25 and R34, R36, and R37, respectively) and -A (F21 and R27, respectively) in combination with the upstream or downstream primers used in Figure 3.4 that define the amplification pattern of DAF-A and -B. The PCR products were fractionated on a 2% agarose gel in 0.5x TBE and visualized by EtBr staining. (**A**) Scheme of the primer sets used and of the amplified regions (not to scale). White and striped boxes are as in Figure 3.4 Black box: DAF-Bx amplicon. E: enhancer. MP: promoter. I: first exon and II: second exon of the uPA gene (white box: untranslated region). (**B**) The amplification pattern of DAF-B is extended in the coding region of the uPA gene by using primers R34 and R36 in combination with F26 and is lost using primer R37. The pattern

could not be extended 5' of DAF-B, using primer F25 (upstream of F26) in combination with R31. (C) Loss of the amplification pattern of DAF-A by using primer F21 in combination with R26 and F22 in combination with R27.

3.1.8. DAF-A, -B and -Bx amplicons represent discrete chromatin structures with different protein contents

Given their proximity to the uPA MP, we asked if the DAF-A, -B and -Bx amplicons were associated with transcription and analyzed their protein content. We focused our attention on three polypeptides: histone H3, since its post-translational modifications are strictly related to the transcriptionally active or inactive state of the gene (Nightingale et al., 2006), HMGN proteins, which are components of active chromatin (Bustin, 1999), and RNAP II. To perform the experiments we used MN-ChIP. ChIP-ready chromatin was digested with MNase for 50 minutes and subsequently immunoprecipitated with the antibodies indicated in Figure 3.9. The resulting genomic DNA was amplified by PCR using the primers sets for DAF-A, -B and –Bx (Figure 3.9A). The results in Figure 3.9B show that DAF-A contains histone H3 both acetylated and dimethylated at lysine 9. This finding is intriguing, since the modifications affect the same residue and have opposite effect on transcriptional activation, but we did not investigate this issue further. The histone modifications associated with DAF-B (H3K4me2, H3K9ac and H3K14ac) are all established marks of transcriptionally active chromatin (Bernstein et al., 2005; Schübeler et al., 2006) (Figure 3.9B). This is in agreement with previous results showing the presence of a DNase I hypersensitive site on the uPA MP in PC3 cells (Ibanez-Tallon et al., 2002). We also found that DAF-B is associated with HMGN1, another hallmark of transcriptionally active

chromatin. Unexpectedly, we found DAF-Bx to be associated only with H3K9ac and H3K14ac (Figure 3.9B), which suggest that DAF-B and -Bx may represent different chromatin populations. This view is supported by the experiment showing that only DAF-B is associated with RNAP II in its elongating form (phosphorylated at serine 2 of the CTD), whereas DAF-A and DAF-Bx are not (Figure 3.9C). Overall the results indicate that the uPA MP region contains three distinct chromatin populations, one of which (DAF-B) is actively engaged in transcription.

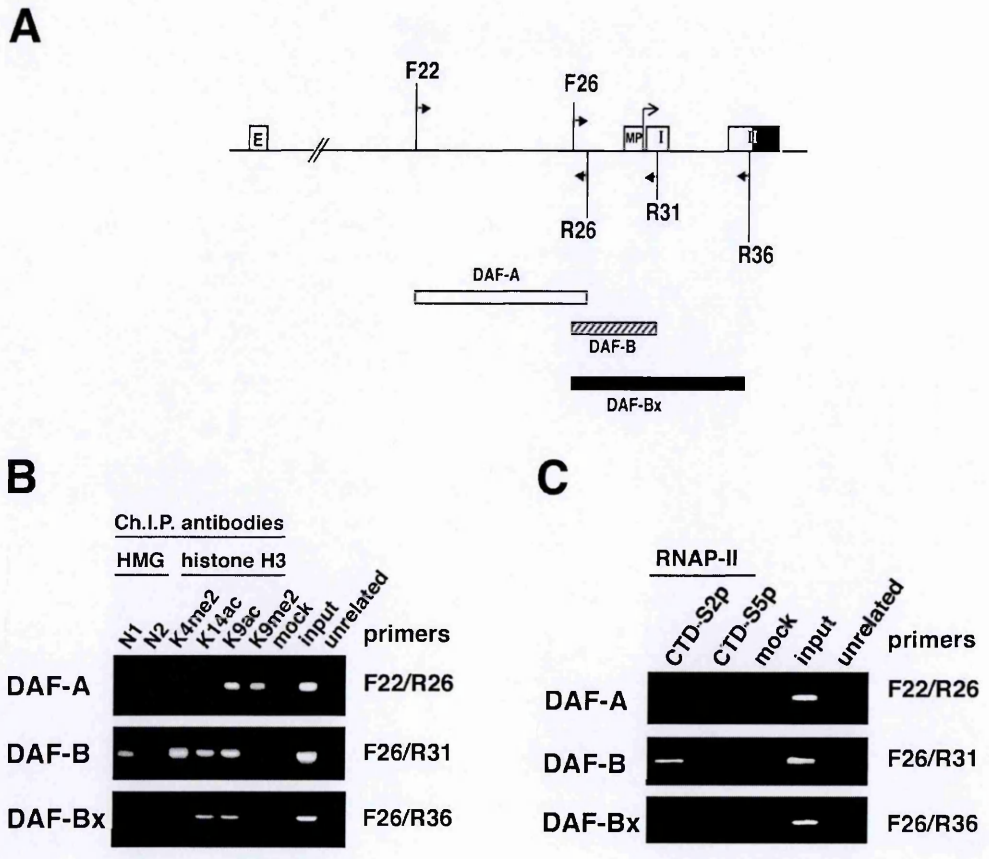

Figure 3.9. Different protein content of DAF-A, -B and -Bx.
ChIP-ready chromatin was digested for 50 minutes with MNase and subsequently immunoprecipitated with the antibodies indicated in the figure, with an antibody against the uPA receptor (unrelated) or treated like the immunoprecipitated samples, but omitting the antibody (mock). The immunoprecipitated, purified genomic DNA was amplified with

the primer sets specific for DAF-A, -B and –Bx and fractionated on a 2% agaose gel. Input DNA was a 1:1000 dilution of the DNA from the 50 minutes digestion time-point prior to immunoprecipitation. (**A**) Scheme of the primer sets used and of the amplified regions (not to scale). Symbols are as in Figure 3.8. (**B**) Amplification of immunoprecipitated genomic DNA with antibodies to histone H3 post-translational modifications and HMGN proteins, whereas in (**C**) amplification material was from DNA immunoprecipitated with antibodies against the functionally different forms of RNAP II. DAF-A, -B and-Bx display substantially different protein contents and only DAF-B is associated with the elongating form of RNAP II (CTD-P-S2) indicating the presence of three distinct chromatin population in the uPA MP region.

3.1.9. The presence of DAF-A, -B and -Bx depends on ongoing transcription.

The protein composition of DAF-A, -B and -Bx and the specific association of DAF-B with the elongating form of RNAP-II prompted the speculation that the amplicons might underlie large complexes of transcriptional nature. Thus we treated PC3 cells with α-amanitin, an inhibitor of RNAP-II (Casse et al., 1999; Nguyen et al., 1996), and asked what was the fate of the DAF amplicons in drug-treated PC3 cells, assuming that complexes not involved in transcription would persist despite the treatment. ChIP-ready chromatin was prepared from α-amanitin-treated cells and then used for a MNase digestion time-course experiment. Purified DNA from each digestion time point was amplified with the specific primers for DAF-A, -B, -Bx and with the F29/R31 primer set, amplifying a nucleosome-size fragment (199 bp) within DAF-B (Figure 3.10A). Figure 3.10B shows that the PCR signal of DAF-B gradually decreased and was not rescued using material from the 50 minutes time point, unlike the experiments in Figure 3.4B. Unexpectedly, also the signals for DAF-A and -Bx decreased throughout the digestion time course. However,

at all digestion time points we were still able to detect nucleosome size genomic fragments located within DAF-B (199 bp in Figure 3.10B) and on the enhancer (150 bp, not shown), suggesting that drug treatment had perturbed the specific structures associated with DAF-A, -B and -Bx, but not the overall structure of the regulatory region. The results indicate that the presence of the DAF amplicons depends on active transcription.

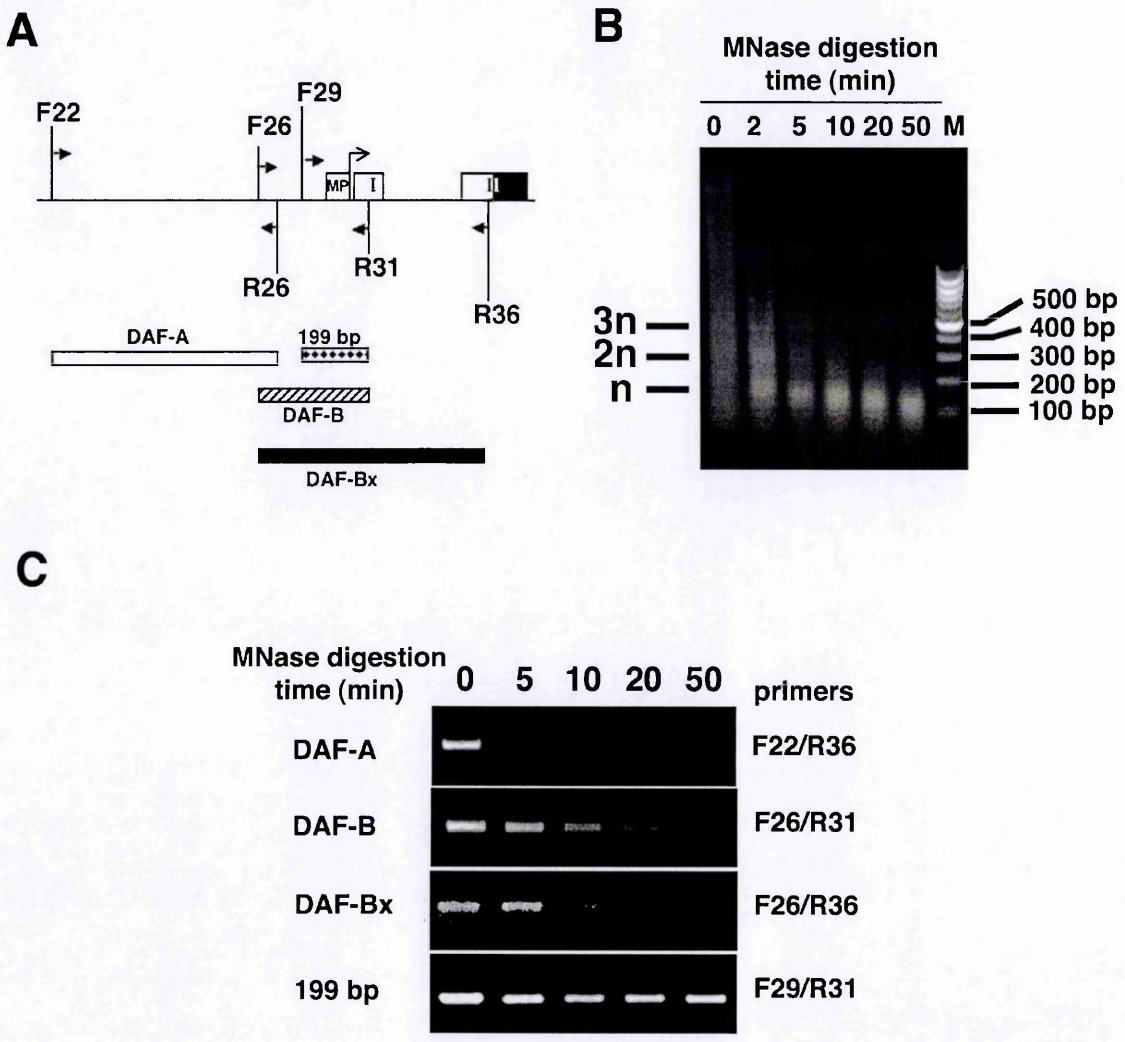

Figure 3.10. The presence of DAF-A, -B and -Bx depends on active transcription. The concentration of α-amanitin to be used in PC3 cells treatment (10 mg/ml for 24 hours) was determined in a dose-response experiment in which the endogenous levels of uPA mRNA were determined by qRT-PCR at each α-amanitin concentration (data not shown). (**A**) Scheme of the amplified regions and the primers used for DAF amplicons are as in

Figure 3.8. Squared box: the 199 bp (nucleosome size) fragment amplified with the F29/R31 primer set is contained in the DAF-B amplicon. (**B**) MNase-digestion of cross-linked chromatin from α-amanitin-treated PC3 cells generates a genomic DNA ladder similar to that obtained from untreated cells (compare with figure 3.3B). n, 2n, 3n: mono-, di- and tri-nucleosome size DNA; M: DNA size marker (fragments length is indicated to the right). (**C**) Loss of the amplification pattern of DAF-A, -B and -Bx using MNase-digested, ChIP-ready chromatin from α-amanitin-treated PC3 cells, as detected on a 2% agarose, 0.5x TBE gel stained with EtBr. The results indicate that the structures associated with the DAF amplicons are sensitive to drug treatment of PC3 cells, but the nucleosomal structure of the uPA regulatory region is maintained.

3.1.10. Chromatin proteins and RNAP II content of nucleosome-size fragments in the uPA enhancer region.

We thought that the presence of specific transcription-dependent chromatin structures in the uPA MP region might facilitate our search for evidences of an interaction between the enhancer and the promoter. Since DAF-B spans the MP and was found associated with RNAP II, this was the most likely candidate for such an interaction. Therefore we asked if the MN-ChIP immunoprecipitates that contained DAF-B (see Figure 3.9) also included one or more fragments (~145 bp to ~190 bp long) encompassing the uPA enhancer, as detailed in the scheme of Figure 3.11A. The results of Figure 3.11B show that all the immunoprecipitates contained fragments spanning the enhancer, with the notable exception of fragment 6, which was not immunoprecipitated by any of the antibodies used (Figure 3.11B). Interestingly fragment 7 corresponding to the DNA sequence immediately upstream of the enhancer was found to associate with the poised form of RNAP-II (CTD-S5p) (Figure 3.11B). However, the only fragment immunoprecipitated by the same combination of antibodies that also immunoprecipitated DAF-B, including α-CTD-S2p

and α-HMGN1, was fragment 1 (Figure 3.11B). We conclude that fragment 1 and DAF-B represent populations of enhancer and MP interacting with each other.

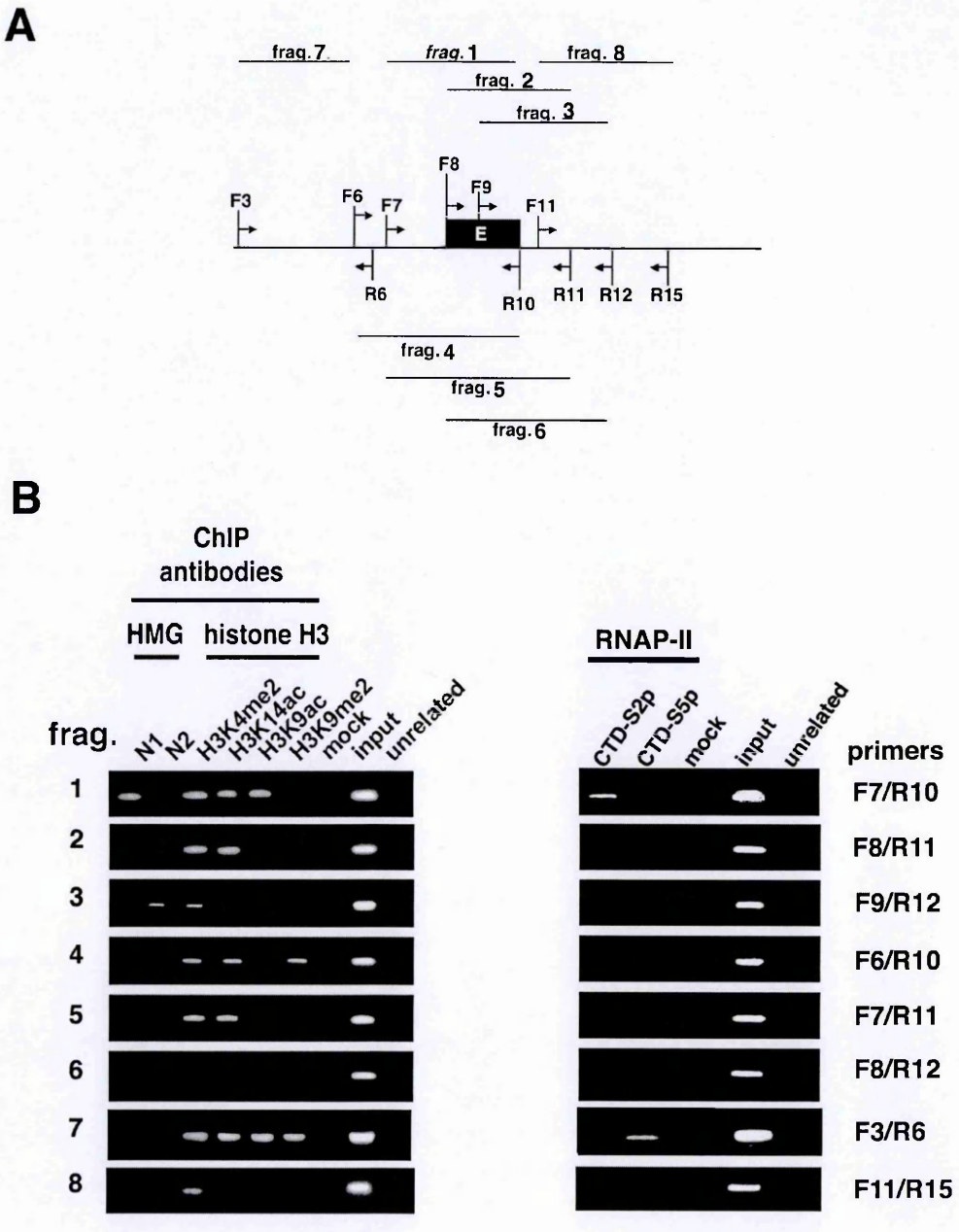

Figure 3.11. Protein association of nucleosome-size fragments in the enhancer region of the uPA gene.

The same material immunoprecipitated for the experiment in Figure 2.9 was amplified with primer sets spanning various genomic fragments at and around the uPA enhancer. PCR products were visualized on a 2% agarose, 0.5x TBE gel by EtBr staining. **(A)** Scheme (not to scale) of the uPA enhancer (black box with E) region, of the primers used and their orientation (black arrowheads and Table I) and of the expected amplification products (frag. 1, 2, 3 and 7, 8: ~145 bp; frag. 4, 5 and 6: ~190 bp amplification products). **(B)** Amplification products of different PCR reactions with the indicated primers. Various genomic fragments were associated with different histone H3 post-translational modifications, HMGN proteins and RNAP-II. Only frag. 1 was associated with the exact same proteins as DAF-B (compare with Figures 2.9B and C).

3.1.11. The presence of RNAP II on the uPA enhancer is due to its interaction with the MP.

The presence of RNAP II on the uPA enhancer raises the possibility that this region is part of an independent transcription unit, nested in the uPA locus. To formally exclude the presence of RNA in the enhancer region we reverse-transcribed total RNA from PC3 cells with random primers and amplified the resulting products with primers spanning fragment 1 and fragments of similar size located 5' (fragment 7) or 3' (fragment 8) of fragment 1 (Figure 3.12A); we also amplified a fragment in the coding region of the uPA gene from + 194 to + 420 as positive control. The results in Figure 3.12B clearly indicate that the enhancer and neighboring regions are devoid of mRNA, which, as expected, is present in the coding region of the uPA gene. Therefore the presence of RNAP II CTD-S2p on the enhancer is likely to be due to its interaction with the MP. This was further supported by the absence of fragment 1 in the MN-ChIP immunoprecipitate (with α-CTD-S5p and α-CTD-S2p) from α-amanitin-treated PC3 cells (Figure 3.12C), in which we observed the loss of DAF-B (Figure 3.10B).

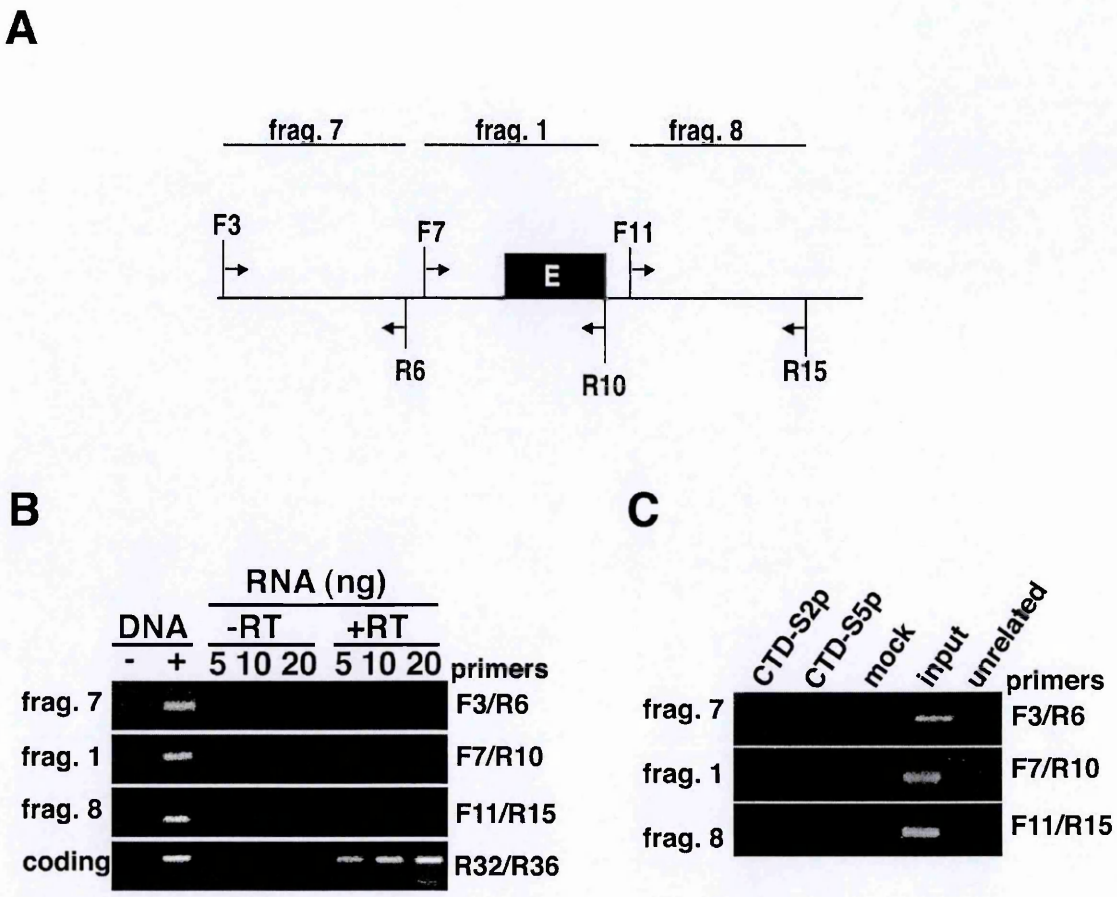

Figure 3.12. The presence of RNAP II on the uPA enhancer is not due to a nested transcription unit and is sensitive to α-amanitin treatment of PC3 cells.
(**A**) Scheme depicting the primer sets used and the amplified fragments in the enhancer region of the uPA gene (not to scale). Black box with E: enhancer. (**B**) Total RNA was extracted, reverse-transcribed and increasing amounts amplified with the primers indicated in panel A, spanning fragments 1, 7 and 8 in the enhancer region and a 226 nt fragment in the coding region (see Table I). As controls, genomic DNA (+) and non-retrotranscribed RNA (-RT) were also amplified with the same primers. PCR products were visualized on a 2% agarose, 0.5x TBE gel stained with EtBr. The lack of mRNA in this region indicates the absence of a cryptic transcription unit. (**C**) MNase-digested (50 minutes), ChIP-ready chromatin from α-amanitin-treated PC3 cells was immunoprecipitated with antibodies against the phosphorylated forms (CTD-S2p and CTD-S5p) of RNAP II. The immunoprecipitated material was amplified with primer sets for fragments 1, 7 and 8 and the PCR products and visualized as above. Following α-amanitin treatment of PC3 cells fragment 1 is no longer associated with RNAP II (CTD-S2p). The results indicate that the presence of RNAP II on the enhancer is due to its interaction with the MP (DAF-B).

3.1.12. c-Jun, that specifically binds the uPA enhancer, is also associated with the DAF-B amplicon.

To reciprocate the experiment of Figure 3.1, we asked whether antibodies against c-Jun, a transcription factor that specifically binds the uPA enhancer and not the MP (Cirillo et al., 1999; Nerlov et al., 1991) could also immunoprecipitate DAF-B. MN-ChIP immunoprecipitated material was amplified with primer sets spanning fragment 1 and fragment 8 on the enhancer and DAF-B on the MP (F7/R10, F11/R15 and F26/R31, respectively; Figure 3.13A). The results showed that both fragment 1 and DAF-B sequences were present in the immunoprecipitate (Figure 3.13B). However fragment 8 (immediately downstream of fragment 1) is devoid of c-Jun (Figure 3.13B). Furthermore the presence of c-Jun in the enhancer and MP regions was abolished by the α-amanitin treatment of PC3 cells (Figure 3.13C), further corroborating the role of these fragments in the interaction. Overall, our results lead us to conclude that fragment 1 and DAF-B are populations of interacting enhancer and MP, as depicted in the model of Figure 3.14.

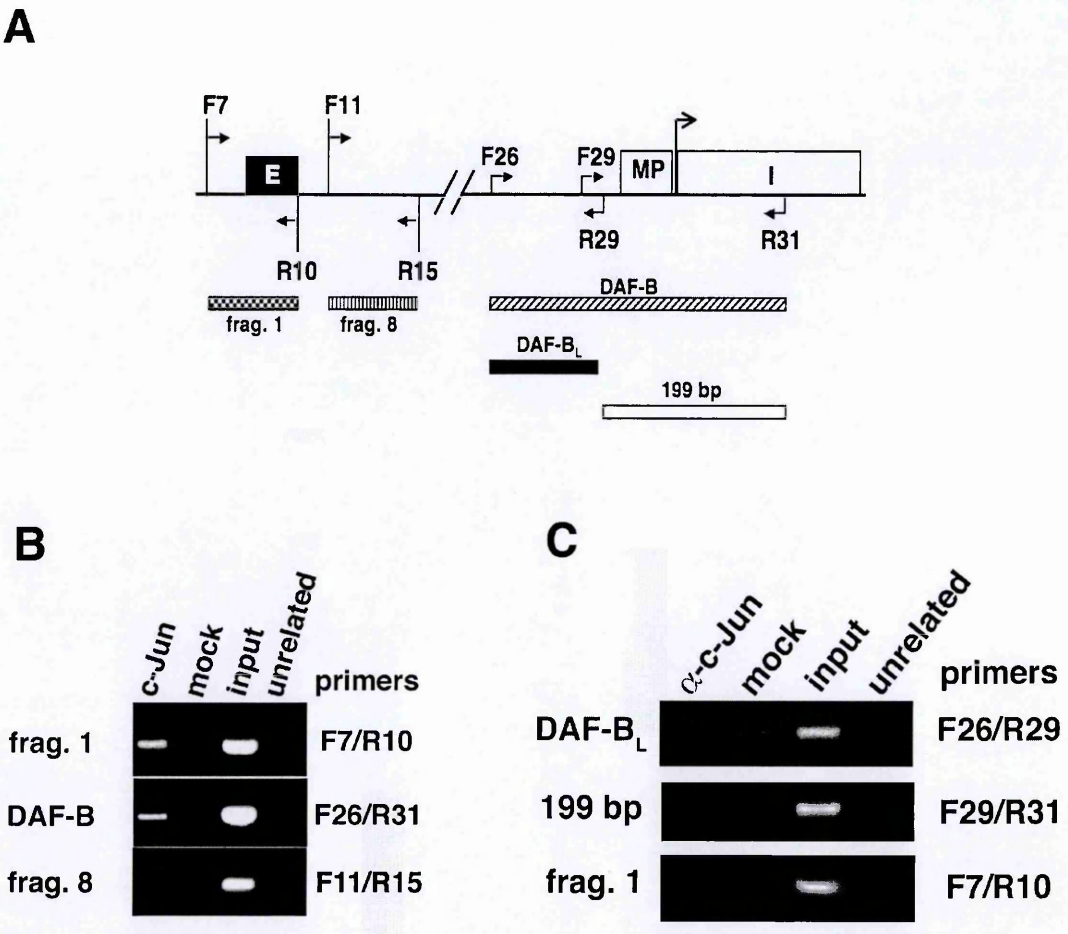

Figure 3.13. c-Jun, a transcription factor specifically binding the uPA enhancer, immunoprecipitates the MP of the gene. The material used for the experiment in Figure 3.9 was also immunoprecipitated with antibodies against c-Jun, a transcription factor that specifically binds the uPA enhancer. The immunoprecipitated genomic DNA was amplified with primer sets specific for enhancer (fragment 1 and fragment 8) and MP (DAF-B) sequences and the products visualized on a 2% agarose, 0.5x TBE gel by EtBr staining. (**A**) Scheme (not to scale) of the primer sets used and of the amplified fragments. Symbols are as in Figures 3.8 and 3.11. (**B**) Amplification of immunoprecipitated material with the appropriate primer sets shows that c-Jun is associated with both enhancer and MP sequences. C-Jun is absent from a sequence located downstream of the enhancer (fragment 8). (**C**) MNase-digested (50 minutes), ChIP-ready chromatin from α-amanitin-treated PC3 cells was immunoprecipitated with antibodies against c-Jun and the resulting purified DNA was subjected to PCR reactions with the overlapping F26/R29 and F29/R31 primer sets, spanning the whole DAF-B fragment, and with the F7/R10 primer set, spanning the enhancer. We chose to amplify fragments smaller than DAF-B in the MP region because the results of Figure 3.10 indicate that such fragment cannot be amplified using genomic DNA from α-amanitin-treated PC3 cells. However, a nucleosome-size DNA fragment can

still be amplified in this region (199 bp amplicon in Figure 3.10). Thus we decided to check whether c-Jun was present on this fragment or on an overlapping fragment, immediately upstream (DAF-B_L). The results show that c-Jun is absent from this region and from the enhancer in the immunoprecipitated material from α-amanitin-treated PC3 cells.

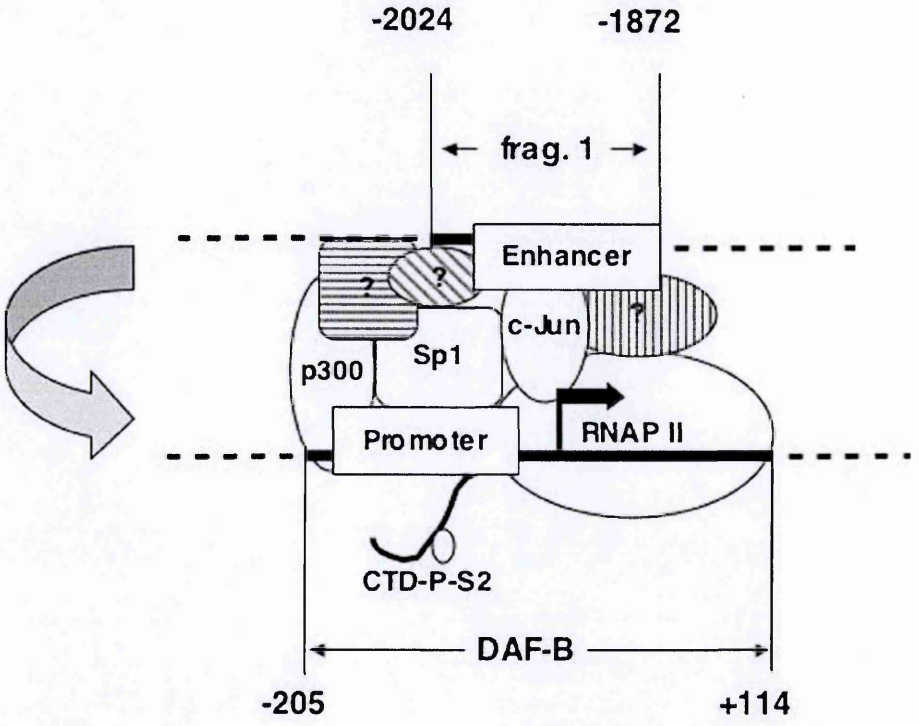

Figure 3.14. Model depicting the interaction between the regulatory elements of uPA. The enhancer and promoter of the uPA gene interact by looping of the IVS (curved arrow). Enhancer and promoter are shown in the position occupied within frag.1 (-2024/-1872) and DAF-B (-205/+114) amplicons (black bars). Sp1 and p300 are shown associated with the promoter and c-Jun associated with the enhancer; both are shown interacting with RNAP II. The elongating form of RNAP II (CTD-S2p) is shown entering the coding region. Striped boxes with question marks: other possible components contributing to the interaction between enhancer and promoter. Broken lines: sequences upstream and downstream of frag.1 and DAF-B.

DISCUSSION -I-

For many years transcription has been thought of as mere consequence of binding of the transcriptional machinery to specific regulatory sequences. However, long-range chromatin interactions between distal regulatory elements have revealed a more complicated scenario (Fraser, 2006). The control of most genes involves the activities of remote elements, which are essential in turning on or off specific subsets of genes in a temporally and spatially regulated manner (Li et al., 1999). Thus it is of fundamental importance to understand the molecular mechanisms involved in this process.

3.2.1. MN-ChIP a new approach to study the interaction between DNA regions.

The β-globin cluster has provided a paradigm for long-distance interactions of regulatory elements. RNA-TRAP and 3C experiments have lead to the identification of interacting sequences (Carter et al., 2002; Tolhuis et al., 2002) and ChIP experiments have characterized the histone content of the chromatin fiber of the cluster (Litt et al., 2001a; Litt et al., 2001b). However, the experiments have been carried out independently and, thus, the protein composition of interacting sequences is inferred from the results. Therefore, formal evidence that specifically interacting structures have a defined protein composition is not yet available. This is, at least in part, due to inherent limitations of the

RNA-TRAP, 3C and ChIP technique. The former does not provide data on the protein composition of the interacting structures. In the latter, the sonication step produces DNA fragments that are too large for a high-resolution analysis, but sufficiently small to establish that interacting sequences (positioned many kilobases apart) are indeed located on different fragments. Extensive digestion of ChIP-ready chromatin with MNase has two advantages: 1) It generates genomic fragments that are physically defined by the endpoint of cleavage, since MNase is a processive enzyme that stops when it finds a (physical) barrier that hinders further cleavage; 2) It allows the study of the protein composition of the specific fragments.

3.2.2. Active transcription and DAF formation.

What generates the possible complexes that give rise to MNase-resistant genomic fragments is an open question. It is unlikely that this is due to nucleosomes sliding in a closely packed configuration since we have previously reported the presence of a DNase I hypersensitive site in PC3 cells in the exact location of the DAF-B amplicon (Ibanez-Tallon et al., 2002). Furthermore, an indirect end-labeling experiment to map nucleosome positioning in this region would not be informative, since PC3 cells have multiple copies of the gene and not all of them are transcriptionally active (Helenius et al., 2001). This would lead to the detection of patterns that, although different, would overlap, resulting in the inability to distinguish the contribution of each structure to the final result. We favor the hypothesis that DAF amplicons are generated by the formation of complexes of a transcriptionally competent nature. This is supported by the evidence that they are

undetectable after α-amanitin treatment of PC3 cells and by the presence of the phoshorylated form of RNAP-II on DAF-B, both implying that ongoing transcription is a requisite for their presence. Nevertheless, DAF-A, -B and -Bx amplicons appear to underlie different chromatin populations, as indicated by their physical boundaries and protein content (see Figures 3.8 and 3.9).

3.2.3. DAF reflects the dynamic "on"/"off" waves of transcription in a steady state gene expression.

As mentioned above, DAF amplicons represent chromatin subpopulations of all the copies of the gene present in immunoprecipitable material. Their amplification pattern becomes visible only when the sensitive population is fully digested by MNase. This occurs only at long digestion time-points, when a large amount of material has been processed to mononucleosomes by the enzyme (see Figure 3.3). The lack of detection of DAFs by Southern blotting analysis suggests that DAFs represents very small chromatin subpopulations. This observation is consistent with quantitation of the steady state uPA mRNA levels in PC3 cells indicate that not all gene copies are transcribed (Helenius et al., 2001). Furthermore, previous reports indicate that constitutively active genes are not continuously transcribed. They shuttle between "on" and "off" states spending more time in the "off" state, so that, at any given time (steady-state level), the number of copies that are effectively engaged in transcription is underepresented (Levsky et al., 2002; Osborne et al., 2004; Ross et al., 1994). It is therefore feasible that DAF-A, -B and -Bx represent different structures formed during the onset of transcription, at steps that occur at low

kinetic rate (Hahn, 2004), such as promoter escape by RNAP II (Krumm et al., 1995; Krumm et al., 1992).

3.2.4. The specific interaction of the uPA enhancer and MP: formation of a single transcription control unit and looping of the IVS.

Besides the presence of the same chromatin proteins (HMGN1) and post-translational modifications (PTM) of histone H3 (H3K4me2; H3K9ac; H3K14ac), the interaction of uPA enhancer and MP is supported by the association of specific genomic fragments (DAF-B and fragment 1, Figure 3.8), spanning the regulatory elements, with the elongating form of RNAP II and with transcription factors that specifically bind either the enhancer (c-Jun) or the MP (Sp1) (Figures 3.13A and 3.1). Interestingly, the association of the same histone H3 post translational modifications and chromatin proteins with both the uPA enhancer and MP indicates the inherent inability of the ChIP approach to determine whether these proteins are actually present on both elements or if they are differentially contributed by enhancer and MP to the final structure. It also suggests, from a functional standpoint, that such a distinction is irrelevant, since both elements (and related chromatin structures) are required for transcriptional activation. More importantly, this is further supported by the association of RNAP-II, Sp1 and c-Jun with both elements, regardless of the location of their specific binding site, indicating that the resulting structure functions as a single transcription control unit.

3.2.5. The interaction between enhancer and MP of uPA persists after transcriptional activation.

The interaction between enhancer elements and proximal promoters culminate in the transcriptional activation event (Carter et al., 2002; Hatzis and Talianidis, 2002; Tolhuis et al., 2002) . However, it is not clear if such an event stems from the transient interaction of regulatory elements or through a more stable structure. Interestingly, we found that one of the sequences embedded in the uPA transcriptional control unit (DAF-B) spans from –205 to +114 thus including a substantial portion of the coding region. This indicates that the interaction between enhancer and MP is maintained during the early stages of transcriptional elongation and suggests that the early step of transcription may require a more stable interaction of the regulatory elements than previously thought

SUMMARY -I-

In this chapter we provide evidences that the interaction between the enhancer and the MP of the uPA gene occurs through specific structures (DAFs), identified and characterized through their sequences, location and protein composition. In particular, the sequences at and around the MP region were discriminated by their distinctive and persistent amplification pattern, as the result of MNase digestion of ChIP-ready chromatin, which depletes genomic DNA of cleavage-sensitive sequences. Importantly, the presence of

DAFs is transcription dependent. The results support a model in which the interaction of enhancer and MP is transcription-dependent, persists during the early stages of transcriptional elongation and causes the extrusion of the intervening sequence (looping).

Part of the data presented in this Chapter have been published in: Ferrai C, Munari D, Luraghi P, Pecciarini L, Cangi M, Doglioni C, Blasi F, Crippa MP. "A transcription-dependent MNase-resistant fragment of the uPA promoter interacts with the enhancer". J Biol Chem. 2007 Feb 28.

RESULTS AND DISCUSSION -II-

Poised uPA occupies a distinct RNAP-II CTD-S5p transcription factory.

RESULTS -II-

4.1.1. MNase digestion of cross-linked chromatin reveals the presence of a cleavage-resistant fragment spanning the uPA promoter before and after transcriptional activation of HepG2 cells.

MN-ChIP, allowed us to physically map the interacting regulatory sequences of the constitutively expressed uPA gene in PC3 cells and to characterize their specific association with nuclear proteins (Ferrai et al., 2007). We then applied this procedure to chromatin from HepG2 cells, in which the uPA gene is transcriptionally induced by the treatment of cells with phorbol esters (Ibanez-Tallon et al., 1999). Figure 4.1A shows that the mRNA levels of endogenous uPA mRNA increase in a time-dependent manner following TPA treatment of HepG2 cells. Thus ChIP-ready chromatin was prepared from HepG2 cells, either untreated or treated for three hours with TPA, and subjected to a digestion time-course with MNase, as previously described (Ferrai et al., 2007). The MNase digestion pattern obtained from ChIP-ready chromatin from TPA-treated HepG2 cells (Figure 4.1B) shows that chromatin was increasingly cleaved by the enzyme to mono- and sub-nucleosomal particles. The same pattern was obtained from untreated HepG2 cells

(not shown). Genomic DNA from the various digestion time-points was then subjected to PCR reactions with sets of primers amplifying increasingly larger (from 145 to 250 bp) fragments in the uPA enhancer region (Figure 4.1C). The results show that only core nucleosome- and chromatosome-size genomic fragments can be amplified using material from all the digestion time-points of untreated and TPA-treated cells (Figure 4.1D). This suggests that the enhancer region maintains its essential nucleosomal structure both before and after TPA treatment of HepG2 cells. A similar analysis performed on the promoter region shows the presence of a MNase-resistant genomic fragment (Persistent Fragment = PF in Figure 4.1E) spanning the minimal promoter of the gene, in agreement with what previously observed (Ferrai et al., 2007). Such fragment can be extended in the 5' direction (Persistent Fragment extended = PFx; Figure 4.1E), but not in the 3' direction (fragment 2; Figure 4.1E). On the other hand, the presence of fragment 1, upstream of PF and overlapping with PFx (Figure 4.1E) is not detected in HepG2 cells, differently from what observed in PC3 cells (Ferrai et al., 2007), suggesting that the detection of some fragments may be cell line-specific. Interestingly, the presence of PF and PFx is detected both before and after TPA treatment of HepG2 cells, indicating that transcriptional induction does not noticeably alter the chromatin structure of the MP region.

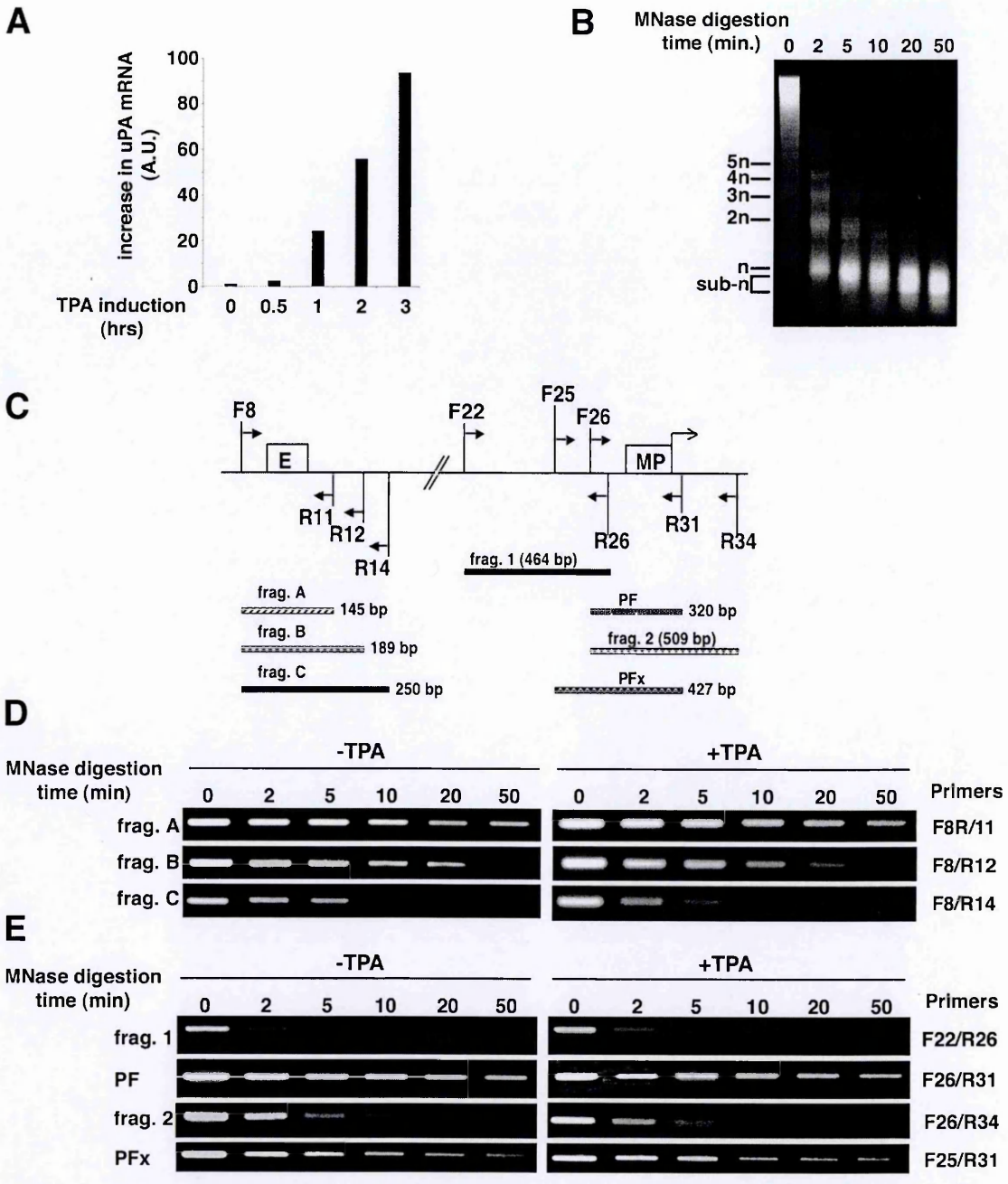

Figure 4.1. TPA do not affects sensitivity to MNase digestion on uPA gene.
(**A**). HepG2 cells were treated with TPA (Ibanez-Tallon et al., 1999) for the indicated times. Total RNA was extracted and processed for quantitative RT-PCR as described in material and methods. The normalized qRT-PCR results for each induction time-point were plotted in a graph. (**B**) Chromatin (treated or not with TPA) was cross-linked, fractionated, digested with MNase (for the times indicated) and genomic DNA purificated as described in material and methods. Bulk chromatin DNA at each digestion time-point was visualized by ehtidium bromide staining of a 2% agarose, 1X TAE gel. (**C**) Scheme

(not to scale) of the uPA gene regulatory region, outlining the enhancer (E), the minimal promoter (MP) and the genomic fragments (and their length) amplified with the indicated primers (see also Table 1). PF: persistent fragment; PFx: persistent fragment extended. **(D)** and **(E)** Genomic DNA from all the MNase digestion time-points of ChIP-ready chromatin, amplified with the indicated primers, was fractionated on agarose gels and visualized by Et-Br staining. The nomenclature of amplified fragments is as in panel (C).

4.1.2. Histone modification analysis shows that the regulatory elements of the uPA gene are in a permissive configuration before transcriptional activation.

We decided to investigate the chromatin composition of uPA regulatory elements before and after TPA induction and we studied the association of the enhancer and of the minimal promoter with histone H3 modifications associated with active (K4me2, K9ac, K14ac) or inactive (K9me2) chromatin (Nightingale et al., 2006). Thus we performed MN-ChIP experiments using ChIP-ready chromatin from untreated and TPA-treated HepG2 cells with antibodies against the specific histone H3 modifications. The rationale for the choice of amplicons (Figure 4.2A) was the following: 1) we have no evidence of a precise positioning of nucleosomes on the enhancer (Ibanez-Tallon et al., 1999) and therefore we wanted to test at least two alternative primer sets and compare them with a set of primers immediately outside the regulatory element; 2) we decided to split the PF amplicon in two smaller, overlapping amplicons (upstream PF and downstream PF = uPF and dPF, respectively; Figure 4.2C) to improve the resolution of the analysis in the MP region. Prior to transcriptional induction, fragment A, spanning the enhancer (Figure 4.2A), is associated with all histone H3 modifications indicating active chromatin (Figure 4.2B),

whereas in fragments D and E (Figure 4.2A) we only observe the presence of methylated and acetylated histone H3 (K4me2 and K14ac; Figure 4.2B). Before induction we do not detect the presence of H3K9me2 in any fragment. Following transcriptional induction (Figure 4.2B) fragment A is associated with the same histone H3 modifications as it is prior to induction (Figure 4.2B). Fragments D and E, on the other hand, are both associated with H3K4me2 and K9ac, but differ in the content of H3K14ac, present on fragment D (Figure 4.2B), and H3K9me2, present on fragment E (Figure 4.2B). A similar analysis was carried out in the promoter region. Figure 4.2D shows that PF was associated with H3K4me2 and H3K9ac prior to induction and only with H3K4me2 following TPA treatment (Figure 4.2D). However, an analysis of the same region with smaller amplicons indicates that they are associated with H3K4me2, K9ac and K14ac both before and after transcriptional induction of the uPA gene with TPA (Figure 4.2D). These results indicate that the chromatin of enhancer and promoter regions of the uPA gene are in a transcriptionally "permissive" configuration before transcriptional activation, in agreement with the "poised" state of chromatin detected by DNaseI hypersensitivity assay (Ibanez-Tallon et al., 1999). Moreover, the content of histone H3 modifications of the uPA regulatory elements is not substantially altered by transcriptional induction.

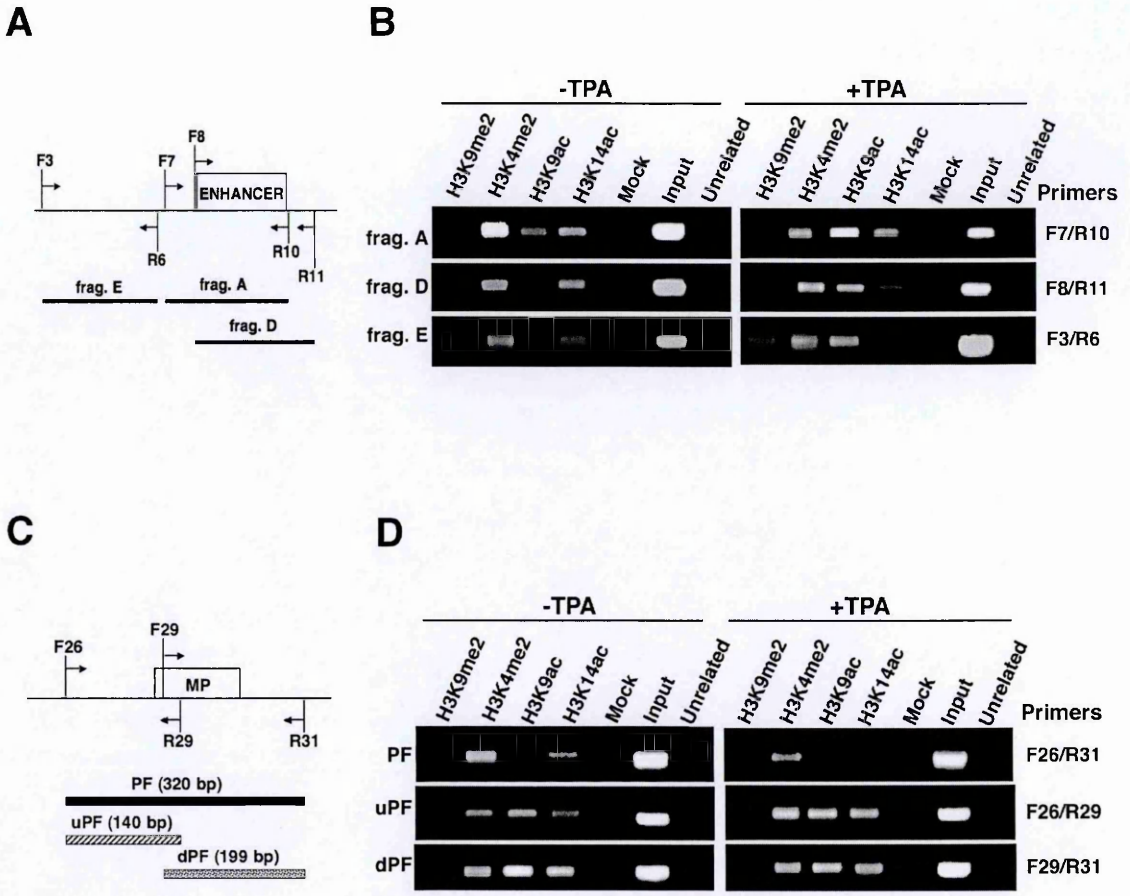

Figure 4.2. The regulatory regions of uPA are in a permissive state also before induction.

(**A**) and (**C**) Schemes (not to scale) of the enhancer and MP regions, respectively, indicating the primers used for amplification, their location and the position of the amplified fragments with respect to the regulatory elements. (**B**) and (**D**) ChIP-ready chromatin was digested with MNase for 50 minutes and the resulting material immunoprecipitated with the indicated antibodies, as described in material and methods. The resulting purified genomic DNA was amplified and visualized on 2% agarose, 1X TAE gels by Et-Br staining. Polyclonal anti-uPAR antibodies were used as the unrelated antibody (see material and methods).

4.1.3. uPA Enhancer and MP are associated with a poised RNAP-II before transcriptional activation.

We further looked for the presence of the RNAP-II in the enhancer and MP chromatin by immunoprecipitating the same material used for the experiments of Figure 4.2 with antibodies against the differentially phosphorylated forms of RNAP-II (CTD-S5p and CTD-S2p). The immunoprecipitated DNA was amplified with the primers shown in Figure 4.3A and C. The results show that prior to transcriptional induction both the uPA enhancer (fragments A and D; Figure 4.3B) and the MP (PF, uPF and dPF; Figure 4.3D) are associated with RNAPII CTD-S5p. Surprisingly also fragment E, upstream of the enhancer, was associated with the same form of RNAPII (Figure 4.3B). These results suggest that the regulatory elements of the uPA gene may be interacting prior to transcriptional induction of the gene and that such interaction involves larger genomic regions than the regulatory elements themselves, in agreement with our previous findings (Ferrai et al., 2007). Following TPA treatment, enhancer fragments A and D become associated with RNAP-II CTD-S2p, whereas fragment E remains associated with RNAP-II CTD-S5p (Figure 4.3B). Similarly the PF fragment, spanning the MP, becomes associated with RNAPII CTD-S2p, while its association with CTD-S5p persists (Figure 4.3D). Thus, the detection of uPA mRNA in HepG2 cells after three hours of TPA treatment (Figure 4.1A), is accompanied by the association of both regulatory elements with the elongating form of RNAP-II. It is feasible that the uPA promoter and enhancer form a non-productive single transcriptional control unit before transcriptional induction, which then becomes productive following TPA treatment.

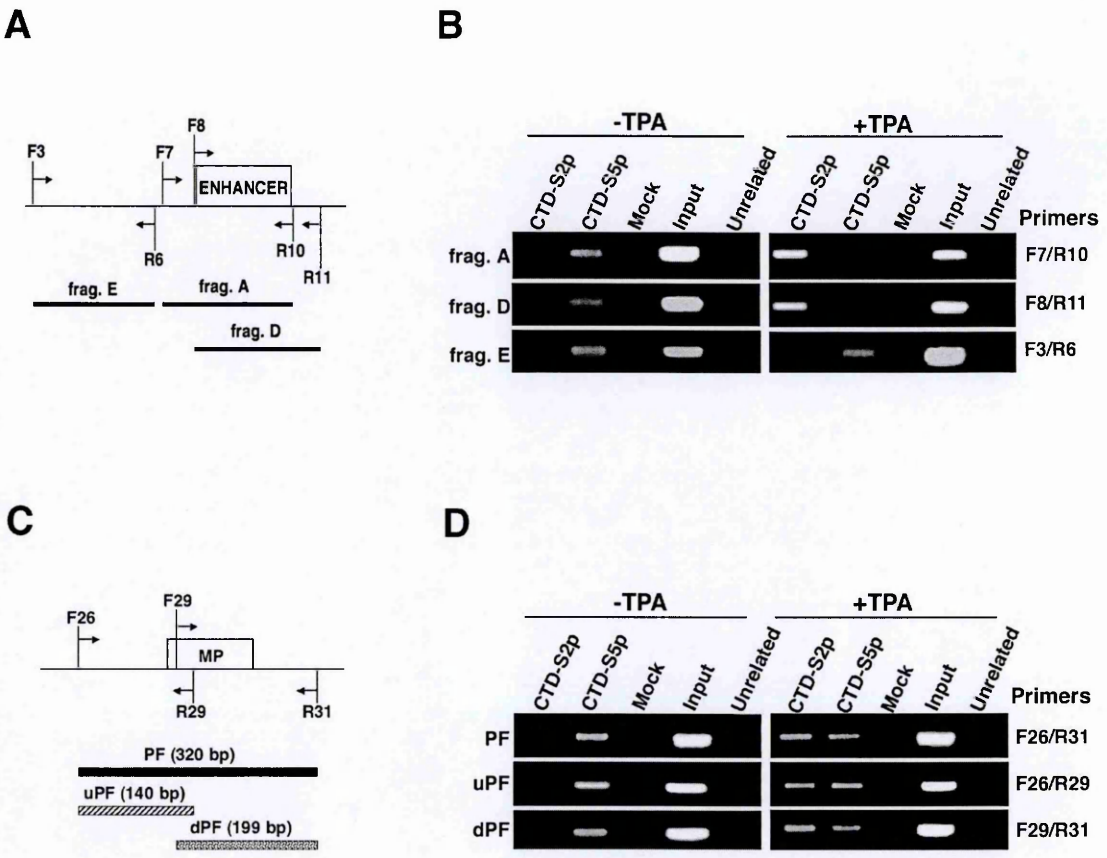

Figure 4.3. Poised RNAP-II associates with the regulatory regions of uPA before induction.

(**A**) and (**C**) Schemes (not to scale) of the enhancer and MP regions, respectively, indicating the primers used for amplification, their location and the position of the amplified fragments with respect to the regulatory elements. (**B**) and (**D**) Material prepared as in Figure 4.2 was immunoprecipitated with anti-CTD-S2p and anti-CTD-S5p antibodies. Further processing was as in Figure 4.2.

4.1.4. TPA treatment induces the conversion of RNAP-II from the hypo- to the hyper-phosphorylated state with an increase of both CTD-S2p and CTD-S5p forms.

The switch in the form of RNAP-II associated with the uPA gene regulatory elements following transcriptional induction (from CTD-S5p to CTD-S2p) raises the question on whether there is a variation in the relative amount of the two forms of RNAP-II in the nucleus following TPA treatment of HepG2 cells. A western blot analysis of the total RNAP-II content of HepG2 cells before and after transcriptional induction shows that the total amount of RNAP-II does not change (Figure 4.4A). However, the distribution between non-phosphorylated and phosphorylated forms is substantially altered, in that the former decreases and the latter increases (Figure 4.4A). We then investigated the content of the CTD-S5p and CTD-S2p forms of RNAP-II in HepG2 cells before and after transcriptional induction. The results (Figure 4.4A) show that both forms of RNAP-II increase following TPA treatment, indicating that phorbol esters induce a general conversion of hypophosphorylated RNAP-II to the hyperphosphorylated form, but not to one particular phosphorylated form.

4.1.5. A poised uPA gene occupies a distinct RNAP-II CTD-S5p transcription factory.

The above results show that the regulatory elements of the uPA gene interact with RNAP-II yielding a non-productive (CTD-S5p) association before TPA treatment and a

productive association (CTD-S2p) after transcriptional induction. Moreover, both forms of RNAP-II are present on the MP following transcriptional activation. Since transcriptionally productive interactions occur within transcription factories, our results raise the question on whether the association of the uPA gene with RNAP-II CTD-S5p occurs stochastically in the nuclear volume or in distinct nuclear structures. To investigate this issue we combined DNA FISH, using a fluorescently labeled BAC probe specific for uPA, with immunofluorescence, using antibodies against the differentially phosphorylated forms of RNAP-II in untreated or TPA-treated HepG2 cells on ultrathin cryosections (Branco and Pombo, 2006). Figure 4.4B shows representative images of the experiment, suggesting the colocalization of CTD-S5p with uPA gene both before and after TPA treatment and a strict colocalization of the uPA gene with CTD-S2p after transcriptional induction. Images from several fields were collected in different preparations and the colocalization of the uPA gene with CTD-S5p or CTD-S2p before and after transcriptional induction was quantified. We find a strong colocalization (approximately 90% of the observed fields) of the uPA gene with CTD-S5p before transcriptional induction, which is maintained (approximately 80% of the observed fields) after TPA treatment (Figure 4.4C). On the other hand, in approximately 70% of the cases the uPA gene localizes away from CTD-S2p-containing structures prior to transcriptional induction and colocalizes with them in about 85% of the cases following induction (Figure 4.4C). We conclude that in uninduced HepG2 cells the association of the uPA gene with RNAP-II CTD-S5p occurs in specific structures, different from actively transcribing transcription factories (characterized by the presence of RNAP-II CTD-S2p). Although the uPA gene strongly associates with RNAP-II CTD-S2p

following TPA treatment, the uPA/RNAP-II CTD-S5p interaction persisted after transcriptional activation, thus corroborating our MN-ChIP findings (Figure 4.3).

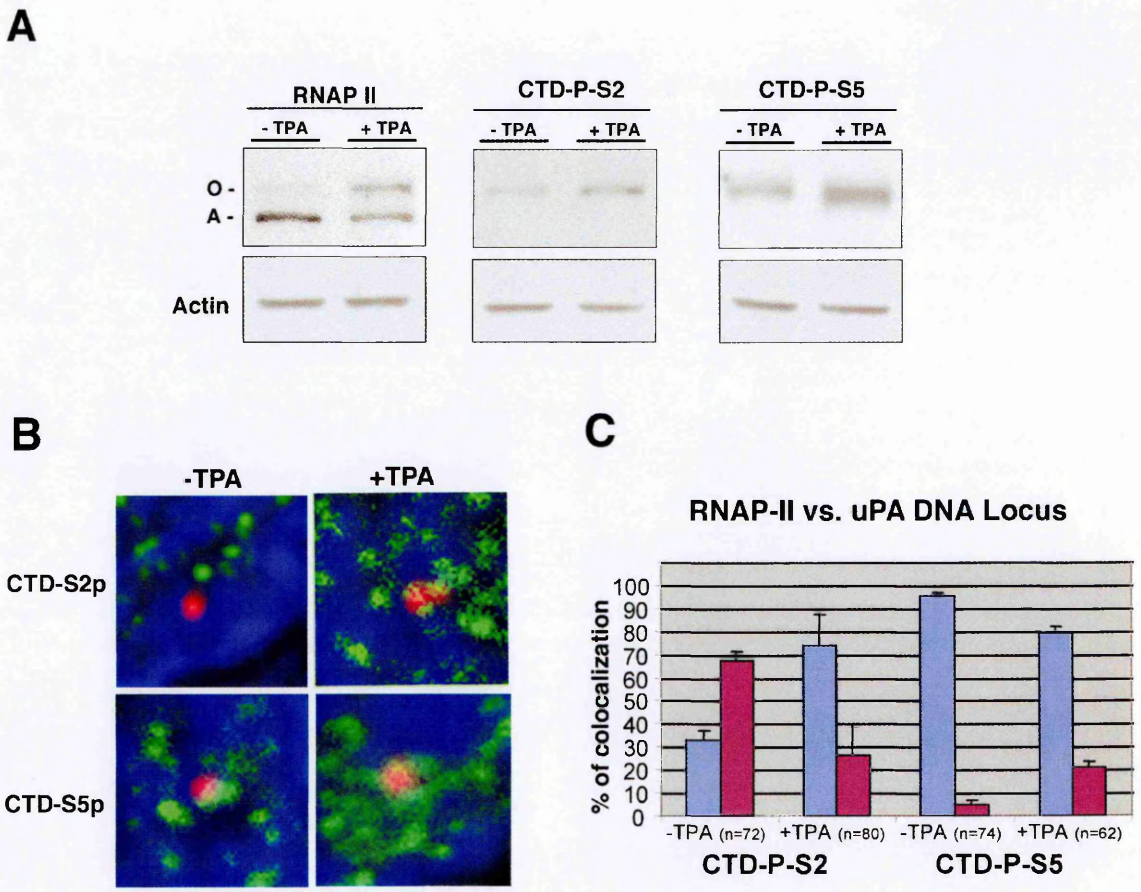

Figure 4.4. RNAP-II forms and association with uPA gene before and after TPA treatment.

In **(A)** equal amounts of total protein extracts were analyzed by WB, as described in material and methods, using antibodies specific for the N-terminal domain of RNAP-II (recognizing the -A- hypo-phosphorylated and -O- hyper-phosphorylated RNAP-II) and for CTD-S2p or CTD-S5p. The signal obtained with anti-actin antibodies was used to normalize RNAP-II, CTD-S2p and CTD-S5p signals. **(B)** Cryo-sections were prepared and were used to perform immuno-FISH experiments as described in (Branco and Pombo, 2006) using anti-CTD-S2p and anti-CTD-S5p antibodies and a BAC probe specific for uPA gene. Representative images of nuclear region containing the uPA gene are shown. uPA gene, RNAP-II forms and DNA are stained in red, green and blue respectively. **(C)** Plot showing the percentage of uPA localization with or away of (blue bars and purple bars respectively) RNAP-II factories containing CTD-S2p or CTD-S5p (mean ± SD from three independent experiments). The number of cells analyzed is reported at the bottom of the bars.

DISCUSSION - II -

Transcription is highly compartmentalized in mammalian nuclei and occurs at specific foci, called transcription factories, enriched in the hyperphosphorylated form of RNAP-II, (Cook, 1999; Jackson et al., 1993; Wansink et al., 1993). It is now increasingly evident that nuclear architecture can influence genome function (Misteli, 2007) and that the process of compartmentalization represents a further level of complexity in the mechanism of transcriptional regulation.

4.2.1. The organization inside the nucleus: transcription is a compartmentalized process.

The limited number of transcription factories/nucleus compared with the larger number of active genes led to the prediction that more than one active gene is transcribed in each factory (Jackson et al., 1998) and this was recently shown to be the case by (Osborne et al., 2004). In particular, since active genes go through transcription cycles, shuttling between an "on" and an "off" state (Levsky et al., 2002; Osborne et al., 2004; Ross et al., 1994), it was reported that two genes co-localize to the same active factory when both are in the "on" phase, whereas when one or both are in the "off" state they relocate away from each other and from the active focus (Osborne et al., 2004). This suggested a model in which active genes are brought to transcription factories to be transcribed (Chakalova et al., 2005; Osborne et al., 2004). The model implies that the association of genes with RNAPII occurs

only within a transcription factory and that the subsequent synthesis of mRNA defines them as transcriptionally active. Here we show that in HepG2 cells, where transcription of the uPA gene can be induced by TPA treatment (Ibanez-Tallon et al., 1999), the gene has permissive chromatin conformation before its active transcription. In particular, both the enhancer and the promoter regions show the presence of specific histone H3 modifications associated with transcriptional activity. This is in agreement with what reported in a recent paper (Azuara et al., 2006) in which non-transcribed genes are associated with markers defining "active" chromatin. We also found that the uPA enhancer and MP are both associated with RNAP-II CTD-S5p prior to induction and become associated with RNAP-II CTD-S2p following TPA treatment. The presence of the poised RNAP-II is particularly interesting, since it suggests that the enhancer and the MP may be interacting before TPA induction. These findings are also in line with what previously reported (Gomes et al., 2006). However, immuno/FISH experiments provide evidence that the association of transcriptionally inactive genes with RNAP-II does not occur stochastically in the nuclear volume, but is confined to specific structures. Our results expand the previous model (Chakalova et al., 2005; Osborne et al., 2004) indicating that the association of some genes with RNAPII in specific nuclear structures occurs without mRNA synthesis and that transcriptional activity is not a prerequisite for their association with a transcription factory.

4.2.2. Transcriptional compartmentalization has functional relevance for gene expression.

The functional importance of transcription compartmentalization may be that of locally concentrating the required factors and to ensure efficient interactions between the components of the transcriptional machinery (Bartlett et al., 2006). Recent results showing that lineage specific genes, remotely located from one another, frequently co-localize to the same transcription factory when actively transcribed (Osborne et al., 2004) strengthened the hypothesis of a possible coordinated gene regulation through their association with the same transcription factory/ies. An attractive hypothesis is the existence of specialized transcription factories (Bartlett et al., 2006) which differ in the content of specific transcriptional components thus creating distinct transcriptional environments (Cook, 1999; Misteli, 2007). However, little experimental evidence supports the differential composition of transcription foci. The presence of discrete foci where genes with a permissive chromatin configuration are associated with the non-elongating form of RNAP-II suggests the presence of "inactive" (or poised) transcription factories as functionally independent entities, distinct from the active ones. Thus, it is feasible that inactive foci, containing clustered RNAP-II CTD-S5p and poised genes, represent a type of specialized transcription factory (Bartlett et al., 2006). In these foci the recruitment of specific components would contribute to create a distinct transcriptional environment (Misteli, 2007), in order to rapidly and efficiently respond to specific extra-cellular signals. Whether inactive factories can be moved in a new position outside the CT and converted to active ones or whether the gene is repositioned to another factory following a transcription-inducing stimulus is still unknown. However, our results emphasize the presence of

dedicated nuclear sub-compartments and strengthen the emerging view of a non-random genome organization, possibly moulded by function (Marenduzzo et al., 2007; Misteli, 2007).

SUMMARY - II -

The main finding reported in this chapter is that a transcriptionally competent, but inactive, uPA gene is associated with the CTD-S5p of RNAP-II in specific nuclear structures. This seemingly exclude that the association of some genes with RNAP-II CTD-S5p occurs stochastically in the nucleus, supporting the idea that the interaction is restricted to specific sub-nuclear compartments and thus, suggesting the existence of specialized RNAP-II transcription factories.

The experiments presented in this chapter include unpublished data part of which (Figure 4.4.B and C) have been obtained through a collaboration with Ana Pombo's group at MRC Clinical Sciences Centre, Faculty of Medicine, Imperial College London, Hammersmith Hospital Campus, London W12 0NN, United Kingdom.

RESULTS AND DISCUSSION -III-

Myosin VI affects RNAP-II transcriptional elongation.

RESULTS -III-

5.1.1. Myosin VI associates with RNAP-II CTD-S2p on DAF-B and enhancer of the uPA gene in PC3 cells.

We have previously shown the presence of the non-conventional Myosin VI protein in the nucleus of HeLa cells and its co-immunoprecipitation with RNAP-II (Vreugde et al., 2006). We decided to use the MN-ChIP assay in PC3 cells in order to test the association of Myosin VI with the regulatory elements of the uPA gene. Therefore we expanded the results of Figures 3.8 and 3.9 by performing immunoprecipitations with antibodies against Myosin VI in parallel with antibodies against the CTD-S5p and CTD-S2p forms of RNAP-II. The imunoprecipitated DNA was analyzed using primer sets specific for frag.1, spanning the enhancer, and DAF-A and -B in the MP region of the uPA gene (see Figure 5.1A and Chapter 3). The results in Figure 5.1B show that frag.1 and DAF-B amplicons

were associated with RNAP-II CTD-S2p, but not with CTD-S5p, as expected (see Figures 3.8 and 3.11) and also with Myosin VI.

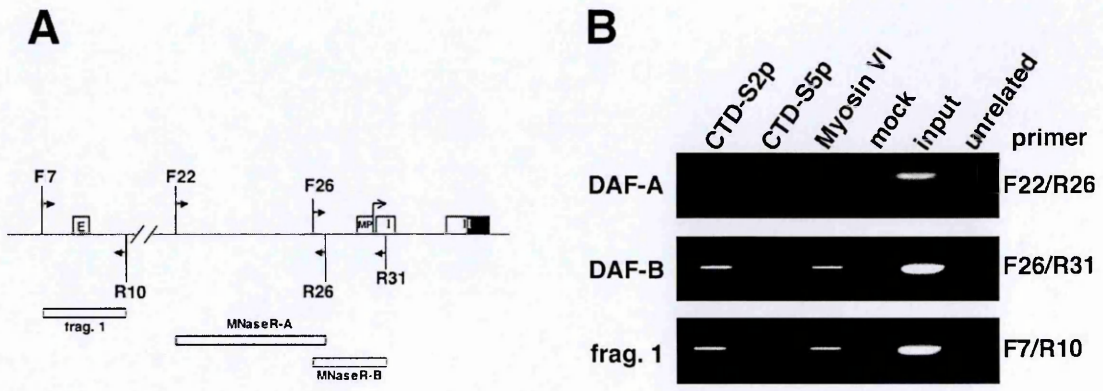

Figure 5.1. Myosin VI associates with DAF-B and frag.1 of uPA in PC3 cells.
ChIP-ready chromatin was digested for 50 minutes with MNase as in Figure 3.9 and subsequently immunoprecipitated with the antibodies indicated in the figure. The immunoprecipitated, purified genomic DNA was amplified with primer sets specific for DAF-A, -B and frag.1 and fractionated on a 2% agarose gel. Input DNA was a 1:1000 dilution of the DNA from the 50 minutes digestion time-point prior to immunoprecipitation. (**A**) Scheme of the primer sets used and of the amplified regions (not to scale). Symbols are as in Figures 3.8 and 3.11. (**B**) Amplifications of immunoprecipitated genomic DNA with antibodies to different forms of RNAP-II (CTD-S2p and CTD-S5p) and Myosin VI. Myosin VI is associated with DAF-B and frag.1 together with the elongating form of RNAP II (CTD-S2p).

5.1.2. Myosin VI associates with the promoters and intragenic regions of selected gene and modulates their transcription in PC3 cells.

We decided to determine if myosin VI specifically associates with the regulatory regions of genes. We performed ChIP assays using cross-linked chromatin from PC3 cells and specific antibodies for CTD-S2p RNAP-II, CTD-S5p RNAP-II and Myosin VI. Primers for the amplification of immunoprecipitated material were designed to include the promoter and intragenic sequences (coding region) of the chosen genes. As a negative control we used sets of primers that amplify an intergenic (non coding) region, upstream of the uPA gene. Quantitative PCR results (Figure 5.2) show that myosin VI is recruited to the promoter and intragenic regions of the uPA, LDLR and the p27BBP/eIF6 genes all of which are expressed in PC3 cells, but not to the promoter and intragenic region of p21WAF1/CIP1 or to the intergenic region (Figure 5.2). Similarly, the CTD-S2p and CTD-S5p forms of RNAP-II are recruited to the promoters and intragenic regions of the selected genes, but not to the intergenic region (Figure 5.2), as expected. Interestingly, CTD-S2p and Myosin VI seemed to be relatively more enriched in intragenic as compared to promoter regions in all the genes tested (Figure 5.2). These results suggest a possible role for nuclear Myosin VI in the elongation phase of transcription. Next we decided to evaluate whether nuclear Myosin VI modulates the expression of the selected genes by monitoring their mRNA levels in Myosin VI-depleted cells. Transient transfections of PC3 cells with a plasmid expressing an antisense (AS) RNA for Myosin VI (Yoshida et al., 2004) efficiently decrease Myosin VI protein levels (Figure 5.3A) and qRT-PCR shows that the mRNA levels of the tested genes (uPA, $p27^{BBP}$/eIF6 and LDLR) also decrease (Figure 5.3B). Importantly, the mRNA levels of the p21WAF1/CIP1 gene, the regulatory

region of which is not associated with myosin VI, are not down-regulated by depletion of myosin VI (Figure 5.3B). Taken together, these data suggest that down-regulation of myosin VI affects the mRNA levels of selected RNAP-II target genes *in vivo*.

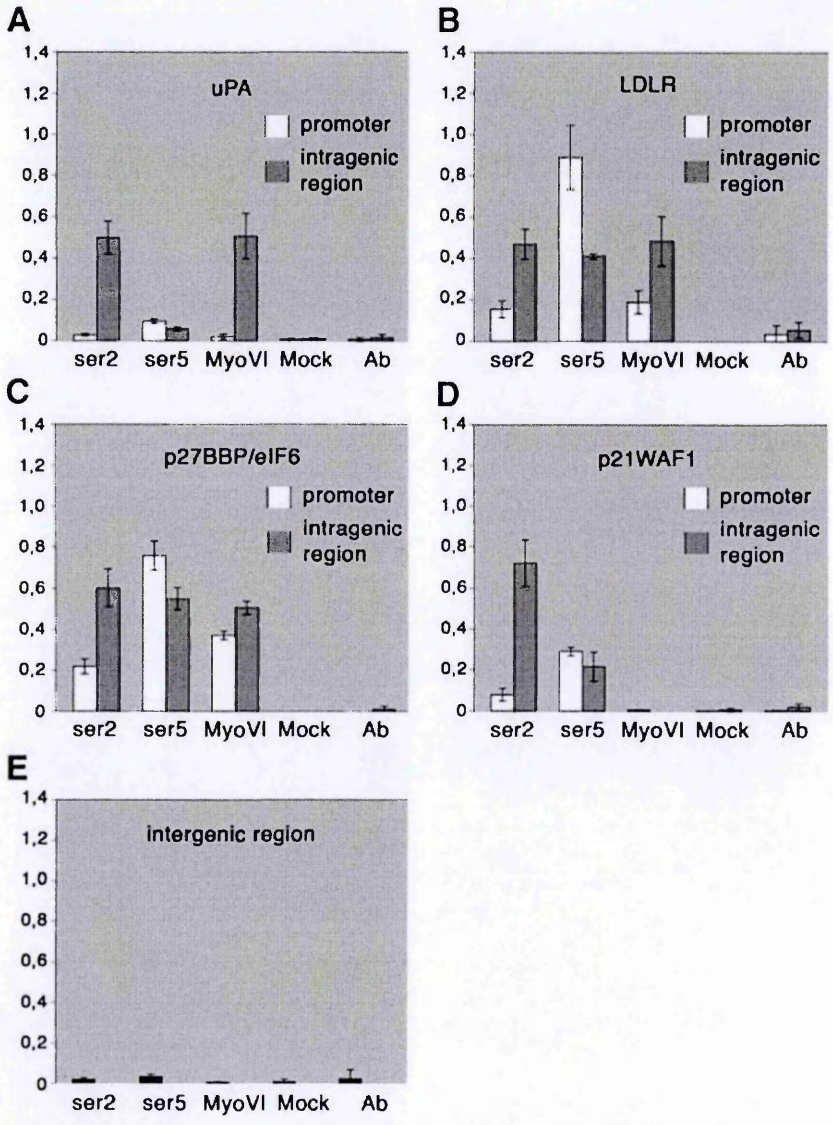

Figure 5.2. Myosin VI associates with promoters and intragenic regions of different genes.

ChIP using PC3 cross-linked chromatin was performed as described in material and methods using antibodies against CTD-S2p, CTD-S5p and Myosin VI as shown in the figure. qPCR amplification of immunoprecipitated material was performed with primers defining the promoter and the intragenic region, respectively, of the uPA, LDLR, p27/eIF6 and p21 genes. Primers amplifying an intergenic region were also used as a negative

control. Values plotted in the graphs correspond to the enrichment detected in the imunoprecipitated material relative to the input DNA for uPA (**A**), LDLR (**B**), p27/eIF6 (**C**) and p21 (**D**) genes and the intragenic region (**E**) (mean ± SD from three independent experiments). The results show that Myosin VI can be found specifically associated with promoter and intragenic regions of expressed genes genes.

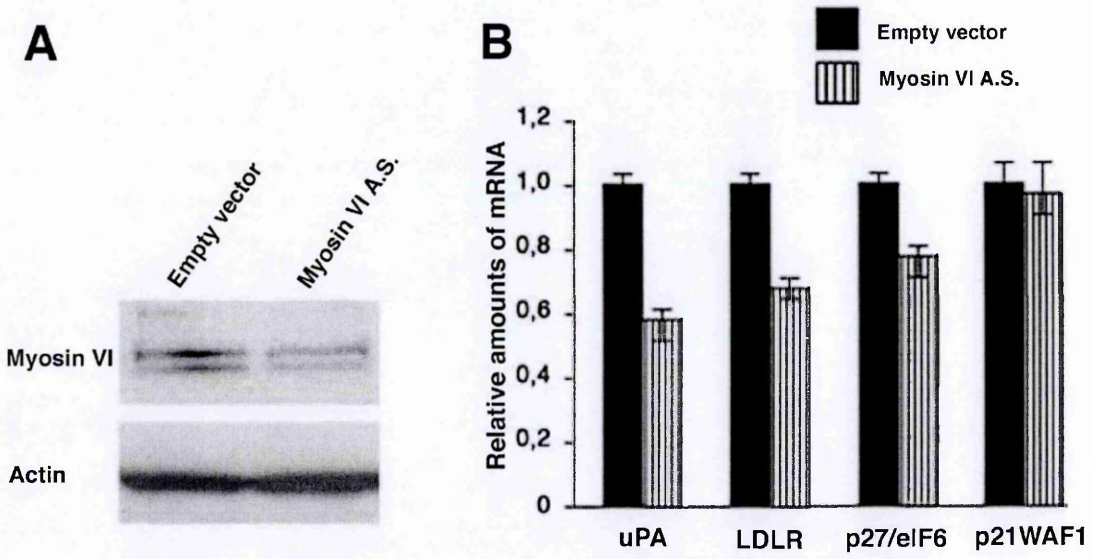

Figure 5.3. Myosin VI knock-down inhibits transcription of selected genes.
PC3 cells were transiently transfected with an empty vector (pIRES-EGFP) or with a vector carring a Myosin VI A.S. (pIRES-EGFP Myosin VI A.S. (Yoshida et al., 2004)). Part of the transfected cells was used to perform total proteins extraction (see material and methods). (**A**) Total protein extracts were resolved on a 5-15% gradient SDS-PAGE and transferred to PVDF membrane. The levels of endogenous Myosin VI were analyzed by immunoblotting with specific polyclonal antibodies and normalized to the actin signal. (**B**) The remaining transfected cells were used for total RNA extraction that was purified, retro-transcribed and a qRT PCR analysis was performed using primers specific for the selected genes (see Material and Methods). The values were normalized to the 18s rRNA and plotted in a graph (mean ± SD from three independent experiments). The results show that knock-down of Myosin VI affects mRNA levels of the genes with which it is associated.

5.1.3. TPA treatment induces the nuclear accumulation of Myosin VI protein.

In order to investigate the response of MyosinVI to transcription-inducing signals, we moved to the inducible HepG2 cell system (see Chapter 4). We first studied the distribution of the endogenous protein by confocal microscopy in untreated and TPA-treated cells that were fixed and stained with specific antibodies. Figure 5.4A shows that MyosinVI is present in the nucleus of untreated cells with the typical speckled distribution (Compare with Figure 1A in (Vreugde et al., 2006). Transcriptional induction by TPA determines a massive increase of the protein in the nuclear compartment. Nuclear accumulation of MyosinVI following transcriptional induction was also observed by confocal microscopy after transiently transfecting HepG2 cells with a plasmid carrying a GFP-tagged full length MyosinVI (Aschenbrenner et al., 2003) and using anti-GFP antibodies (Figure 5.4B). A WB analysis of total, nuclear and cytoplasmic extracts of untreated and TPA-treated HepG2 cells (Figure 5.5) confirmed the nuclear accumulation of endogenous MyosinVI after transcriptional induction. Its increase in the nuclear compartment is not associated with an increase of the total protein amount, as shown by the comparable levels of MyosinVI in total extracts before and after TPA treatment. Moreover, a concomitant decrease of MyosinVI is detected in the cytoplasm after transcriptional induction. We conclude that transcriptional activation induces a relocation of MyosinVI to the nuclear compartment.

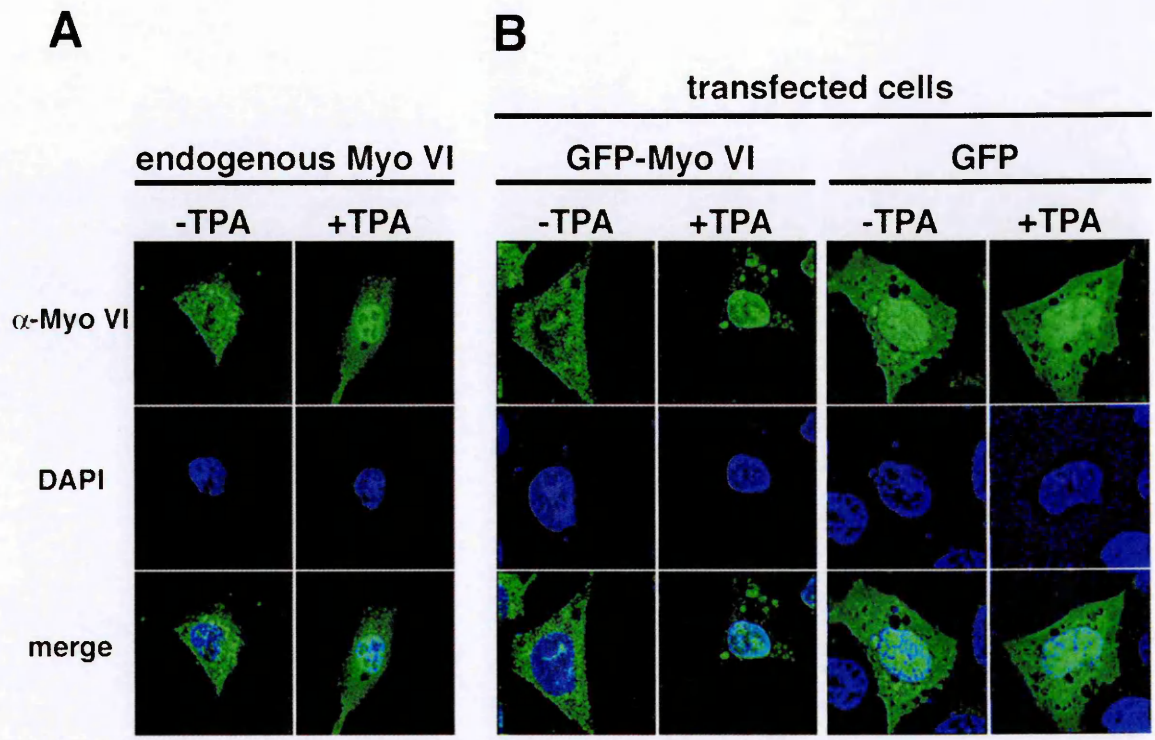

Figure 5.4. TPA induction determines the nuclear accumulation of Myosin VI in HepG2 cells.

HepG2 cells untreated or treated with TPA (see Chapter 4 Figure 5.1) were fixed with para-formaldehyde, permeabilized and immuno-stained using antibodies specific for Myosin VI (see material and methods). DAPI staining was used to visualize the nuclei. **(A)** Confocal images show that TPA induction determines an accumulation of the protein in the nuclear compartment. To confirm this pattern HepG2 cells were transfected with a construct containing the full length Myosin VI tagged with GFP (Aschenbrenner et al., 2003), transfection with GFP empty vector was used as a control. Cells were treated with or without TPA after transfection and immuno-stained using antibodies specific for GFP (as described above) to enhance GFP signal. **(B)** Confocal images show that GFP-Myosin VI is mostly cytoplasmic before TPA treatment and strongly accumulates in the nucleus after transcriptional induction. No such difference was observed in control cells transfected with the GFP (empty vector)

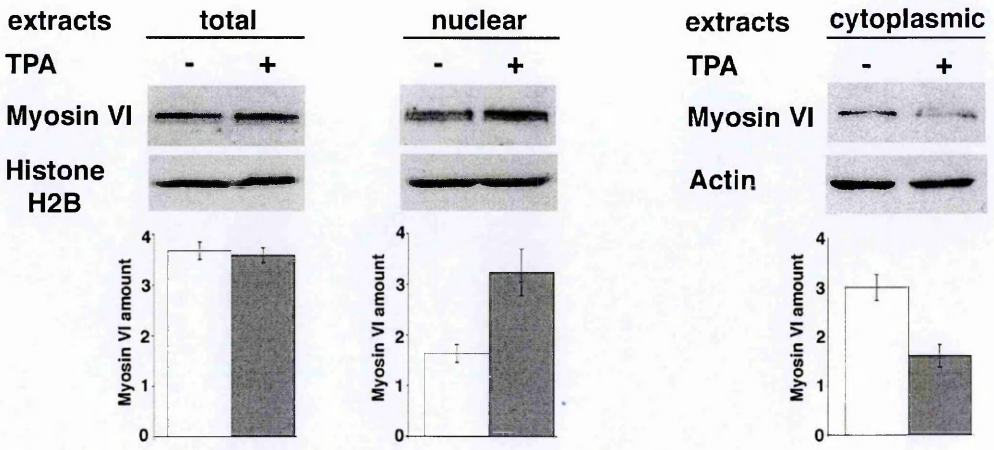

Figure 5.5. TPA induces nuclear accumulation of Myosin VI in HepG2 cells.
Total, nuclear and cytoplasmic proteins were extracted from untreated and TPA treated HepG2 cells (see material and methods) resolved on a 5-15% gradient SDS-PAGE and transferred to PVDF membrane. The protein levels of Myosin VI were analyzed by immunoblotting with specific polyclonal antibodies. The signal obtained with an anti-Histone H2B or anti-actin was used for normalization. Densitometric analysis was carried for each lane and the normalized O.D. values for each band were plotted in the respective graphs (mean ± SD from three independent experiments).

5.1.4. Myosin VI is recruited to the promoter of induced genes after transcriptional activation.

TPA treatment transcriptionally induces several genes in HepG2 cells. To look for a connection between MyosinVI and transcriptional induction we examined the association of the promoters of the LDLR and uPA genes (Huang et al., 2004; Ibanez-Tallon et al., 1999) with MyosinVI, RNAP-II CTD-S5p and RNAP-II CTD-S2p in untreated and TPA treated HepG2 cells by ChIP assay. Figure 5.6 shows that prior to TPA treatment chromatin immunoprecipitated with anti-Myosin VI antibodies is not enriched in the

promoter sequences of the LDLR and uPA genes, as it is not enriched in the intergenic region used as a negative control. Following transcriptional induction we observed a clear recruitment of MyosinVI to the promoter of the genes, but not in the intergenic region (Figure 5.6). Transcriptional induction also affected the detection of the specific forms of RNAP-II. CTD-S5p was observed on the promoter of the LDLR and uPA genes before and after induction (Figure 5.6). As expected, we observed a clear PCR amplification signal of the genes promoter in CTD-S2p immunoprecipitated material after TPA treatment (Figure 5.6) correlating with their transcriptional induction. In all cases the intergenic region displayed no signal for either form of RNAP-II. Our results indicate that MyosinVI is recruited to the promoters of TPA-induced genes and that its recruitment it is accompanied by the switch from a poised to an elongating RNAP-II form.

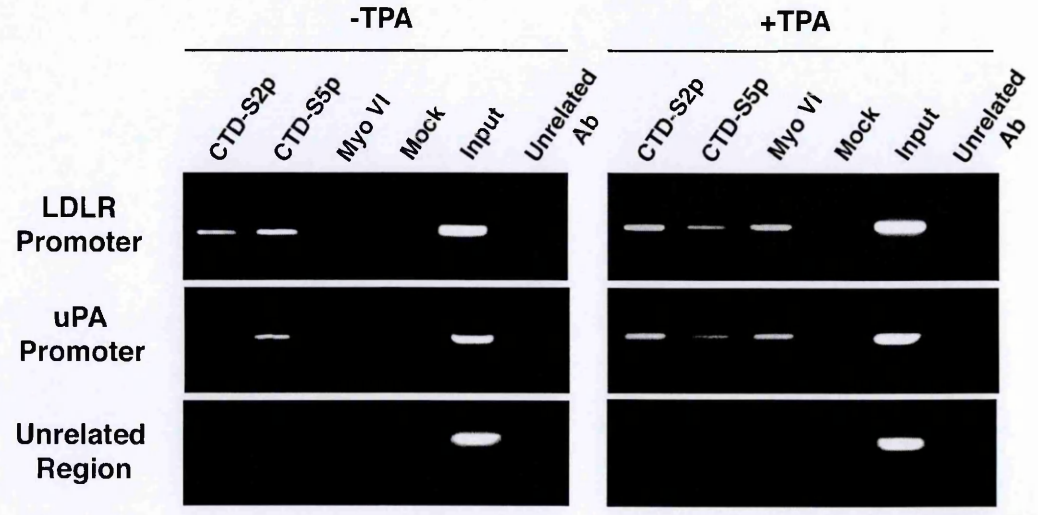

Figure 5.6. Myosin VI associates with promoters of different genes upon TPA induction.
ChIP using cross-linked chromatin from HepG2 treated or not with TPA was performed as described in material and methods, using antibodies against CTD-S2p, CTD-S5p and Myosin VI, as reported in the figure. PCR amplification of immunoprecipitated material was performed with primers defining the promoter of the uPA and LDLR genes (Table II).

Primers amplifying an intergenic region (Table II) upstream of the uPA promoter gene were also used as a negative control. Amplified material was visualized on 2% agarose, 1X TAE gels by Et-Br staining. The results show that Myosin VI is specifically associated with the promoter region of the genes following transcriptional induction.

5.1.5. The down regulation of Myosin VI protein levels affects RNAP-II CTD-S2p levels.

We previously showed that down regulation of MyosinVI inhibits transcription (Vreugde et al., 2006) through a yet unidentified mechanism. Since the results of Figure 5.2 and Figure 5.6 show that transcriptional activity correlate with the association of CTD-S2p and Myosin VI with the promoters and intragenic regions of specific genes, we speculated that depletion of MyosinVI might prevent RNAP-II from proceeding to the elongating phase. Thus, we developed a HepG2 cell line stably expressing the AS RNA for MyosinVI previously used (see above). The plasmid containing the AS sequence is a pIRES-EGFP bicistronic vector, thus allowing us to distinguish untransfected vs. transfected cells. The presence of RNAP-II differentially phosphorylated forms (CTD-S5p and CTD-S2p) was analyzed in such cells before and after transcriptional induction by confocal microscopy using specific antibodies. We did not observe detectable differences in the CTD-S5p signal distribution by comparing AS MyosinVI-transfected untreated vs. treated cells with vector-transfected untreated vs. treated cells Figure 5.7. Strikingly, however, the CTD-S2p form shows substantial differences in the immunofluorescence signal in AS MyosinVI–transfected, untreated cells as compared to untreated cells transfected with the

vector only. Figure 5.8 shows that AS Myosin VI expression causes a dramatic drop in the immunofluorescence signal for CTD-S2p.

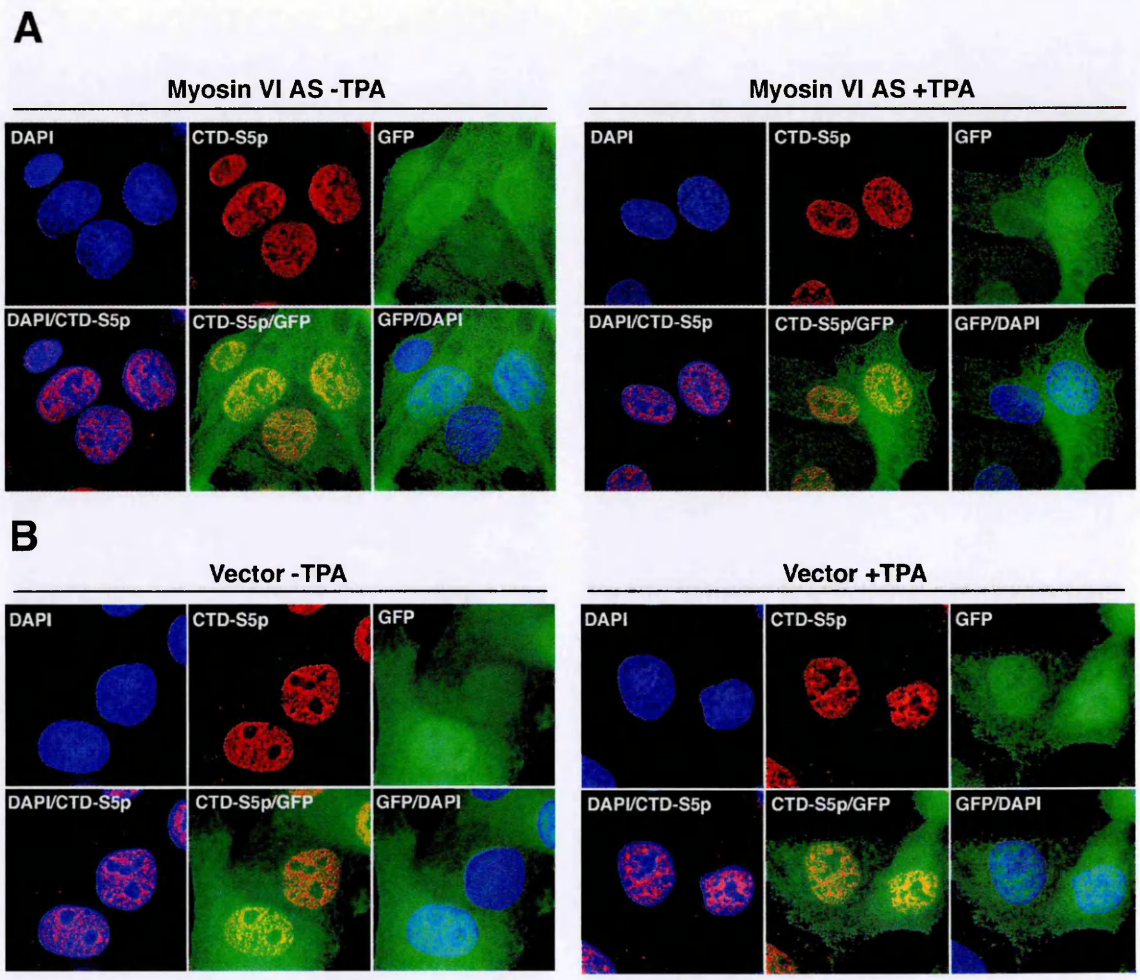

Figure 5.7. Knock-down of Myosin VI does not affect CTD-S5p in HepG2 cells. Pools of HepG2 cells stably transfected with a pIRES-EGFP plasmid either carrying a Myosin VI A.S. sequence (Yoshida et al., 2004), or not were either treated with TPA or not (see Chapter 4, Figure 4.1), fixed with para-formaldehyde, permeabilized and co-immuno-stained using antibodies specific for the poised form of RNAP-II (CTD-S5p) and GFP (see material and methods). DAPI staining was used to visualize the nuclei. Confocal images of Myosin VI A.S. transfected cells in **(A)** and Vector transfected cells in **(B)** show that no major differences can be observed between the two pools of cells with respect to CTD-S5p staining, meaning that knock-down of Myosin VI does not alter the distribution pattern of CTD-S5p.

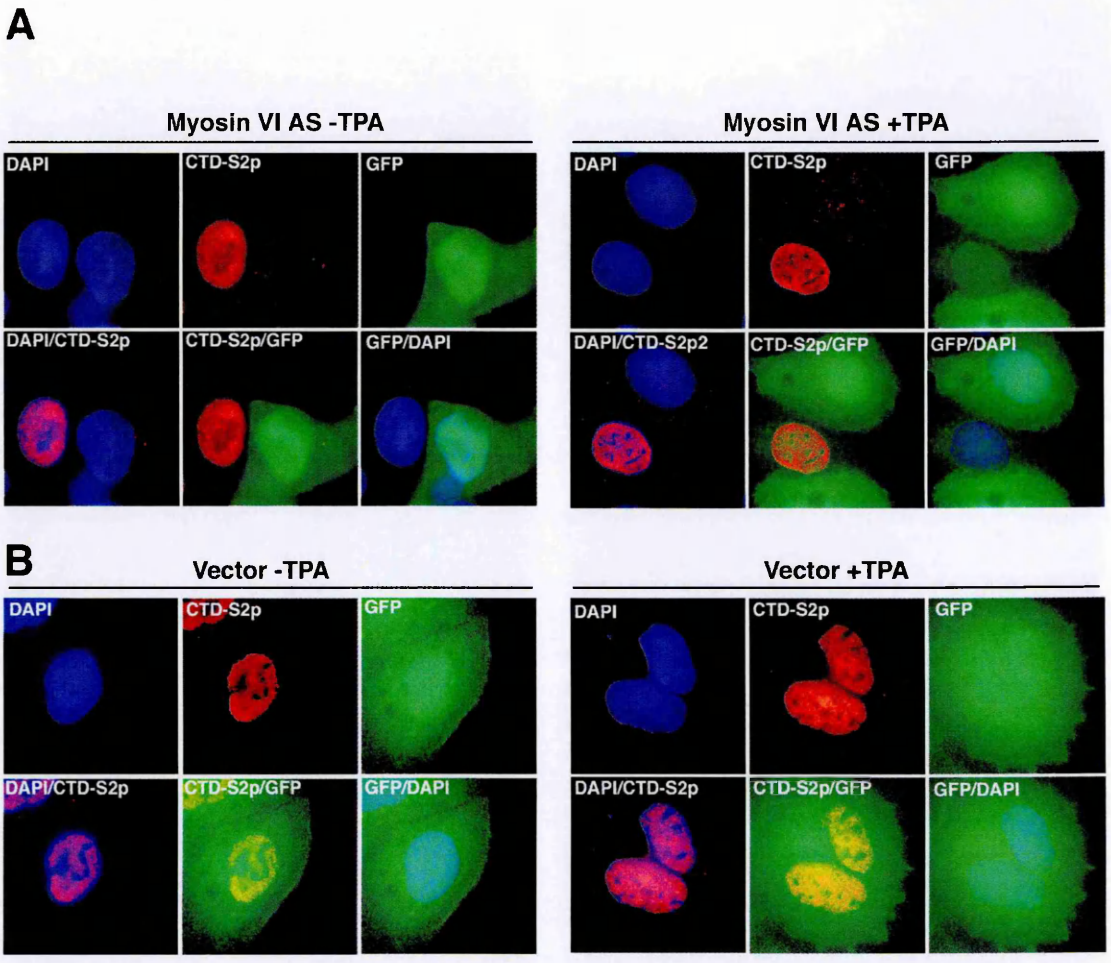

Figure 5.8. CTD-S2p is affected by knock-down of Myosin VI in HepG2 cells.
The pools of HepG2 cells stably used in the experiment shown in Figure 5.7 were co-immuno-stained with antibodies specific for the elongating form of RNAP-II (CTD-S2p) and GFP (see material and methods). DAPI staining was used to visualize the nuclei. Confocal images of Myosin VI A.S. transfected cells in **(A)** and Vector transfected cells in **(B)** show that a strong difference can be observed between the two pools of cells with respect to CTD-S2p staining. In fact in cells expressing Myosin VI A.S. the staining relative to CTD-S2p is dramatically dropped. Conversely, CTD-S2p staining is not overall altered in control vector transfected cells.

Thus, AS MyosinVI-and vector-transfected cells were sorted in order to select those with the higher GFP (and consequently AS Myosin VI expression) levels and then used to perform a WB analysis of the levels of MyosinVI before and after transcriptional induction. In AS-transfected cells the decrease in endogenous MyosinVI levels was approximately 50% in untreated cells and around 80% in TPA-treated cells, as compared to untreated vs. treated cells stably transfected with the vector only (Figure 5.9A). The same extracts were also used to analyze CTD-S5p and CTD-S2p levels. Both AS MyosinVI- and vector-transfected cells showed equivalent levels of CTD-S5p before TPA treatment and a two fold of increase following TPA treatment (Figure 5.9B), as expected (see Figure 4.4A). The levels of CTD-S2p in sorted cells, however, were lower in AS MyosinVI- than in vector-transfected cells prior to TPA induction (Figure 5.9C). Following induction the CTD-S2p levels in vector-transfected cells increased two fold, as compared with the untreated control, whereas we observed a 50% decrease in the CTD-S2p signal in AS-transfected cells, as compared to the untreated control (Figure 5.9C). Moreover, the decrease of CTD-S2p levels in AS-transfected, TPA-treated cells reached 75% when the comparison was done with vector-transfected TPA induced cells (Figure 5.9C). These results indicate that of Myosin VI specifically modulates the levels of RNAP II CTD-S2p and, thus, plays a role in transcription by affecting the elongation step.

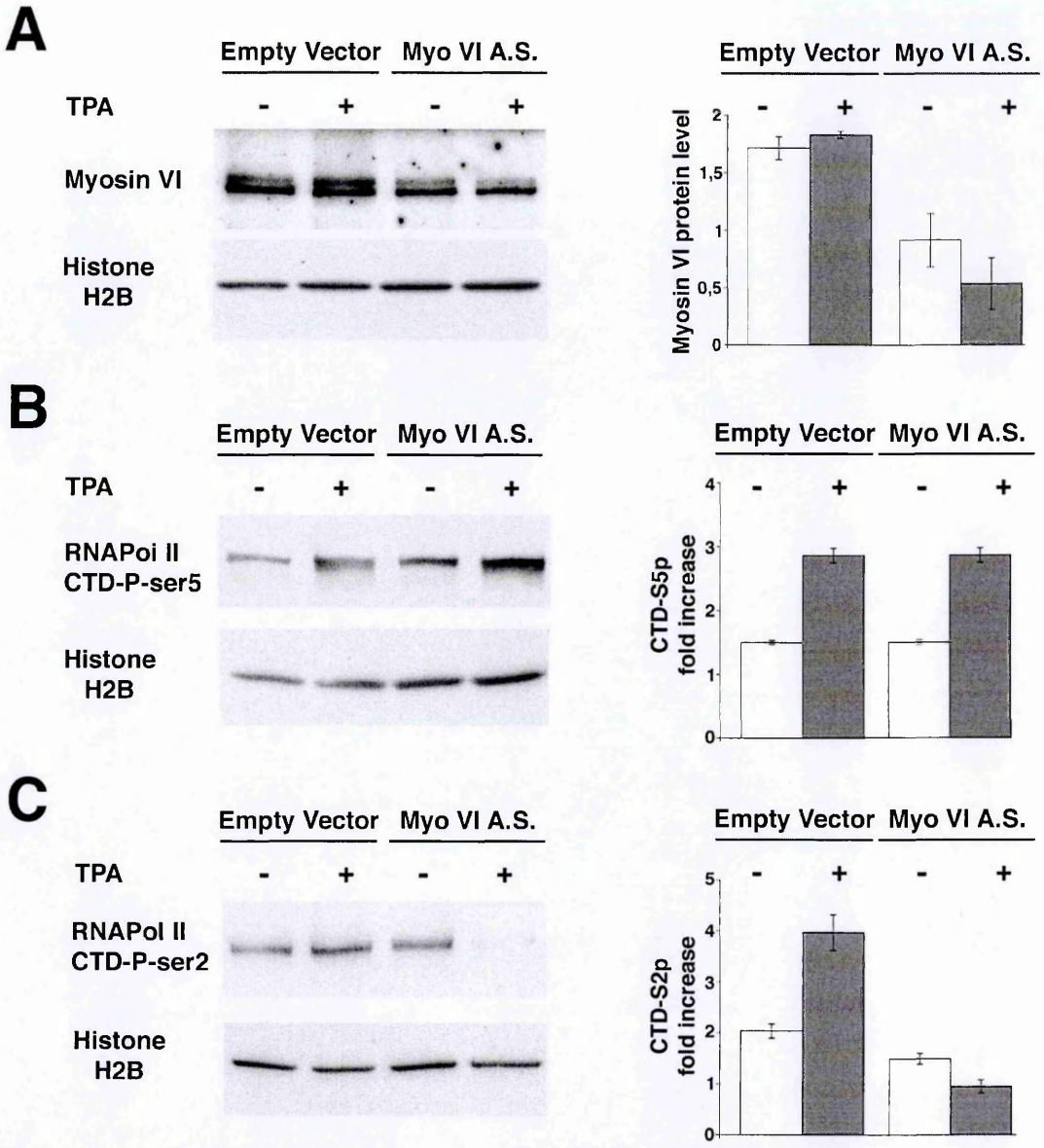

Figure 5.9. Myosin VI knock-down affects CTD-S2p of RNAP-II.
The pools of HepG2 cells previously used (Figures 5.7 and 5.8) were sorted to select cells with a high level of EGFP expression. Sorted cells were plated, treated or not with TPA (as described above) and total proteins were extracted (see material and methods). The extracts were fractionated on a 5-15% gradient SDS-PAGE and transferred to PVDF membrane. The levels of Myosin VI and specific RNAP-II phosporylated forms (CTD-S5p and CTD-S2p) were analyzed by immunoblotting with specific antibodies and Histone H2B was used for normalization (**left panels A, B and C,**). Densitometric analysis was carried for each lane and the normalized O.D. values for each band were plotted in a graph (**right panels A, B and C**) (mean ± SD from three independent experiments).

5.1.6. Myosin VI affects transcriptional elongation.

To substantiate this finding and to analyze whether the effect on CTD-S2p raffected transcription we carried out *in vivo* run-on assays. Stably AS MyosinVI- and vector-only-transfected cells were permeabilized, incubated with BrUTP and its incorporation into nascent transcripts was detected by immunofluorescence with polyclonal anti-BrUTP antibodies. As expected, control cells (vector transfected) did not show any difference in the levels of nascent transcripts either before or after TPA treatment (Figure 5.10B). Notably, BrUTP incorporation was almost abolished in AS MyosinVI cells as compared to the relative control, indicating substantially decreased transcription (Figure 5.10A). This behavior parallels what observed with RNAP II CTD-S2p and further confirms the involvement of myosin VI in the elongation step of transcription.

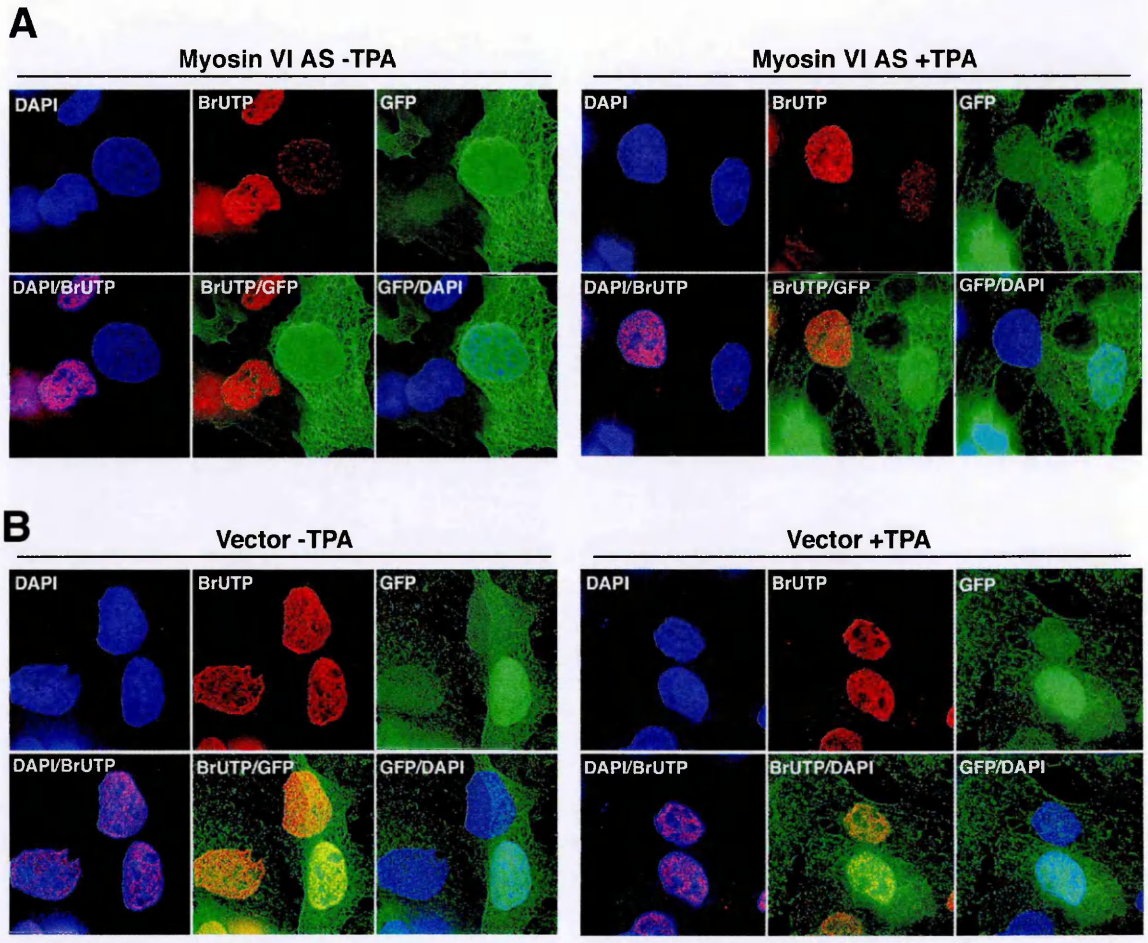

Figure 5.10. Myosin VI knock-down affects BrUTP incorporation in HepG2 cells. Nascent transcripts were monitored by BrUTP incorporation (see material and methods) in the pools of HepG2 cells used in the experiments shows in Figures 5.7 and 5.8. After permebilization the cells were incubated in a buffer containing BrUTP, and after fixation, coimmuno-staining using antibodies specific for BrUTP and GFP was performed (see material and methods). DAPI staining was used to visualize nuclei. Confocal images of Myosin VI A.S. transfected cells in **(A)** and Vector transfected cells in **(B)** show a strong difference in BrUTP incorporation: in cells with a high expression level of the Myosin VI A.S. BrUTP staining was dramatically low. Conversely no major differences in the BrUTP pattern is observed in the control vector-transfected cells.

DISCUSSION - III -

Transcription of DNA requires large protein complexes. The synergistic action of the proteins that compose the basal transcriptional machinery together with transcription factors and chromatin remodeling proteins contribute to modulating this highly regulated process and determining correct gene expression. Recent work showed the presence of β-actin, NMI and a number of related proteins in the nucleus (de Lanerolle et al., 2005). However, even though there is agreement on their implication in transcriptional regulation, their mechanism of action is still not known.

5.2.1. Motor protein in transcription, a growing family.

Despite the early proposal of an actin-based mechanism in gene transcription (Egly et al., 1984) (Scheer et al., 1984), evidences for such a direct implication have only been gathered recently. A number of reports indicate that β-actin associates with components of ATP-dependent chromatin remodeling complexes (Bettinger et al., 2004; Olave et al., 2002), RNP particles (Percipalle et al., 2001)) and RNA polymerases in the eukaryotic cell nucleus and *in vitro* (Hofmann et al., 2004; Hu et al., 2004; Kukalev et al., 2005; Philimonenko et al., 2004), strengthening its implication as a crucial component of the transcription process. However, until now, only one Myosin (NMI) has been reported to be present in the mammalian nucleus (Pestic-Dragovich et al., 2000) and was shown to have an essential role in the RNAP-I dependent transcription of ribosomal RNA genes

(Philimonenko et al., 2004). Here we report the presence in the nucleus of non-conventional Myosin VI. We find that in mammalian cells Myosin VI is associated with the DNA of active genes, where it modulates RNAP-II activity. These findings support the hypothesis that an acto-myosin-based mechanism is involved in the transcription of RNAP-II genes (Kukalev et al., 2005). Wile β-actin is the only form of actin reported to be present in the nucleus and to interact with all three classes of polymerases, at least two myosins (NMI and Myosin VI) are found in the nucleus. An intriguing hypothesis is that myosin might confer target selectivity to the acto-myosin system.

5.2.2. Myosin VI response to extra-cellular stimuli.

A compelling question is whether motor proteins can modulate the overall transcriptional activity in response to extra-cellular signals. A feasible mechanism is that an external stimulus would activate the motor proteins that, in turn, will regulate specific subset of genes. Our results in an inducible cell system show that cells respond to a transcriptional inducing stimulus by relocating Myosin VI to the nuclear compartment. The nuclear accumulation of the protein is paralleled by its recruitment on the regulatory region of specifically induced genes. This suggests a direct involvement of Myosin in gene activation, but does not elucidate its mechanism of action. We have therefore further characterized the role of nuclear myosin VI in transcriptional regulation to clarify this issue.

5.2.3. Molecular mechanism of action of Myosin VI.

Actin seems to be important in the process of transcription of the all tree RNAP (Philimonenko et al., 2004). However the way in which it exerts its action is not yet known. An emerging idea is that actin may act as a molecular platform for protein–protein interactions through a mechanism that requires ongoing RNA synthesis (Kukalev et al., 2005) (Philimonenko et al., 2004). In fact abortive transcription-initiation assays showed that actin inhibits elongation, but does not affect the synthesis of the first nucleotides (Hofmann et al., 2004; Philimonenko et al., 2004). Myosin VI is also able to affect RNAP-II dependent transcription (Vreugde et al., 2006). Interestingly, ChIP assays show that Myosin VI associates with intragenic regions of active genes (Figure 5.2) suggesting that it may have a role in the mRNA elongation step. Experiments in the HepG2 inducible system also showed that Myosin VI is recruited on TPA-induced genes. Moreover the recruitment of Myosin VI coincides with the association of said genes with the elongating form of RNAP-II (CTD-S2p). Our results also show that the depletion of Myosin VI severely impairs the phosphorylation of RNAP-II-CTD at serine 2 (Figures 5.8 and 5.9C), but not at serine 5 (Figures 5.7 and 5.9B), determining a dramatic decrease in BrUTP incorporation (Figures 5.10). These data establish a connection between RNAP-II and Myosin VI suggesting its involvement in the elongation step. The molecular mechanism by which Myosin VI modulates CTD-S2p phosphorylation is presently under investigation. A feasible possibility is that it could contribute to the recruitment a series of cofactors such as CDK9, the specific kinase indicated to be involved in CTD-S2p phosphorylation.

SUMMARY -III-

In this chapter we report the presence in the nucleus of non-conventional Myosin VI and show that is implicated in modulating the RNAP-II transcription process in PC3 cells. We also show that transcriptional induction of HepG2 cells triggers a massive recruitment of MyosinVI in the nucleus and its association with the elongating form of RNAP-II (CTD-S2p). We also provide evidence that MyosinVI depletion specifically affects the levels of RNAP-II CTD-S2p and decreases transcriptional activity. This suggests that MyosinVI responds to transcription-inducing stimuli by promoting RNAP-II elongation.

The experiments presented in this chapter includes a part of data (Figures 5.2 and 5.3) that have been published in: Vreugde S, Ferrai C, Miluzio A, Hauben E, Marchisio PC, Crippa MP, Bussi M, Biffo S. "Nuclear myosin VI enhances RNA polymerase II-dependent transcription". Mol Cell. 2006 Sep 1;23(5):749-755.

RESULTS AND DISCUSSION -IV-

Recruitment of Myosin VI to specific target genes through its interaction with the transcription factor Prep1.

RESULTS -IV

6.1.1. Myosin VI is present in a Prep1-containing complex.

The results in the Chapter 5 suggest that Myosin VI is involved in the transcriptional elongation step. However, no information is available on the mechanism by which Myosin VI is recruited to specific genes. Our laboratory has a long-time interest in Prep1, a homeodomain transcription factor essential for many biological functions such as, for instance, embryonic development (Berthelsen et al., 1998; Ferretti et al., 2006), hematopoietic lineage determination (Penkov et al., 2005) and apoptosis regulation (Deflorian et al., 2004). In order to study the Prep1 interactome, a Prep1-containing complex was purified using the Tandem Affinity Purification (TAP) technique (Puig et al., 2001). A C-terminally tagged Prep1 was stably expressed in NIH 3T3 cells and a Prep1-

containing complex was isolated, fractionated on SDS-PAGE and analyzed by mass spectrometry (Diaz et al., in Preparation). β-actin was among the proteins that copurified with Prep1 and raised the question on whether also Myosin VI could be present in the complex. We thus analyzed the Prep1 TAP associated material by immunoblotting with specific anti-Myosin VI antibodies. The results in Figure 6.1 show that RNAP-II and Myosin VI are present in the complex obtained from nuclear extracts. A weak band for both proteins could also be detected in cytoplasmic extracts. Although the presence of Myosin VI in the cytoplasm is expected RNAP-II in this fraction is possibly due to a nuclear contamination of cytoplasmic extracts.

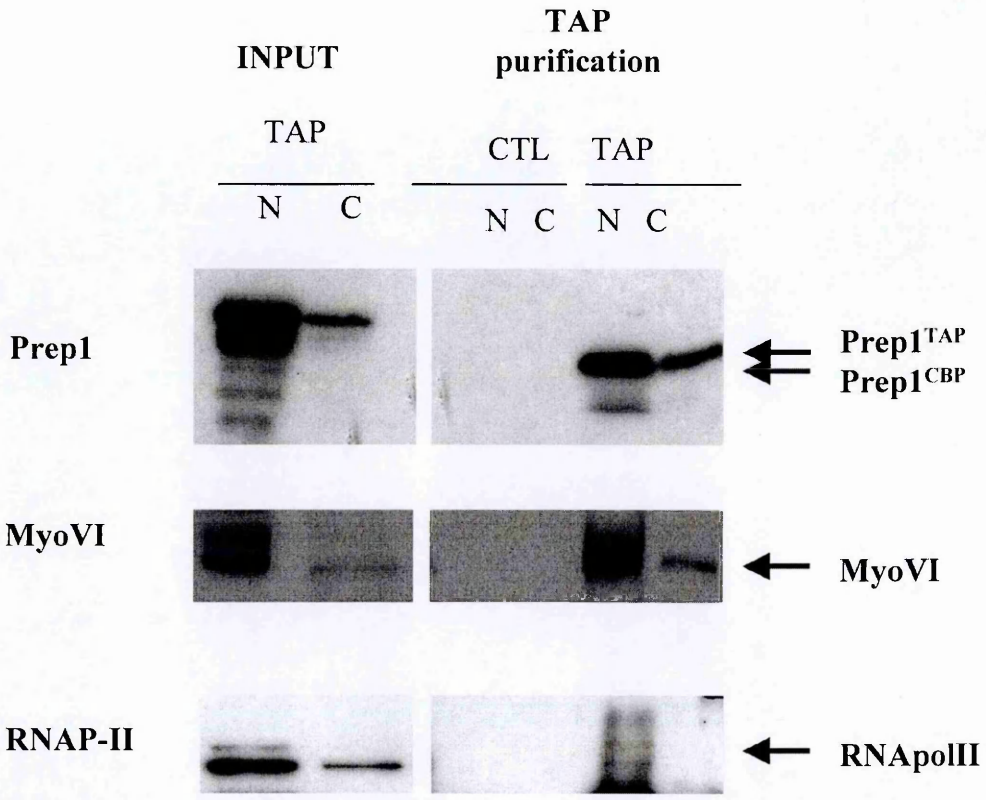

Figure 6.1. Immunoblotting analysis of the Prep1-associated proteins .
NIH-3T3 cells were infected either with a retovirus expressing Prep1-TAP fusion protein (TAP) or an empty vector (CTL) and the cytoplasmic (C) and nuclear (N) extracts purified by TAP (Diaz *et al.*, in preparation). Fraction of inputs and eluates proteins were resolved on a 5-15% gradient SDS-PAGE and transferred on PVDF membrane. The presence of Prep1, Myosin VI and RNAP-II were analyzed by immunoblotting with specific antibodies.

6.1.2. Prep1 and Myosin VI are recruited to the HoxB2 regulatory region upon transcriptional activation.

The human NT2-D1 cell line is known to differentiate in neuronal like cells upon RA

stimulation (Pleasure et al., 1992). RA-induced differentiation is accompanied by the transcriptional activation of the genes of the HoxB cluster (Simeone et al., 1990) in a sequential and time dependent manner, in which Prep1 is required (Longobardi et al., In preparation). TSA treatment of transcriptionally induced NT2-D1 cells reverts the RA effect and, moreover, abolishes the binding of Prep1 to its cognate sequence in the enhancer of the HoxB2 gene (Longobardi et al., in Preparation). ChIP assays carried out on chromatin from untreated, RA- and RA+TSA-treated cells confirmed that Prep1 is recruited to the enhancer of HoxB2 after RA treatment, and is absent in RA+TSA treated cells *in vivo* (Longobardi et al., in Preparation). We decided to analyze the presence of Myosin VI on the enhancer of the HoxB2 gene in the same uninduced, transcriptionally induced (RA) and induction-reversed (RA+TSA) NT2-D1 cells. As shown in Figure 6.2 the HoxB2 enhancer was not immunoprecipitated by MyosinVI antibodies under basal conditions, i.e. when the gene is not transcribed. On the other hand Myosin VI antibodies readily immunoprecipitated the HoxB2 enhancer upon RA induction, but Myosin VI was no longer associated to the regulatory region of HoxB2 when RA-induced NT2-D1 cells were treated with TSA Figure 6.2. An identical result was obtained with anti-RNAP-II CTD-S2p antibodies, which imunoprecipitated the HoxB2 enhancer only RA-treated NT2-D1 cells Figure 6.2. Interestingly, the poised form of RNAP-II (CTD-S5p) was associated with the HoxB2 enhancer in all conditions independently of transcriptional state of the gene. These results establish a link between Myosin VI, Prep1 and the transcriptional induction of HoxB2 gene.

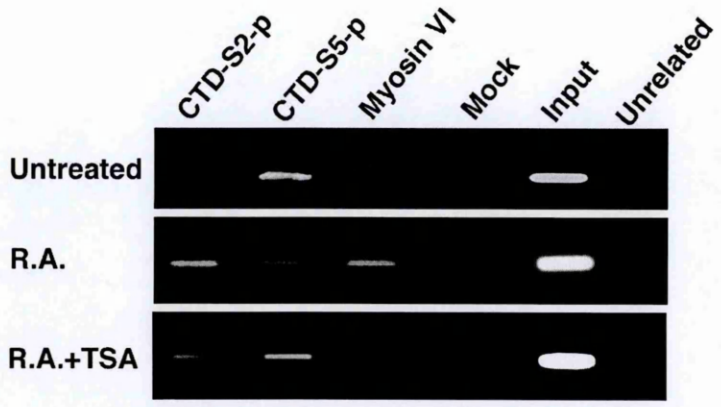

Figure 6.2. . Myosin VI associates with the enhancer of HoxB2 when the gene is transcribed.
ChIP using cross-linked chromatin from NT2-D1, treated or not with TPA, was performed as described in material and methods using antibodies against CTD-S2p, CTD-S5p and Myosin VI, as shown in the Figure. PCR amplification of immunoprecipitated material was performed with primers spanning the enhancer of the HoxB2 gene (Table II). The amplified material was visualized on 2% agarose, 1X TAE gels by Et-Br staining. The results show that Myosin VI is associated with the regulatory region of the HoxB2 gene upon RA transcriptional induction, whereas when the gene is not expressed (RA+TSA or untreated), no association was detected.

6.1.3. Myosin VI is required for the RA transcriptional activation of HoxB2.

We next evaluated whether nuclear Myosin VI regulates the expression of the HoxB2 gene by monitoring its mRNA levels in RA treated cells depleted of Myosin VI. First, we transiently transfected NT2-D1 cells with the AS Myosin VI construct (see chapter 5) or with the empty vector. Transfected cells were sorted in order to select those with a high level of EGFP expression (see Chapter 5). A western blot analysis shows that Myosin VI protein levels were efficiently down-regulated by AS RNA, as compared to control

transfected cells (Figure 6.3A and B). Sorted cells were than treated, or not, with RA and total RNA extracted. qRT-PCR shows a significant decrease (approximately 50%) of HoxB2 mRNA levels in RA-induced, AS Myosin VI transfected cells (Figure 6.3C). The result suggests that Myosin VI is required for the RA induction of HoxB2 transcription.

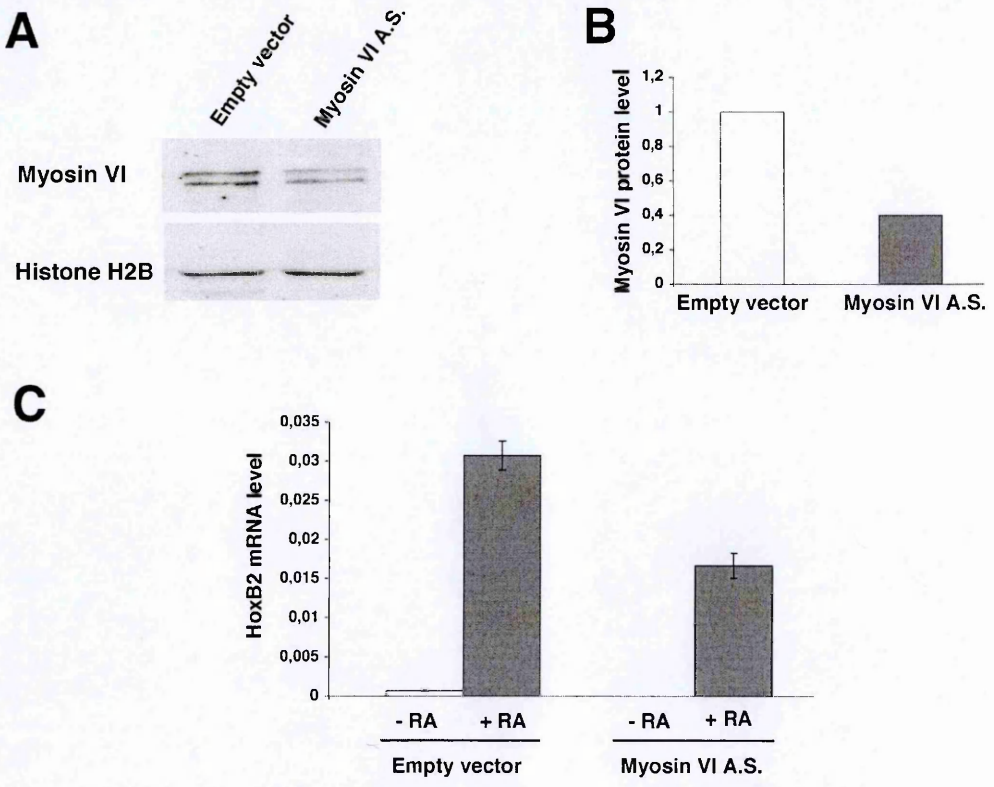

Figure 6.3. Myosin VI knock-down inhibits HoxB2 induction by RA treatment.
Transiently transfected NT2-D1 cells with an empty vector (pIRES-EGFP) or with a vector carring a Myosin VI A.S. (Yoshida et al., 2004)) were sorted to select transfected cells with a high level of EGFP expression. Part of the sorted cells was used to perform total proteins extraction (see material and methods). These extracts were resolved on a 5-15% gradient SDS-PAGE and transferred to PVDF membrane. (**A**) Myosin VI protein levels were analyzed by immunoblotting with specific polyclonal antibody and Histone H2B was used for normalization. (**B**) Densitometric analysis was carried out for each lane and the normalized O.D. values for each band were plotted in the graph shown. (**C**) The remainer of the sorted cells were not treated or treated with RA. Total RNA was purified, retro-transcribed and a qRT PCR analysis was performed using primers specific for HoxB2 mRNA (see Material and Methods). The data were normalized to the endogenous β-actin mRNA and plotted in a graph (mean ± SD from two independent PCRs done in triplicate).

6.1.4. Recruitment of Myosin VI in the nuclear compartment by RA treatment is reverted by TSA in NT2-D1 cells.

Previous results in HepG2 cells showed that a specific transcription-inducing stimulus determine the recruitment of Myosin VI from the cytoplasmic to the nuclear compartment (see chapter 5 and Figures 5.4 and 5.5). We decided to perform immunofluorence experiments by confocal microscopy on NT2-D1 cells in order to check whether RA or RA+TSA treatments affect the nucleo-cytoplasmic localization of Myosin VI. Figure 6.4A shows that MyosinVI is present in the nucleus of untreated cells with the typical speckled distribution (Vreugde et al., 2006), whereas RA-treated cells display a very strong nuclear staining. When NT2-D1 cells, were treated with TSA in the presence of RA, the nuclear accumulation of Myosin VI was reverted and the protein reacquired the cytoplasmic distribution observed in untreated cells (Figure 6.4A). Immunoblot analysis of total extracts of NT2-D1 cells shows that the amount of the protein does not change in all the conditions used (Figure 6.4B). Nevertheless the analysis of nuclear extracts by western blotting shows that RA-treated cells have a higher Myosin VI content than untreated or RA+TSA-treated cells (Figure 6.4B). These results therefore indicate that RA induces the nuclear accumulation of Myosin VI and that this re-localization is reverted by TSA treatment.

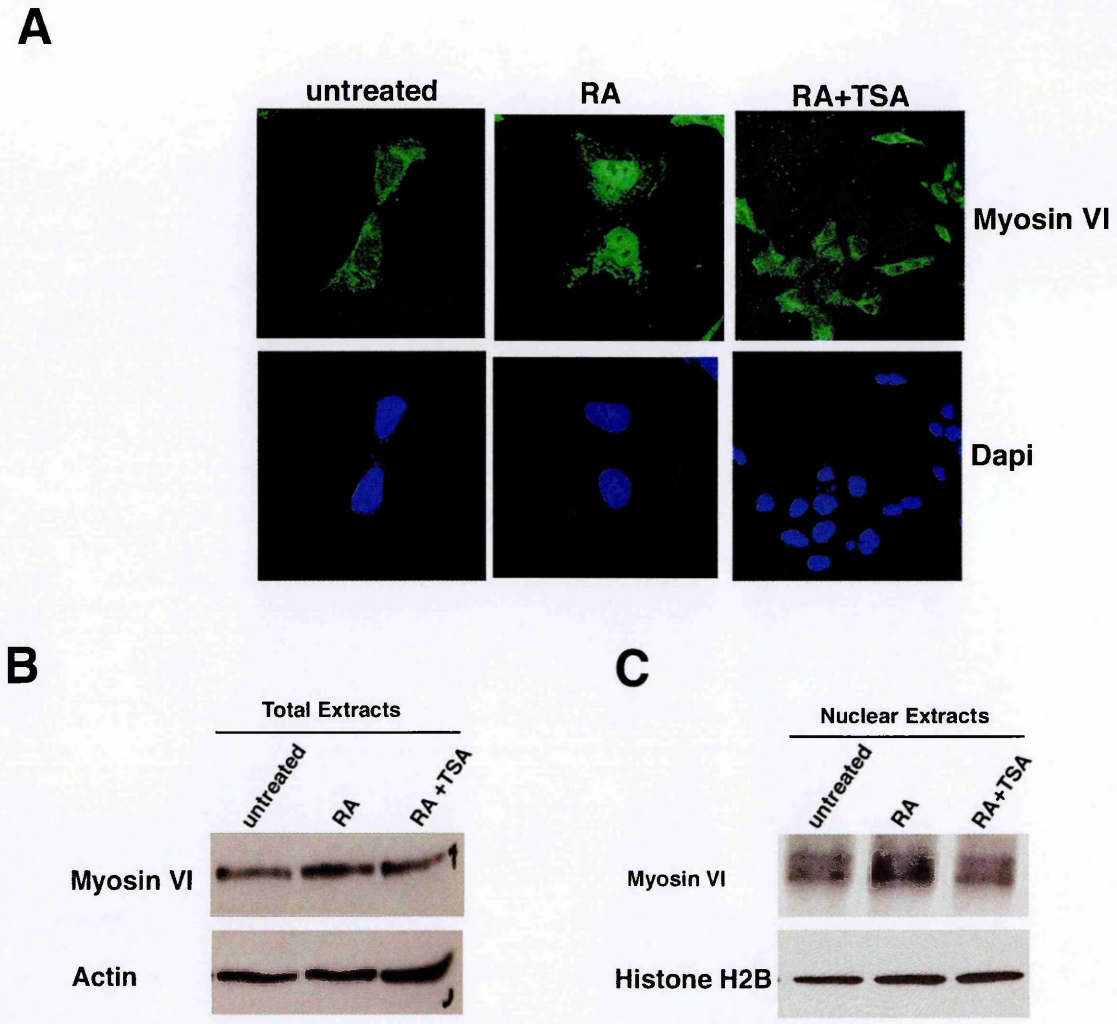

Figure 6.4. Different stimuli affects nuclear /cytoplasmic distribution of Myosin VI in NT2-D1 cells.

NT2-D1 cells untreated, treated with RA or with RA+TSA (see material and methods) were fixed with para-formaldehyde, permeabilized and immuno-stained using antibodies specific for Myosin VI (see material and methods). DAPI staining was used to visualize nuclei. **(A)** Confocal images showing the cellular distribution of Myosin VI show that in untreated cells the protein is mostly cytoplasmic. A certain amount of Myosin VI can be found also in the nuclear compartment where is distributed throughout the nucleoplasm in discrete foci. Treatment with RA determines a nuclear accumulation of Myosin VI whereas TSA treatment in the presence of RA restores the cytoplasmic distribution of the protein. **(B)** and **(C)** To confirm the microscopy results total and nuclear extracts were prepared from NT2-D1 cells subjected to the same treatments as above (see material and methods) resolved on a 5-15% gradient SDS-PAGE and transferred to PVDF membrane. Myosin VI protein levels were analyzed by immunoblotting with specific polyclonal antibodies. Anti-actin antibodies were used to normalize total protein extracts whereas nuclear extracts were normalized with an anti-Histone H2B.

6.1.5. The absence of Prep1 prevents the binding of Myosin VI to the regulatory regions of the transcription factor target genes.

Prep1 and Myosin VI are both associated with the enhancer of the HoxB2 gene after RA-induced transcriptional activation (Longobardi et al., in preparation and Figure 6.2). On the other hand the lack of Prep1 binding upon TSA treatment (Longobardi et al., in preparation) is accompanied by the loss of Myosin VI from the HoxB2 enhancer. These results suggest that Prep1 may be responsible for the recruitment of Myosin VI to the regulatory region of HoxB2. However, the results of Figure 6.4 do not clarify whether the absence of Myosin VI is the consequence of the loss of Prep1 binding or an independent event, such as the exit of Myosin VI from the nucleus. It has been recently found that the BCL-X and p53 genes are targets of Prep1 (see Introduction) and results of ChIP experiments carried out on MEF from WT and Prep1$^{i/i}$ (hypomorphic) mice showed the association of Prep1 with the regulatory sequences of these genes in the former but not in the latter (Micali et al., in preparation). An immunoblot analysis shows that Myosin VI endogenous protein levels do not vary between WT and Prep1$^{i/i}$ MEF (Figure 6.5A). In order to understand if Prep1 is required for Myosin VI recruitment on its target genes we repeated the ChIP assay using antibodies against Prep1 and Myosin VI on cross-linked chromatin from WT and Prep1$^{i/i}$ MEF and immunoprecipitated DNA was subjected to quantitative PCR. The results show that Myosin VI associates with the regulatory regions of the selected genes on chromatin from WT MEF, while no association of the protein with such sequences was found in immunoprecipitates from Prep1$^{i/i}$ MEF chromatin. These

results suggest that Prep1 is required for the recruitment of Myosin VI to the regulatory region of specific genes.

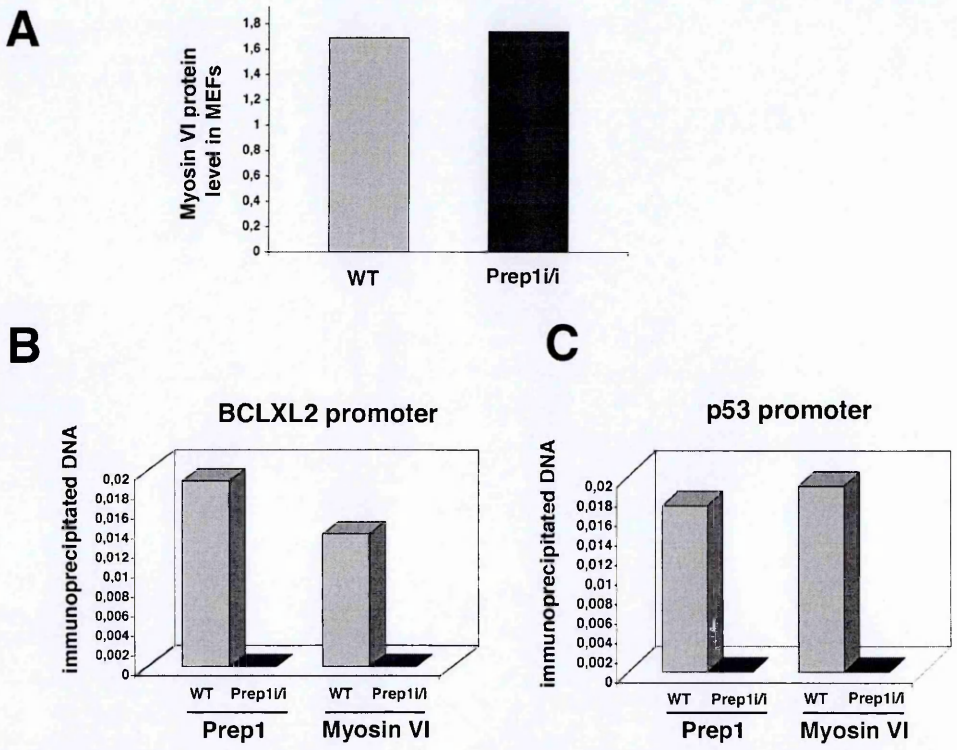

Figure 6.5. Prep1 is required to recruit Myosin VI on the regulatory regions of specific genes.

(**A**) Total proteins were extracted from WT and Prep1 $^{i/i}$ MEF (see material and methods) resolved on a 5-15% gradient SDS-PAGE and transferred to PVDF membrane. Myosin VI protein levels were analyzed by immunoblotting with specific polyclonal antibodies. Histone H2B was used for normalization. Densitometric analysis was carried for each lane and the normalized O.D. values for each band were plotted in the graph. (**B**) and (**C**) ChIP was performed as described in materials and methods. Cross-linked chromatin from WT and Prep1 $^{i/i}$ MEF was immunoprecipitated with antibody against Prep1, Myosin VI and uPAR as unrelated antibody (see Materials and Methods). qRT PCR amplification was performed using specific primers for the regulatory regions of the BCL-X and p53 genes. qPCR results were normalized to input DNA values. The results obtained from unrelated (uPAR) antibodies immunoprecipitated material was subtracted from the results obtained for BCL-X and p53 genes and the final numbers were plotted.

DISCUSSION -IV-

The data presented in Chapter 5 suggest that Myosin VI has a crucial role in modulating the transcriptional activity of RNAP-II by promoting its progression into the elongation phase. However, no information is available on how Myosin VI is recruited to target genes. We hypothesized that the transcription factor Prep1 might be involved in this process. We have approached this issue by using the NT2-D1 cell system in which RA-treatment induces the expression of the HoxB2 gene through the recruitment of Prep1 and in which the effect is reverted by TSA treatment.

6.2.1. Myosin VI is necessary to RA induction of HoxB2 gene.

Transcription factors modulate transcription by binding to specific DNA motifs localized in the regulatory regions of their target genes. The Prep1 homeodomain transcription factor is essential for embryonic development (Berthelsen et al., 1998; Ferretti et al., 2006) and is required for the expression of the HoxB gene cluster (Ferretti et al., 2005; Ferretti et al., 2000; Jacobs et al., 1999; Ryoo et al., 1999). Here we provide evidences that the binding of Prep1 and Myosin VI to the enhancer of the HoxB2 gene correlates with its expression. Myosin VI depletion with a specific AS RNA shows that the reduction of protein levels

correlates with a decrease of HoxB2 mRNA levels following RA treatment of NT2-D1 cells. These data indicate that Myosin VI is required for the transcriptional induction of the HoxB2 gene by RA.

6.2.2. Myosin VI promotes RNAP-II entry in the elongation phase.

In line with what previously observed in HepG2 cells ChIP assays using antibodies against the phosphorylated forms of RNAP-II reveal a clear association of the CTD-S2p with the enhancer of HoxB2 only after RA treatment of NT2-D1 cells. In these conditions also Myosin VI and Prep1 are associated with the regulatory element. Conversely the poised form RNAP-II (CTD-S5p) associates with the HoxB2 enhancer in untreated cells or after RA+TSA treatment, when the gene is not transcribed or is reverted to a transcriptionally inactive state. This indicates that RNAP-II is always associated with the HoxB2 enhancer, but transcription can proceed only when RA induces the RNAP-II switch to the CTD-S2p form. Moreover, these data confirm, in a different experimental system, that the presence of Myosin VI correlates with the association of RNAP-II CTD-S2p with the regulatory element of transcriptionally induced genes, strengthening the suggestion that Myosin VI is involved in promoting the access of RNAP-II to the elongation step. In light of what we reported in Chapter 4 the observation that the HoxB2 enhancer associates with the poised form of RNAP-II in control cells is intriguing. Albeit we have no evidence showing the physical association of the HoxB2 gene with specific factories, the ChIP data suggest that the gene might be located in a poised factory.

6.2.3. Stimulus-dependent behaviour of Myosin VI.

Treatment of NT2-D1 cells with RA determines a relocation of Myosin VI to the nuclear compartment, similarly to what previously observed in TPA treated HepG2 cells. This effect appears to be stimulus-specific, since TSA treatment fails to generate the same result and actually restore the protein distribution observed in untreated cells. These evidences raise questions on how different stimuli can affect Myosin VI behaviour: Which signaling cascade affects Myosin VI behavior? How can different stimuli, conveyed through Myosin VI affect the activation of different gene programs? How does Myosin VI associate with the regulatory region of target genes in order to favor their activation in response to specific stimuli?

6.2.4. Prep1 recruits Myosin VI to specific target genes.

A feasible scenario is the interaction of Myosin VI with transcription factors. The combinatorial action of different transcription factors confers position and temporal specificity to gene expression programs in an organism. Here we show that Myosin VI is part of a Prep1 complex. Both Prep1 and Myosin VI are associated with the enhancer of a transcriptionally induced HoxB2 gene and are absent after transcriptional inhibition by TSA. However, we still do not know if the recruitment of Myosin VI to the HoxB2 enhancer is a Prep1 mediated or an independent event. An indication that such recruitment may be a Prep1-mediated event comes from experiments in Prep1$^{i/i}$ MEF, showing that the absence of Prep1 prevents Myosin VI recruitment to the regulatory region of Prep1-target

genes. This finding supports the idea that a transcription factor may target Myosin VI to the regulatory region of a gene. Whether Myosin VI/Prep1 recruitment occurs through a direct interaction or is mediated by other proteins is presently under investigation.

6.2.5. Nucleus and motor proteins: Could an active nuclear transport be required for transcriptional regulation?

Chromosomes have been shown to have a spatially defined distribution in the interphase nucleus, each occupying a discrete volume defined as CT (Cremer and Cremer, 2001; Parada and Misteli, 2002). It is known that transcription of a specific gene and its position relatively to the CT is an important feature in modulating expression. FISH experiments suggest that, at least for some genes, there is a correlation between transcriptional activity and their localization outside the CTs, with the chromatin fiber containing the transcribed genes looping out of the CT (Chambeyron and Bickmore, 2004a; Mahy et al., 2002). Moreover, gene activation may also lead to the relocation of a gene locus from the periphery to the inner nuclear space (Kosak et al., 2002; Zink et al., 2004). Altogether these observations suggest a model in which some genes change their nuclear radial position following an activating stimulus (Misteli, 2004). In particular the HoxB cluster moves from the chromosomal territory to an extra-territorial location (Chambeyron et al., 2005). While it is clear that genes can change their positions, to date no mechanisms of active nuclear transport has been shown (Gorski et al., 2006). It is tempting to hypothesize the existence of a nucleoskeletal transport and/or gene localization mechanism involving nuclear motor proteins like Myosin VI. No information is available to date on the

reversibility of the processes by which genes protrude out of the CT. However, it is possible that different yet unidentified motor proteins, acting in different orientations, may be required for the displacement and relocation of chromosomal segments. The results shown in Chapter 5 together with those of this Chapter indicate that specific stimuli determine a dramatic redistribution of Myosin VI to the nuclear compartment. On the other hand our data, obtained in different cellular systems, suggest that the functional relevance of Myosin VI is linked to promoting RNAP-II elongation. However, the involvement of motor proteins in relocating genes in the nuclear space has yet to be shown.

SUMMARY -IV-

In this chapter we show that Myosin VI associates with a Prep1 complex and that Prep1 is implicated in the recruitment of Myosin VI to specific target genes. Moreover we provide evidences that Myosin VI selectively responds to specific extra-cellular signals. This suggests that different stimuli can converge onto Myosin VI, which may then modulate selected arrays of genes by the concerted interaction with specific transcription factors.

The experiments presented in this chapter include unpublished data part of which have been obtained in collaboration with other members of my laboratory. In particular: the

material used for the immunoblot experiments shown in Figure 6.1 has been obtained from a Prep1 TAP immunoprecipitation performed by Dr. Victor Manuel Diaz. The material used in the experiment shown in Figure 6.5 was obtained from MEF prepared by Dr. Nicola Micali.

REFERENCES

Abranches, R., Beven, A.F., Aragon-Alcaide, L. and Shaw, P.J. (1998) Transcription sites are not correlated with chromosome territories in wheat nuclei. *J Cell Biol*, **143**, 5-12.

Altman, D., Sweeney, H.L. and Spudich, J.A. (2004) The mechanism of myosin VI translocation and its load-induced anchoring. *Cell*, **116**, 737-749.

Andersen, J.S., Lam, Y.W., Leung, A.K., Ong, S.E., Lyon, C.E., Lamond, A.I. and Mann, M. (2005) Nucleolar proteome dynamics. *Nature*, **433**, 77-83.

Andersen, J.S., Lyon, C.E., Fox, A.H., Leung, A.K., Lam, Y.W., Steen, H., Mann, M. and Lamond, A.I. (2002) Directed proteomic analysis of the human nucleolus. *Curr Biol*, **12**, 1-11.

Andreasen, P.A., Kjoller, L., Christensen, L. and Duffy, M.J. (1997) The urokinase-type plasminogen activator system in cancer metastasis: a review. *Int J Cancer*, **72**, 1-22.

Aschenbrenner, L., Lee, T. and Hasson, T. (2003) Myo6 facilitates the translocation of endocytic vesicles from cell peripheries. *Mol Biol Cell*, **14**, 2728-2743.

Azuara, V., Perry, P., Sauer, S., Spivakov, M., Jorgensen, H.F., John, R.M., Gouti, M., Casanova, M., Warnes, G., Merkenschlager, M. and Fisher, A.G. (2006) Chromatin signatures of pluripotent cell lines. *Nat Cell Biol*, **8**, 532-538.

Bartlett, J., Blagojevic, J., Carter, D., Eskiw, C., Fromaget, M., Job, C., Shamsher, M., Trindade, I.F., Xu, M. and Cook, P.R. (2006) Specialized transcription factories. *Biochem Soc Symp*, 67-75.

Bartova, E., Kozubek, S., Kozubek, M., Jirsova, P., Lukasova, E., Skalnikova, M. and Buchnickova, K. (2000) The influence of the cell cycle, differentiation and irradiation on the nuclear location of the abl, bcr and c-myc genes in human leukemic cells. *Leuk Res*, **24**, 233-241.

Benasciutti, E., Pagès, G., Kenzior, O., Folk, W., Blasi, F. and Crippa, M.P. (2004) MAPK and JNK transduction pathways can phosphorylate Sp1 to activate the uPA minimal promoter elements and endogenous gene transcription. *Blood*, **104**, 256-262.

Bernstein, B.E., Kamal, M., Lindblad-Toh, K., Bekiranov, S., Bailey, D.K., Huebert, D.J., McMahon, S., Karlsson, E.K., Kulbolas, E.J.I., Gingeras, T.R., Schreiber, S.L. and Lander, E.S. (2005) Genomic maps and comparative analysis of histone modifications in human and mouse. *Cell*, **120**, 169-181.

Berthelsen, J., Kilstrup-Nielsen, C., Blasi, F., Mavilio, F. and Zappavigna, V. (1999) The subcellular localization of PBX1 and EXD proteins depends on nuclear import and export signals and is modulated by association with PREP1 and HTH. *Genes Dev*, **13**, 946-953.

Berthelsen, J., Zappavigna, V., Ferretti, E., Mavilio, F. and Blasi, F. (1998) The novel homeoprotein Prep1 modulates Pbx-Hox protein cooperativity. *E.M.B.O. Journal*, **17**.

Besser, D., Verde, P., Nagamine, Y. and Blasi, F. (1996) Signal transduction and the uPA/uPAR system. *Fibrinolysis*, **10**, 215-237.

Bettinger, B.T., Gilbert, D.M. and Amberg, D.C. (2004) Actin up in the nucleus. *Nat Rev Mol Cell Biol*, **5**, 410-415.

Bolzer, A., Kreth, G., Solovei, I., Koehler, D., Saracoglu, K., Fauth, C., Muller, S., Eils, R., Cremer, C., Speicher, M.R. and Cremer, T. (2005) Three-dimensional maps of all chromosomes in human male fibroblast nuclei and prometaphase rosettes. *PLoS Biol*, **3**, e157.

Boyle, S., Gilchrist, S., Bridger, J.M., Mahy, N.L., Ellis, J.A. and Bickmore, W.A. (2001) The spatial organization of human chromosomes within the nuclei of normal and emerin-mutant cells. *Hum Mol Genet*, **10**, 211-219.

Branco, M.R. and Pombo, A. (2006) Intermingling of chromosome territories in interphase suggests role in translocations and transcription-dependent associations. *PLoS Biol*, **4**, e138.

Brown, K.E., Baxter, J., Graf, D., Merkenschlager, M. and Fisher, A.G. (1999) Dynamic repositioning of genes in the nucleus of lymphocytes preparing for cell division. *Mol Cell*, **3**, 207-217.

Buratowski, S. (1994) The basics of basal transcription by RNA polymerase II. *Cell*, **77**, 1-3.

Buss, F., Arden, S.D., Lindsay, M., Luzio, J.P. and Kendrick-Jones, J. (2001) Myosin VI isoform localized to clathrin-coated vesicles with a role in clathrin-mediated endocytosis. *Embo J*, **20**, 3676-3684.

Buss, F., Kendrick-Jones, J., Lionne, C., Knight, A.E., Cote, G.P. and Paul Luzio, J. (1998) The localization of myosin VI at the golgi complex and leading edge of fibroblasts and its phosphorylation and recruitment into membrane ruffles of A431 cells after growth factor stimulation. *J Cell Biol*, **143**, 1535-1545.

Buss, F., Spudich, G. and Kendrick-Jones, J. (2004) Myosin VI: cellular functions and motor properties. *Ann. Rev. Cell Dev. Biol.*, **20**, 649-676.

Bustin, M. (1999) Regulation of DNA-dependent activities by the functional motifs of the high-mobility-group chromosomal proteins. *Mol Cell Biol*, **19**, 5237-5246.

Cai, S., Han, H.J. and Kohwi-Shigematsu, T. (2003) Tissue-specific nuclear architecture and gene expression regulated by SATB1. *Nat Genet*, **34**, 42-51.

Carter, D., Chakalova, L., Osborne, C.S., Dai, Y.F. and Fraser, P. (2002) Long-range chromatin regulatory interactions in vivo. *Nat Genet.*, **32**, 623-626.

Casse, C., Giannoni, F., Nguyen, V.T., Dubois, M.F. and Bensaude, O. (1999) The transcriptional inhibitors, actinomycin D and alpha-amanitin, activate the HIV-1 promoter and favor phosphorylation of the RNA polymerase II C-terminal domain. *J. Biol. Chem.*, **274**, 16097-16106.

Chakalova, L., Debrand, E., Mitchell, J.A., Osborne, C.S. and Fraser, P. (2005) Replication and transcription: shaping the landscape of the genome. *Nat Rev Genet*, **6**, 669-677.

Chambeyron, S. and Bickmore, W.A. (2004a) Chromatin decondensation and nuclear reorganization of the HoxB locus upon induction of transcription. *Genes Dev*, **18**, 1119-1130.

Chambeyron, S. and Bickmore, W.A. (2004b) Does looping and clustering in the nucleus regulate gene expression? *Curr. Opin. Cell Biol.*, **16**, 256-262.

Chambeyron, S., Da Silva, N.R., Lawson, K.A. and Bickmore, W.A. (2005) Nuclear re-organisation of the Hoxb complex during mouse embryonic development. *Development*, **132**, 2215-2223.

Chaumeil, J., Le Baccon, P., Wutz, A. and Heard, E. (2006) A novel role for Xist RNA in the formation of a repressive nuclear compartment into which genes are recruited when silenced. *Genes Dev*, **20**, 2223-2237.

Chi, T., Lieberman, P., Ellwood, K. and Carey, M. (1995) A general mechanism for transcriptional synergy by eukaryotic activators. *Nature*, **377**, 254-257.

Christmann, J.L. and Dahmus, M.E. (1981) Phosphorylation of rat ascites tumor non-histone chromatin proteins. Differential phosphorylation by two cyclic nucleotide-independent protein kinases and comparison to in vivo phosphorylation. *J Biol Chem*, **256**, 3326-3331.

Cirillo, G., Casalino, L., Vallone, D., Caracciolo, A., De Cesare, D. and Verde, P. (1999) Role of distinct mitogen-activated protein kinase pathways and cooperation between Ets-2, ATF-2, and Jun family members in human urokinase-type plasminogen activator gene induction by interleukin-1 and tetradecanoyl phorbol acetate. *Mol. Cell. Biol.*, **19**.

Cook, P.R. (1999) The organization of replication and transcription. *Science*, **284**, 1790-1795.

Cook, P.R. (2002) Predicting three-dimensional genome structure from transcriptional activity. *Nat Genet*, **32**, 347-352.

Corden, J.L. (1990) Tails of RNA polymerase II. *Trends Biochem Sci*, **15**, 383-387.

Cremer, T. and Cremer, C. (2001) Chromosome territories, nuclear architecture and gene regulation in mammalian cells. *Nat Rev Genet*, **2**, 292-301.

Cremer, T., Cremer, C., Baumann, H., Luedtke, E.K., Sperling, K., Teuber, V. and Zorn, C. (1982) Rabl's model of the interphase chromosome arrangement tested in Chinese hamster cells by premature chromosome condensation and laser-UV-microbeam experiments. *Hum Genet*, **60**, 46-56.

Cremer, T., Cremer, M., Dietzel, S., Muller, S., Solovei, I. and Fakan, S. (2006) Chromosome territories--a functional nuclear landscape. *Curr Opin Cell Biol*, **18**, 307-316.

Cremer, T., Kreth, G., Koester, H., Fink, R.H., Heintzmann, R., Cremer, M., Solovei, I., Zink, D. and Cremer, C. (2000) Chromosome territories, interchromatin domain compartment, and nuclear matrix: an integrated view of the functional nuclear architecture. *Crit Rev Eukaryot Gene Expr*, **10**, 179-212.

Cremer, T., Kurz, A., Zirbel, R., Dietzel, S., Rinke, B., Schrock, E., Speicher, M.R., Mathieu, U., Jauch, A., Emmerich, P., Scherthan, H., Ried, T., Cremer, C. and Lichter, P. (1993) Role of chromosome territories in the functional compartmentalization of the cell nucleus. *Cold Spring Harb Symp Quant Biol*, **58**, 777-792.

Crippa, M.P. (2007) Urokinase-type plasminogen activator. *Int J Biochem Cell Biol*, **39**, 690-694.

Dahmus, M.E. (1981) Phosphorylation of eukaryotic DNA-dependent RNA polymerase. Identification of calf thymus RNA polymerase subunits phosphorylated by two purified protein kinases, correlation with in vivo sites of phosphorylation in HeLa cell RNA polymerase II. *J Biol Chem*, **256**, 3332-3339.

Danø, K., Rømer, J., Nielsen, B.S., Bjorn, S., Pyke, C., Rygaard, J. and Lund, L.R. (1999) Cancer invasion and tissue remodeling: cooperation of protease systems and cell types. *APMIS*, **107**, 120-127.

de Lanerolle, P., Johnson, T. and Hofmann, W.A. (2005) Actin and myosin I in the nucleus: what next? *Nat Struct Mol Biol*, **12**, 742-746.

Deflorian, G., Tiso, N., Ferretti, E., Meyer, D., Blasi, F., Bortolussi, M. and Argenton, F. (2004) Prep1.1 has essential genetic functions in hindbrain development and cranial neural crest cell differentiation. *Development*, **131**, 613-627.

Dehghani, H., Dellaire, G. and Bazett-Jones, D.P. (2005) Organization of chromatin in the interphase mammalian cell. *Micron*, **36**, 95-108.

Dekker, J., Rippe, K., Dekker, M. and Kleckner, N. (2002) Capturing chromosome conformation. *Science*, **295**, 1306-1311.

Dellaire, G. and Bazett-Jones, D.P. (2004) PML nuclear bodies: dynamic sensors of DNA damage and cellular stress. *Bioessays*, **26**, 963-977.

Dillon, N. (2006) Gene regulation and large-scale chromatin organization in the nucleus. *Chromosome Res*, **14**, 117-126.

Dillon, N. and Sabbattini, P. (2000) Functional gene expression domains: defining the functional unit of eukaryotic gene regulation. *Bioessays*, **22**, 657-665.

Dreyfuss, G., Kim, V.N. and Kataoka, N. (2002) Messenger-RNA-binding proteins and the messages they carry. *Nat Rev Mol Cell Biol*, **3**, 195-205.

Dynan, W.S. (1989) Modularity in promoters and enhancers. *Cell*, **58**, 1-4.

Egly, J.M., Miyamoto, N.G., Moncollin, V. and Chambon, P. (1984) Is actin a transcription initiation factor for RNA polymerase B? *Embo J*, **3**, 2363-2371.

Eivazova, E.R. and Aune, T.M. (2004) Dynamic alterations in the conformation of the Ifng gene region during T helper cell differentiation. *Proc Natl Acad Sci U S A*, **101**, 251-256.

Ferrai, C., Munari, D., Luraghi, P., Pecciarini, L., Cangi, M., Doglioni, C., Blasi, F. and Crippa, M.P. (2007) A transcription-dependent MNase-resistant fragment of the uPA promoter interacts with the enhancer. *J Biol Chem*.

Ferretti, E., Cambronero, F., Tumpel, S., Longobardi, E., Wiedemann, L.M., Blasi, F. and Krumlauf, R. (2005) Hoxb1 enhancer and control of rhombomere 4 expression: complex interplay between PREP1-PBX1-HOXB1 binding sites. *Mol Cell Biol*, **25**, 8541-8552.

Ferretti, E., Marshall, H., Popperl, H., Maconochie, M., Krumlauf, R. and Blasi, F. (2000) Segmental expression of Hoxb2 in r4 requires two separate sites that integrate cooperative interactions between Prep1, Pbx and Hox proteins. *Development*, **127**, 155-166.

Ferretti, E., Villaescusa, J.C., Di Rosa, P., Fernandez-Diaz, L.C., Longobardi, E., Mazzieri, R., Miccio, A., Micali, N., Selleri, L., Ferrari, G. and Blasi, F. (2006) Hypomorphic

mutation of the TALE gene Prep1 (pKnox1) causes a major reduction of Pbx and Meis proteins and a pleiotropic embryonic phenotype. *Mol Cell Biol*, **26**, 5650-5662.

Fomproix, N. and Percipalle, P. (2004) An actin-myosin complex on actively transcribing genes. *Exp Cell Res*, **294**, 140-148.

Fraser, P. (2006) Transcriptional control thrown for a loop. *Curr Opin Genet Dev*, **16**, 490-495.

Friedman, T.B., Sellers, J.R. and Avraham, K.B. (1999) Unconventional myosins and the genetics of hearing loss. *Am J Med Genet*, **89**, 147-157.

Gaylis, F.D., Keer, H.N., Wilson, M.J., Kwaan, H.C., Sinha, A.A. and Kozlowski, J.M. (1989) Plasminogen activators in human prostate cancer cell lines and tumors: correlation with the aggressive phenotype. *J Urol*, **142**, 193-198.

Goldman, R.D., Gruenbaum, Y., Moir, R.D., Shumaker, D.K. and Spann, T.P. (2002) Nuclear lamins: building blocks of nuclear architecture. *Genes Dev*, **16**, 533-547.

Gomes, N.P., Bjerke, G., Llorente, B., Szostek, S.A., Emerson, B.M. and Espinosa, J.M. (2006) Gene-specific requirement for P-TEFb activity and RNA polymerase II phosphorylation within the p53 transcriptional program. *Genes Dev*, **20**, 601-612.

Gorski, S.A., Dundr, M. and Misteli, T. (2006) The road much traveled: trafficking in the cell nucleus. *Curr Opin Cell Biol*, **18**, 284-290.

Grosveld, F., Blom van Assendelft, G., Greaves, D., Kollias, G. (1987) position-indipendent, high level expression of the human b-globin gene in transgenic mice. *Cell*, **51**, 975-985.

Hahn, S. (2004) Structure and mechanism of the RNA polymerase II transcription machinery. *Nature Struct. Mol. Biol.*, **11**, 394-403.

Handwerger, K.E. and Gall, J.G. (2006) Subnuclear organelles: new insights into form and function. *Trends Cell Biol*, **16**, 19-26.

Hatzis, P. and Talianidis, I. (2002) Dynamics of enhancer-promoter communication during differentiation-induced gene activation. *Mol. Cell*, **10**, 1467-1477.

Helenius, M.A., Saramaki, O.R., Linja, M.J., Tammela, T.L. and Visakorpi, T. (2001) Amplification of urokinase gene in prostate cancer. *Cancer Res.*, **61**, 5340-5344.

Hofmann, W.A., Stojiljkovic, L., Fuchsova, B., Vargas, G.M., Mavrommatis, E., Philimonenko, V., Kysela, K., Goodrich, J.A., Lessard, J.L., Hope, T.J., Hozak, P. and de Lanerolle, P. (2004) Actin is part of pre-initiation complexes and is necessary for transcription by RNA polymerase II. *Nat Cell Biol*, **6**, 1094-1101.

Hofmann, W.A., Vargas, G.M., Ramchandran, R., Stojiljkovic, L., Goodrich, J.A. and de Lanerolle, P. (2006) Nuclear myosin I is necessary for the formation of the first phosphodiester bond during transcription initiation by RNA polymerase II. *J Cell Biochem*, **99**, 1001-1009.

Horikoshi, M., Hai, T., Lin, Y.S., Green, M.R. and Roeder, R.G. (1988) Transcription factor ATF interacts with the TATA factor to facilitate establishment of a preinitiation complex. *Cell*, **54**, 1033-1042.

Hozak, P., Cook, P.R., Schofer, C., Mosgoller, W. and Wachtler, F. (1994) Site of transcription of ribosomal RNA and intranucleolar structure in HeLa cells. *J Cell Sci*, **107 (Pt 2)**, 639-648.

Hsu, D.W., Efird, J.T. and Hedley-Whyte, E.T. (1995) Prognostic role of urokinase-type plasminogen activator in human gliomas. *Am J Pathol*, **147**, 114-123.

Hu, P., Wu, S. and Hernandez, N. (2004) A role for beta-actin in RNA polymerase III transcription. *Genes Dev*, **18**, 3010-3015.

Huang, W., Mishra, V., Batra, S., Dillon, I. and Mehta, K.D. (2004) Phorbol ester promotes histone H3-Ser10 phosphorylation at the LDL receptor promoter in a protein kinase C-dependent manner. *J Lipid Res*, **45**, 1519-1527.

Ibanez-Tallon, I., Caretti, G., Blasi, F. and Crippa, M.P. (1999) In vivo analysis of the state of the human uPA enhancer following stimulation by TPA. *Oncogene*, **18**, 2836-2845.

Ibanez-Tallon, I., Ferrai, C., Longobardi, E., Facetti, I., Blasi, F. and Crippa, M.P. (2002) Binding of Sp1 to the proximal promoter links constitutive expression of the human uPA gene and invasive potential of PC3 cells. *Blood*, **100**, 3325-3332.

Iborra, F.J., Pombo, A., Jackson, D.A. and Cook, P.R. (1996) Active RNA polymerases are localized within discrete transcription "factories' in human nuclei. *J Cell Sci*, **109 (Pt 6)**, 1427-1436.

Inostroza, J.A., Mermelstein, F.H., Ha, I., Lane, W.S. and Reinberg, D. (1992) Dr1, a TATA-binding protein-associated phosphoprotein and inhibitor of class II gene transcription. *Cell*, **70**, 477-489.

Jackson, D.A., Hassan, A.B., Errington, R.J. and Cook, P.R. (1993) Visualization of focal sites of transcription within human nuclei. *Embo J*, **12**, 1059-1065.

Jackson, D.A., Iborra, F.J., Manders, E.M. and Cook, P.R. (1998) Numbers and organization of RNA polymerases, nascent transcripts, and transcription units in HeLa nuclei. *Mol Biol Cell*, **9**, 1523-1536.

Jacobs, Y., Schnabel, C.A. and Cleary, M.L. (1999) Trimeric association of Hox and TALE homeodomain proteins mediates Hoxb2 hindbrain enhancer activity. *Mol Cell Biol*, **19**, 5134-5142.

Kim, S.H., McQueen, P.G., Lichtman, M.K., Shevach, E.M., Parada, L.A. and Misteli, T. (2004) Spatial genome organization during T-cell differentiation. *Cytogenet Genome Res*, **105**, 292-301.

Kim, Y.J., Bjorklund, S., Li, Y., Sayre, M.H. and Kornberg, R.D. (1994) A multiprotein mediator of transcriptional activation and its interaction with the C-terminal repeat domain of RNA polymerase II. *Cell*, **77**, 599-608.

Kimura, H., Sugaya, K. and Cook, P.R. (2002) The transcription cycle of RNA polymerase II in living cells. *J Cell Biol*, **159**, 777-782.

Kimura, H., Tao, Y., Roeder, R.G. and Cook, P.R. (1999) Quantitation of RNA polymerase II and its transcription factors in an HeLa cell: little soluble holoenzyme but significant amounts of polymerases attached to the nuclear substructure. *Mol Cell Biol*, **19**, 5383-5392.

Komarnitsky, P., Cho, E.J. and Buratowski, S. (2000) Different phosphorylated forms of RNA polymerase II and associated mRNA processing factors during transcription. *Genes Dev*, **14**, 2452-2460.

Kosak, S.T., Skok, J.A., Medina, K.L., Riblet, R., Le Beau, M.M., Fisher, A.G. and Singh, H. (2002) Subnuclear compartmentalization of immunoglobulin loci during lymphocyte development. *Science*, **296**, 158-162.

Kozubek, S., Lukasova, E., Jirsova, P., Koutna, I., Kozubek, M., Ganova, A., Bartova, E., Falk, M. and Pasekova, R. (2002) 3D Structure of the human genome: order in randomness. *Chromosoma*, **111**, 321-331.

Krumm, A., Hickey, L.B. and Groudine, M. (1995) Promoter-proximal pausing of RNA polymerase II defines a general rate-limiting step after transcription initiation. *Genes Dev.*, **9**, 559-572.

Krumm, A., Meulia, T., Brunvand, M. and M., G. (1992) The block to transcriptional elongation within the human c-myc gene is determined in the promoter-proximal region. *Genes Dev.*, **6**, 2201-2213.

Kukalev, A., Nord, Y., Palmberg, C., Bergman, T. and Percipalle, P. (2005) Actin and hnRNP U cooperate for productive transcription by RNA polymerase II. *Nat Struct Mol Biol*, **12**, 238-244.

Kumaran, R.I., Muralikrishna, B. and Parnaik, V.K. (2002) Lamin A/C speckles mediate spatial organization of splicing factor compartments and RNA polymerase II transcription. *J Cell Biol*, **159**, 783-793.

Kurz, A., Lampel, S., Nickolenko, J.E., Bradl, J., Benner, A., Zirbel, R.M., Cremer, T. and Lichter, P. (1996) Active and inactive genes localize preferentially in the periphery of chromosome territories. *J Cell Biol*, **135**, 1195-1205.

Laemmli, U.K. (1970) Cleavage of structural proteins during the assembly of the head of bacteriophage T4. *Nature*, **227**, 680-685.

Lamond, A.I. and Spector, D.L. (2003) Nuclear speckles: a model for nuclear organelles. *Nat Rev Mol Cell Biol*, **4**, 605-612.

Lemon, B. and Tjian, R. (2000) Orchestrated response: a symphony of transcription factors for gene control. *Genes Dev*, **14**, 2551-2569.

Levsky, J.M., Shenoy, S.M., Pezo, R.C. and Singer, R.H. (2002) Single-cell gene expression profiling. *Science*, **297**, 836-840.

Li, Q., Harju, S. and Peterson, K.R. (1999) Locus control regions: coming of age at a decade plus. *Trends Genet.*, **15**, 403-408.

Lin, Y.S. and Green, M.R. (1991) Mechanism of action of an acidic transcriptional activator in vitro. *Cell*, **64**, 971-981.

Litt, M.D., Simpson, M., Gaszner, M., Allis, C.D. and Felsenfeld, G. (2001a) Correlation between histone lysine methylation and developmental changes at the chicken β-globin locus. *Science*, **293**, 2453-2455.

Litt, M.D., Simpson, M., Recillas-Targa, F., Prioleau, M.N. and Felsenfeld, G. (2001b) Transitions in histone acetylation reveal boundaries of three separately regulated neighboring loci. *EMBO J.*, **20**, 2224-2235.

Liu, Z. and Garrard, W.T. (2005) Long-range interactions between three transcriptional enhancers, active Vkappa gene promoters, and a 3' boundary sequence spanning 46 kilobases. *Mol Cell Biol*, **25**, 3220-3231.

Look, M.P. and Foekens, J.A. (1999) Clinical relevance of the urokinase plasminogen activator system in breast cancer. *Apmis*, **107**, 150-159.

Mahy, N.L., Perry, P.E. and Bickmore, W.A. (2002) Gene density and transcription influence the localization of chromatin outside of chromosome territories detectable by FISH. *J Cell Biol*, **159**, 753-763.

Marenduzzo, D., Faro-Trindade, I. and Cook, P.R. (2007) What are the molecular ties that maintain genomic loops? *Trends Genet.*, **23**, 126-133.

Martin, S. and Pombo, A. (2003) Transcription factories: quantitative studies of nanostructures in the mammalian nucleus. *Chromosome Res*, **11**, 461-470.

McDonald, D., Carrero, G., Andrin, C., de Vries, G. and Hendzel, M.J. (2006) Nucleoplasmic beta-actin exists in a dynamic equilibrium between low-mobility polymeric species and rapidly diffusing populations. *J Cell Biol*, **172**, 541-552.

Milanini, J., Viñals, F., Pouysségur, J. and Pagès, G. (1998) p42/p44 MAP kinase module plays a key role in the transcriptional regulation of the vascular endothelial growth factor gene in fibroblasts. *J.Biol.Chem.*, **273**, 18156-18172.

Milanini-Mongiat, J., Pouysségur, J. and Pagès, G. (2002) Identification of two p42/p44 mitogen activated kinases phosphorilation sites on Sp1: Their implication in vascular endothelial growth factor gene transcription. *J.Biol.Chem.*, **In press**.

Misteli, T. (2001a) Protein dynamics: implications for nuclear architecture and gene expression. *Science*, **291**, 843-847.

Misteli, T. (2001b) The concept of self-organization in cellular architecture. *J Cell Biol*, **155**, 181-185.

Misteli, T. (2004) Spatial positioning; a new dimension in genome function. *Cell*, **119**, 153-156.

Misteli, T. (2005) Concepts in nuclear architecture. *Bioessays*, **27**, 477-487.

Misteli, T. (2007) Beyond the sequence: cellular organization of genome function. *Cell*, **128**, 787-800.

Miyake, H., Hara, I., Yamanaka, K., Arakawa, S. and Kamidono, S. (1999a) Elevation of urokinase-type plasminogen activator and its receptor densities as new predictors of disease progression and prognosis in men with prostate cancer. *Int J Oncol*, **14**, 535-541.

Miyake, H., Hara, I., Yamanaka, K., Gohji, K., Arakawa, S. and Kamidono, S. (1999b) Elevation of serum levels of urokinase-type plasminogen activator and its receptor is associated with disease progression and prognosis in patients with prostate cancer. *Prostate*, **39**, 123-129.

Murrell, A., Heeson, S. and Reik, W. (2004) Interaction between differentially methylated regions partitions the imprinted genes Igf2 and H19 into parent-specific chromatin loops. *Nature Genetics*, **36**, 889-893.

Nakajima, T., Uchida, C., Anderson, S.F., Lee, C.G., Hurwitz, J., Parvin, J.D. and Montminy, M. (1997) RNA helicase A mediates association of CBP with RNA polymerase II. *Cell*, **90**, 1107-1112.

Nerlov, C., De Cesare, D., Pergola, F., Caracciolo, A., Blasi, F., Johnsen, M. and Verde, P. (1992) A regulatory element that mediates co-operation between a PEA3/AP-1 element and an AP-1 site is required for phorbol ester induction of urokinase enhancer activity in HepG2 hepatoma cells. *E.M.B.O. Journal*, **11**, 4573-4582.

Nerlov, C., Rørth, P., Blasi, F. and Johnsen, M. (1991) Essential AP-1 and PEA3 binding elements in the human urokinase enhancer display cell type-specific activity. *Oncogene*, **6**, 1583-1592.

Nguyen, V.T., Giannoni, F., Dubois, M.F., Seo, S.J., Vigneron, M., Kedinger, C. and Bensaude, O. (1996) In vivo degradation of RNA polymerase II largest subunit triggered by alpha-amanitin. *Nucl. Acids Res.*, **24**, 2924-2929.

Nickerson, J. (2001) Experimental observations of a nuclear matrix. *J Cell Sci*, **114**, 463-474.

Nightingale, K.P., O'Neill, L.P. and Turner, B.M. (2006) Histone modifications: signalling receptors and potential elements of a heritable epigenetic code. *Curr Opin Genet Dev*, **16**, 125-136.

Olave, I.A., Reck-Peterson, S.L. and Crabtree, G.R. (2002) Nuclear actin and actin-related proteins in chromatin remodeling. *Annu Rev Biochem*, **71**, 755-781.

Orlando, V., Strutt, H. and Paro, R. (1997) Analysis of chromatin structure by in vivo formaldehyde cross-linking. *Methods*, **11**, 205-214.

Osborne, C.S., Chakalova, L., Brown, K.E., Carter, D., Horton, A., Debrand, E., Goyenechea, B., Mitchell, J.A., Lopes, S., Reik, W. and Fraser, P. (2004) Active genes dynamically colocalize to shared sites of ongoing transcription. *Nat Genet*, **36**, 1065-1071.

Parada, L. and Misteli, T. (2002) Chromosome positioning in the interphase nucleus. *Trends Cell Biol*, **12**, 425-432.

Pederson, T. (2000) Half a century of "the nuclear matrix". *Mol Biol Cell*, **11**, 799-805.

Penkov, D., Di Rosa, P., Fernandez Diaz, L., Basso, V., Ferretti, E., Grassi, F., Mondino, A. and Blasi, F. (2005) Involvement of Prep1 in the alphabeta T-cell receptor T-lymphocytic potential of hematopoietic precursors. *Mol Cell Biol*, **25**, 10768-10781.

Percipalle, P., Zhao, J., Pope, B., Weeds, A., Lindberg, U. and Daneholt, B. (2001) Actin bound to the heterogeneous nuclear ribonucleoprotein hrp36 is associated with Balbiani ring mRNA from the gene to polysomes. *J Cell Biol*, **153**, 229-236.

Pestic-Dragovich, L., Stojiljkovic, L., Philimonenko, A.A., Nowak, G., Ke, Y., Settlage, R.E., Shabanowitz, J., Hunt, D.F., Hozak, P. and de Lanerolle, P. (2000) A myosin I isoform in the nucleus. *Science*, **290**, 337-341.

Philimonenko, V.V., Zhao, J., Iben, S., Dingova, H., Kysela, K., Kahle, M., Zentgraf, H., Hofmann, W.A., de Lanerolle, P., Hozak, P. and Grummt, I. (2004) Nuclear actin and myosin I are required for RNA polymerase I transcription. *Nat Cell Biol*, **6**, 1165-1172.

Pleasure, S.J., Page, C. and Lee, V.M. (1992) Pure, postmitotic, polarized human neurons derived from NTera 2 cells provide a system for expressing exogenous proteins in terminally differentiated neurons. *J Neurosci*, **12**, 1802-1815.

Pombo, A., Jackson, D.A., Hollinshead, M., Wang, Z., Roeder, R.G. and Cook, P.R. (1999) Regional specialization in human nuclei: visualization of discrete sites of transcription by RNA polymerase III. *Embo J*, **18**, 2241-2253.

Puig, O., Caspary, F., Rigaut, G., Rutz, B., Bouveret, E., Bragado-Nilsson, E., Wilm, M. and Seraphin, B. (2001) The tandem affinity purification (TAP) method: a general procedure of protein complex purification. *Methods*, **24**, 218-229.

Pyke, C., Kristensen, P., Ralfkjær, E., Grondahl-Hansen, J., Eriksen, J., Blasi, F. and Danø, K. (1991) Urokinase-type plasminogen activator is expressed in stromal cells and its receptor in cancer cells at invasive foci in human colon adenocarcinomas. *Am J Pathol*, **138**, 1059-1067.

Ragoczy, T., Telling, A., Sawado, T., Groudine, M. and Kosak, S.T. (2003) A genetic analysis of chromosome territory looping: diverse roles for distal regulatory elements. *Chromosome Res*, **11**, 513-525.

Riccio, A., Grimaldi, G., Verde, P., Sebastio, G., Boast, S. and Blasi, F. (1985) The human urokinase-plasminogen activator gene and its promoter. *Nucl. Acids Res.*, **13**, 2759-2771.

Roix, J.J., McQueen, P.G., Munson, P.J., Parada, L.A. and Misteli, T. (2003) Spatial proximity of translocation-prone gene loci in human lymphomas. *Nat Genet*, **34**, 287-291.

Rorth, P., Nerlov, C., Blasi, F. and Johnsen, M. (1990) Transcription factor PEA3 participates in the induction of urokinase plasminogen activator transcription in murine keratinocytes stimulated with epidermal growth factor or phorbol-ester. *Nucl. Acids Res.*, **18**, 5009-5017.

Ross, I.L., Browne, C.M. and Hume, D.A. (1994) Transcription of individual genes in eukaryotic cells occurs randomly and infrequently. *Immunol Cell Biol*, **72**, 177-185.

Ryoo, H.D., Marty, T., Casares, F., Affolter, M. and Mann, R.S. (1999) Regulation of Hox target genes by a DNA bound Homothorax/Hox/Extradenticle complex. *Development*, **126**, 5137-5148.

Scheer, U., Hinssen, H., Franke, W.W. and Jockusch, B.M. (1984) Microinjection of actin-binding proteins and actin antibodies demonstrates involvement of nuclear actin in transcription of lampbrush chromosomes. *Cell*, **39**, 111-122.

Schübeler, D., MacAlpine, D.M., Scalzo, D., Wirbelauer, C., Kooperberg, C., van Leeuwen, F., Gottschling, D.E., O'Neill, L.P., Turner, B.M., Delrow, J., Bell, S.P. and Groudine, M. (2006) The histone modification pattern of active genes revealed through genome-wide chromatin analysis of a higher eukaryote. *Genes Dev.*, **18**, 1263-1271.

Simeone, A., Acampora, D., Arcioni, L., Andrews, P.W., Boncinelli, E. and Mavilio, F. (1990) Sequential activation of HOX2 homeobox genes by retinoic acid in human embryonal carcinoma cells. *Nature*, **346**, 763-766.

Sims, R.J., 3rd, Belotserkovskaya, R. and Reinberg, D. (2004) Elongation by RNA polymerase II: the short and long of it. *Genes Dev*, **18**, 2437-2468.

Skok, J.A., Brown, K.E., Azuara, V., Caparros, M.L., Baxter, J., Takacs, K., Dillon, N., Gray, D., Perry, R.P., Merkenschlager, M. and Fisher, A.G. (2001) Nonequivalent nuclear location of immunoglobulin alleles in B lymphocytes. *Nat Immunol*, **2**, 848-854.

Skriver, L., Larsson, L.I., Kielberg, V., Nielsen, L.S., Andresen, P.B., Kristensen, P. and Dano, K. (1984) Immunocytochemical localization of urokinase-type plasminogen activator in Lewis lung carcinoma. *J Cell Biol*, **99**, 752-757.

Spilianakis, C.G. and Flavell, R.A. (2004) Long-range intrachromosomal interactions in the T helper type 2 cytokine locus. *Nature Immunology*, **5**, 1017-1027.

Stiller, J.W. and Cook, M.S. (2004) Functional unit of the RNA polymerase II C-terminal domain lies within heptapeptide pairs. *Eukaryot Cell*, **3**, 735-740.

Sullivan, G.J., Bridger, J.M., Cuthbert, A.P., Newbold, R.F., Bickmore, W.A. and McStay, B. (2001) Human acrocentric chromosomes with transcriptionally silent nucleolar organizer regions associate with nucleoli. *Embo J*, **20**, 2867-2874.

Sun, F.L. and Elgin, S.C. (1999) Putting boundaries on silence. *Cell*, **99**, 459-462.

Tolhuis, B., Palstra, R.J., Splinter, E., Grosveld, F. and de Laat, W. (2002) Looping and interaction between hypersensitive sites in the active β-globin locus. *Mol. Cell.*, **10**, 1453-1465.

Towbin, H., Staehelin, T. and Gordon, J. (1979) Electrophoretic transfer of proteins from polyacrylamide gels to nitrocellulose sheets: procedure and some applications. *Proc Natl Acad Sci U S A*, **76**, 4350-4354.

Turner, B.M. (2001) *Chromatin and Gene Regulation. Molecular Mechanisms in Epigenetics*. Blackwell Science Ltd.

Turner, B.M. (2005) Reading signals on the nucleosome with a new nomenclature for modified histones. *Nat. Struct. Mol. Biol.*, **12**, 110-112.

van Holde, K.E. (1989) *Chromatin*. Springer-Verlag, New York.

Van Veldhuizen, P.J., Sadasivan, R., Cherian, R. and Wyatt, A. (1996) Urokinase-type plasminogen activator expression in human prostate carcinomas. *Am J Med Sci*, **312**, 8-11.

Vecerova, J., Koberna, K., Malinsky, J., Soutoglou, E., Sullivan, T., Stewart, C.L., Raska, I. and Misteli, T. (2004) Formation of nuclear splicing factor compartments is independent of lamins A/C. *Mol Biol Cell*, **15**, 4904-4910.

Verde, P., Boast, S., Franze, A., Robbiati, F. and Blasi, F. (1988) An upstream enhancer and a negative element in the 5' flanking region of the human urokinase plasminogen activator gene. *Nucleic Acids Res*, **16**, 10699-10716.

Verschure, P.J., van der Kraan, I., Manders, E.M., Hoogstraten, D., Houtsmuller, A.B. and van Driel, R. (2003) Condensed chromatin domains in the mammalian nucleus are accessible to large macromolecules. *EMBO Rep*, **4**, 861-866.

Verschure, P.J., van Der Kraan, I., Manders, E.M. and van Driel, R. (1999) Spatial relationship between transcription sites and chromosome territories. *J Cell Biol*, **147**, 13-24.

Volpi, E.V., Chevret, E., Jones, T., Vatcheva, R., Williamson, J., Beck, S., Campbell, R.D., Goldsworthy, M., Powis, S.H., Ragoussis, J., Trowsdale, J. and Sheer, D. (2000) Large-scale chromatin organization of the major histocompatibility complex and other regions of human chromosome 6 and its response to interferon in interphase nuclei. *J Cell Sci*, **113 (Pt 9)**, 1565-1576.

Vreugde, S., Ferrai, C., Miluzio, A., Hauben, E., Marchisio, P.C., Crippa, M.P., Bussi, M. and Biffo, S. (2006) Nuclear myosin VI enhances RNA polymerase II-dependent transcription. *Mol Cell*, **23**, 749-755.

Wansink, D.G., Schul, W., van der Kraan, I., van Steensel, B., van Driel, R. and de Jong, L. (1993) Fluorescent labeling of nascent RNA reveals transcription by RNA polymerase II in domains scattered throughout the nucleus. *J Cell Biol*, **122**, 283-293.

Wasser, M. and Chia, W. (2000) The EAST protein of drosophila controls an expandable nuclear endoskeleton. *Nat Cell Biol*, **2**, 268-275.

Wells, A.L., Lin, A.W., Chen, L.Q., Safer, D., Cain, S.M., Hasson, T., Carragher, B.O., Milligan, R.A. and Sweeney, H.L. (1999) Myosin VI is an actin-based motor that moves backwards. *Nature*, **401**, 505-508.

West, A.G., Gaszner, M. and Felsenfeld, G. (2002) Insulators: many functions, many mechanisms. *Genes Dev*, **16**, 271-288.

Williams, R.R., Broad, S., Sheer, D. and Ragoussis, J. (2002) Subchromosomal positioning of the epidermal differentiation complex (EDC) in keratinocyte and lymphoblast interphase nuclei. *Exp Cell Res*, **272**, 163-175.

Wu, X., Yoo, Y., Okuhama, N.N., Tucker, P.W., Liu, G. and Guan, J.L. (2006) Regulation of RNA-polymerase-II-dependent transcription by N-WASP and its nuclear-binding partners. *Nat Cell Biol*, **8**, 756-763.

Yang, J.L., Seetoo, D., Wang, Y., Ranson, M., Berney, C.R., Ham, J.M., Russell, P.J. and Crowe, P.J. (2000) Urokinase-type plasminogen activator and its receptor in colorectal cancer: independent prognostic factors of metastasis and cancer-specific survival and potential therapeutic targets. *Int J Cancer*, **89**, 431-439.

Yoshida, H., Cheng, W., Hung, J., Montell, D., Geisbrecht, E., Rosen, D., Liu, J. and Naora, H. (2004) Lessons from border cell migration in the Drosophila ovary: A role for myosin VI in dissemination of human ovarian cancer. *Proc Natl Acad Sci U S A*, **101**, 8144-8149.

Zink, D., Amaral, M.D., Englmann, A., Lang, S., Clarke, L.A., Rudolph, C., Alt, F., Luther, K., Braz, C., Sadoni, N., Rosenecker, J. and Schindelhauer, D. (2004) Transcription-dependent spatial arrangements of CFTR and adjacent genes in human cell nuclei. *J Cell Biol*, **166**, 815-825.

Zirbel, R.M., Mathieu, U.R., Kurz, A., Cremer, T. and Lichter, P. (1993) Evidence for a nuclear compartment of transcription and splicing located at chromosome domain boundaries. *Chromosome Res*, **1**, 93-106.

ACKNOWLEDGMENTS

During my PhD I travelled through wonderful stimulating experiences and by daily tackling difficulties I grew scientifically and professionally. However I would never be what I am now without someone very special. "Sometime you can't make it on your own" and in this big trip I have never been alone. So I would like to express all my gratitude to these persons who tought me, fought with me, took care of me and allowed me to run and touch this important appointment. First I would like to thank my director of studies Massimo P. Crippa for giving me this opportunity, I will never forget it. Many thanks also to my supervisors Bryan M. Turner and Lawerence Wrabetz for their precious help in some crucial steps of my walk. Of course thanks also to Francesco Blasi, the big eye. A special thank to Ana Pombo and her group for stimulating discussions and crucial help with Immuno-FISH experiments. Many thanks also to Sarah Vreugde, Stefano Biffo and all Biffo's group from whom I learnt a lot working with. How to forget the dream-team Paolo Luraghi and Davide Munari: working together has been an honour. Many thanks also to Elena Longobardi, Victor Diaz, and Nicola Micali for useful discussions and collaborative efforts. Thanks to Cesare Covino for help and patience in introducing me to the beautiful confocal imaging world and also to Alessio Palini who helped me in cell-sorting experiments. Thanks to the "Meldolesians angels" Rosalba Dalessandro, Laura Stucchi. Serena Bellani, Vitor Sousa, Luisa Stefano, Andrijana Klain and Malik Yussuf for their constant great support. Special aknowledgements to Luis Fernandez and Andrea Orsi:

science will never die with persons like that. I would like to say thanks to the PhD community in particular to Paola Scaffidi, Dario Bonanomi, Alessandro Nodari and Stefano Biressi: you may believe that behind a beer often there are the highest philosophic discussions. Fantastic friends like Laura Astolfi, Celia Pardini, Tiziana Giordano and Giada Bianchi simply became a piece of my soul. Thanks to the past and the future of our laboratory Silvia Olivari, Elisa Benasciutti, Giorgia Colciago, Monika Wozinska and to all Blasi's laboratory. My thought necessarily goes to the big population of friends, the ones that are always around of me and the ones that unfortunately are not... they gave me so much... I hope to have the opportunity to give back at least a part of what I received! I would like to say thanks also to Annalisa Di Sabato, I have no words, but look in my eyes... I think it's enough. Very special thanks goes to Gianpietro Ferrai, Angela Loi, Mariagrazia Ferrai, Veneranda Ferrai, Giulia Ferrai and Valeria Tegas...my Family...I am in you exactly like you are in me. Thanks to my grandfather Eugenio (noto Egidio) Loi: he simply tought me to smile, to be brave in every situation of life and to respect everything and everyone. But in particular he tought me to be damned curious and to realize that truth is made of many voices.

- Thanks for the gift, for any day of this shared time, made special by pleasant daily habits -

- Grazie per il regalo, per una giornata qualunque di questo tempo condiviso, nel tempo reso speciale da una bella quotidianità -

Carmelo

Appendix A

List of abbreviations:

Cromosome Territories	(CT)
RNA Polymerase	(RNAP)
urokinase Plasminogen Activator	(uPA)
Retinoic Acid	(RA)
TricoStatin A	(TSA)
Tetradecanoyl Phorbol Acetate	(TPA)
Chromatin Immuno Precipitation	(ChIP)
Polymerase Chain Reaction	(PCR)
Tandem Affinity Purification	(TAP)
Mouse Embryo Fibroblasts	(MEF)
Fluorescence In Situ Hybridization	(FISH)
Minimal Promoter	(MP)
InterVening Sequence	(IVS)
Carboxy Terminal Domain	(CTD)
Distinct Amplification Fragment	(DAF)
Micrococcal Nuclease	(MNase)
MNase digestion coupled with ChIP	(MN-ChIP)
Locus Controlm Regions	(LCRs)
RNA Tagging and Recovery of Associated Proteins	(RNA TRAP)
Chromosomal Conformation Capture	(3C)

Pro Myelocytic Leukemia	(PML)
CT- Inter-Chromosome-domains	(CT-IC)
Inter-chromatin Compartment	(IC)
Electron Spectroscopic Imaging	(ESI)
Nucleolar Organization Region	(NOR)
Pre Initiation Complex	(PIC)
Fluorescence Recovery After Photobleaching	(FRAP)
Fluorescence Loss In Photobleaching	(FLIP)
Nuclear Myosin I	(NMI)
Heterogeneous nuclear RiboNuclear Particles	(hnRNPs)
Transcription Initiation Factor-IA	(TIF-IA)
Helix-Loop-Helix	(HLH)
Helix-Turn-Helix	(HTH)
Electrophoretic Mobility Shift Assay	(EMSA)
Activator Responsive Element	(ARE)
Dulbecco's Modified Eagle's Medium	(DMEM)
Fetal Bovine Serum	(FBS)
SDS PolyAcrylamide Gel Electrophoresis	(SDS-PAGE)
Phosphate Buffered Saline	(PBS)
Cross-linked sonicated chromatin	(ChIP ready chromatin)